Three-Dimensional (3D) Reconstruction of Microstructures via Serial Sectioning

By

Adam Hareezi Abdul Aziz

Dissertation Report submitted in partial fulfillment of

the requirements for the

Bachelor of Engineering (Hons)

(Mechanical Engineering)

JUNE 2010

Universiti Teknologi PETRONAS
Bandar Seri Iskandar
31750 Tronoh
Perak Darul Ridzuan

CERTIFICATION OF APPROVAL

Three-Dimensional (3D) Reconstruction of Microstructures

via Serial Sectioning

by

Adam Hareezi Bin Abdul Aziz

A project dissertation submitted to the
Mechanical Engineering Programme
Universiti Teknologi PETRONAS
in partial fulfilment of the requirement for the
BACHELOR OF ENGINEERING (Hons)
(MECHANICAL ENGINEERING)

Approved by,

_____

(DR. AZMI ABDUL WAHAB)

UNIVERSITI TEKNOLOGI PETRONAS
TRONOH, PERAK
JUNE 2010

CERTIFICATION OF ORIGINALITY

This is to certify that I am responsible for the work submitted in this project, that the original work is my own except as specified in the references and acknowledgements, and that the original work contained herein have not been undertaken or done by unspecified sources or persons.

_____

ADAM HAREEZI BIN ABDUL AZIZ

ABSTRACT

A study to generate three-dimensional (3D) reconstruction images of microstructures by using serial sectioning method is performed in which, proper processes and procedures of serial sectioning method need to be established. Serial sectioning method is a material-removal technique, which only practical for a range of material-removal rates of the materials to be studied. The basic serial sectioning material removal methods are involving manual or semiautomated polishing, which can remove between approximately 0.05 to 1.0 micron per section of the material. The material used in this project is Carbon Fiber Reinforced Polymer (CFRP) which is a very strong, light, and expensive composite material or fiber-reinforced polymer. In the project, a few tasks and experiments have been conducted including grinding and polishing, measuring by micrometer and image recording by using optical microscope. Both images from 5X magnification and 50X magnification have been successfully developed and reconstructed into 3D volume by using ImageJ computer software program. Several features and characteristics of CFRP which are the inclination angle measurement and fiber rich area are also discussed in a section of this report.

ACKNOWLEDGEMENT

First and foremost, the author would like to express his deepest gratitude to God for making the Final Year Project (FYP) successful and beneficial for him. Special thanks also goes to Dr. Azmi Abdul Wahab, FYP Supervisor for his support, guidance and time spent throughout the semesters despite his other commitments and packed schedule as a lecturer in UTP. Under his constant supervision, the author managed to start his project with a proper planning and proceed until completion according to the timeframe scheduled.

Apart from these, the author would like to express his sincere thanks to the Mr. Mohd Ridzuan Abdul Latif for providing the samples and also to FYP Coordinator, Dr Saravanan Karuppanan in handling all the undergraduates' FYP successfully. Most importantly, ample time was given to fully complete the project. Besides, the author would like to take this opportunity to express deepest gratitude to the Lab Technicians for their respective professionalism and contribution to this research.

Lastly, heartfelt appreciation goes to beloved parents, family and friends for their support and company in making this research something to be proud of. Thank you to all of you.

TABLE OF CONTENTS

LIST OF FIGURES

LIST OF TABLES

ABBREVIATIONS & NOMENCLATURES

3D	–	three dimensional
2D	–	two dimensional
CFRP	–	Carbon Fiber Reinforced Polymer
UHM	–	Ultra High Modulus
HM	–	High Modulus
IM	–	Intermediate Modulus
HT	–	High Tensile
SHT	–	Super High Tensile
FIB	–	Focused Ion Beam
GIMP	–	Gnu Image Manipulation Program
SEM	–	Scanning Electron Microscope
PPM	–	Portable Pixel Map

CHAPTER 1
PROJECT BACKGROUND

1.1 Background of Study

3D analysis of microstructures already began at least from 1918 with Fortman's effort to understand the 3D structure of pearlite. Solid models of cementite lamellas were constructed by him by projecting the images of each section onto cardboard layers of appropriate thickness. As the time goes by and technologies are developing rapidly, improvements in image processing and 3D visualization capabilities have made 3D reconstruction and visualization of microstructures much more practical. In 1991, Hull et al. were among the first to use computer software in the 3D analysis of microstructures. In this case, he used to contain the titanium prior-beta grain sizes and shapes into 3D wire-frame drawings. Probably, the first to take full advantage of advanced computer reconstruction of microstructures was Shiftlet's group at the University of Virginia. (Kral et al., 1999)

Nowadays, there are many methods that can be used to analyze the microstructures in 3D images such as serial sectioning, focused ion beam tomography, atom probe tomography and x-ray micro-tomography. However, in this project, the author is focusing more in the serial sectioning method in order to generate the 3D images of microstructures.

1.2 Problems Identification

Typically, two-dimensional (2D) metallographic methods provide single polished-and-etched sections for observation and the 2D images of microstructures generated from these methods provide only a planar view of the material. Details of some parameters and characterizations of a microstructures or materials cannot be studied deeply due to this limitation. Thus, proper processes and procedures must be generated in order to obtain the 3D images of microstructures. By reconstructing the 2D images, 3D volumes of microstructures can be generated to provide of more

precise descriptions of sizes, spatial distribution, shapes and interconnectivities of complex microstructural features which can be used in the detail studies of microstructures.

Since the method of the reconstruction of 3D images of microstructures has not been widely developed yet in Malaysia, the author took the challenge to be one of the first to produce the official processes and procedures of 3D reconstruction of microstructures.

1.3 Objectives and Scope of Study

The main objective of this project is to generate three-dimensional (3D) reconstruction images of microstructures by using serial sectioning method. Also, proper processes and procedures of serial sectioning method need to be established as it is the method to be used in this project.

The scope of study of the materials in this project are the materials that consist of minimum two phases. It can be the combination of ferrite and pearlite, austentite and ferrite or austentite and pearlite. Two phases materials are chosen because they have simple structures and is not too complicated to generate their volume.

In order to complete this project, a few tasks and experiments need to be carried out. Grinding and polishing, measuring by micrometer and image recording by using optical microscope are the processes that need to be performed. Also, the uses of computer software are involved in order to generate the 3D volume of microstructures.

CHAPTER 2
LITERATURE REVIEW

2.1 Carbon Fiber Reinforced Polymer

Carbon Fiber Reinforced Polymer (CFRP) is a Polymer Matrix Composite material reinforced by carbon fibers. The reinforcing dispersed phase may be in the form of either continuous or discontinuous carbon fibers commonly woven into a cloth. Carbon fibers are very expensive but they possess the highest specific mechanical properties such as modulus of elasticity and strength. Carbon fibers are used for reinforcing polymer matrix due to the following their properties:

- Very high modulus of elasticity exceeding that of steel;
- High tensile strength, which may reach 1000 ksi (7 GPa);
- Low density: 114 lb/ft³ (1800 kg/m³);
- High chemical inertness. (Kopeliovich, 2010)

The types of carbon fibers are as follows:

- UHM (ultra high modulus): Modulus of elasticity > 65400 ksi (450GPa).
- HM (high modulus): Modulus of elasticity is in the range 51000-65400 ksi (350-450GPa).
- IM (intermediate modulus): Modulus of elasticity is in the range 29000-51000 ksi (200-350GPa).
- HT (high tensile, low modulus): Tensile strength > 436 ksi (3 GPa), modulus of elasticity < 14500 ksi (100 GPa).
- SHT (super high tensile). Tensile strength > 650 ksi (4.5GPa). (Kopeliovich, 2010)

Carbon fibers are also classified according to the manufacturing method:

i. PAN-based carbon fibers (the most popular type of carbon fibers).
   In this method carbon fibers are produced by conversion of polyacrylonitrile (PAN) precursor through the following stages:

- Stretching filaments from polyacrylonitrile precursor and their thermal oxidation at 400°F (200°C). The filaments are held in tension.
- Carbonization in Nitrogen atmosphere at a temperature about 2200 °F (1200°C) for several hours. During this stage non-carbon elements (O,N,H) volatilize resulting in enrichment of the fibers with carbon.
- Graphitization at about 4500 °F (2500°C).

ii. Pitch-based carbon fibers.

Carbon fibers of this type are manufactured from pitch:

- Filaments are spun from coal tar or petroleum asphalt (pitch).
- The fibers are cured at 600°F (315°C).
- Carbonization in nitrogen atmosphere at a temperature about 2200 °F (1200°C). (Kopeliovich, 2010)

The most popular matrix materials for manufacturing Carbon Fiber Reinforced Polymers (CFRP) are thermosets such as epoxy, polyester and thermoplastics such as nylon (polyamide). Carbon Fiber Reinforced Polymers (CFRP) materials usually have laminate structure, providing reinforcing in two perpendicular directions. Carbon Fiber Reinforced Polymers (CFRP) are manufactured by open mold processes, closed mold processes and Pultrusion method. (Kopeliovich, 2010)

Carbon Fiber Reinforced Polymers (CFRP) are characterized by the following properties:

- Light weight;
- High strength-to-weight ratio;
- Very High modulus elasticity-to-weight ratio;
- High Fatigue strength;
- Good corrosion resistance;
- Very low coefficient of thermal expansion;
- Low impact resistance;
- High electric conductivity;
- High cost.

Carbon Fiber Reinforced Polymers (CFRP) are used for manufacturing: automotive marine and aerospace parts, sport goods (golf clubs, skis, tennis racquets, fishing rods), bicycle frames. The main disadvantage of carbon (Graphite) fibers is catastrophic mode of failure (carbon fibers are brittle). (Kopeliovich, 2010)

2.2 Three-Dimensional (3D) Reconstruction Techniques

When using traditional metallographic techniques, materials scientists often make assumptions about the shape, distribution and connectivity of 3D features that lie buried within the material. Recent work has shown that these assumptions can be incorrect. An approach to 3D analysis of microstructures has been taken nowadays and with recent improvements in image processing and 3D visualization capabilities which are helped by the computer-aided programs, many techniques to reconstruct the 3D volume of microstructures have been developed. Therefore, here are the brief descriptions of some of the techniques that are used in 3D reconstruction of microstructure. (Kral et al., 1999)

2.2.1 Serial Sectioning

Serial sectioning method is a material-removal technique, which is only practical for a range of material-removal rates of the materials to be studied. Anyone undertaking this project should identify a microstructural feature for which some 3D information is desired. The basic serial sectioning material removal methods involves manual or semiautomated polishing, which can usually remove approximately 0.05 to 1.0 micron per section of the material. Also, there are other stages of experimental parameters that may be applicable in this techniques which are number of sections required, applying fiducial marks, etching requirements, images recording, images acquisition and visualization software. (Kral et al., 2004)

2.2.2 Focused Ion Beam (FIB) Tomography

In this technique, focused ion beam instruments are operated by rastering a focused beam of ions over the surface of the sample. Direct imaging of the sample surface is

produced when there are interactions between the ion beam and the samples, and the interaction also result in material removal through sputtering. (Kral et al., 2004)

For modern FIB systems, the ion beam spot sizes are routinely of the order of tens of nanometers. This means that these instruments are capable of both high-precision material removal and high-resolution imaging of microstructures. (Kral et al., 2004)

2.2.3 Atom Probe Tomography

In atom probe tomography, the sampled volume is reconstructed atom by atom from many hundred thousands of 2D layers, each of them contains a few atoms. A short-duration high voltage pulse that is superimposed on a standing voltage is used to remove individual atoms from the surface of a needle-shaped specimen at a precise time. (Kral et al., 2004)

Usually, a small aperture in the microchannel plate and phosphor screen assembly is used to view the field ion image in the original atom probe. However, in atom probe tomography technique, the volume analysis is defined by the number of layers of atoms field evaporated from the specimen and by the effective lateral extents of the position-sensitive detector. (Kral et al., 2004)

2.2.4 X-Ray Microtomography

X-Ray tomography is based on the realization that as an x-ray beam passes through an object, it samples a prismatic volume consisting of many small volume elements along its path. If some of the property of the sample such as attenuation of the beam density or the fluorescence yield is measured, it can be used to help reconstruct the structure along the beam path. (Kral et al., 2004)

In order to accurately determine the internal structure of the object, different combination of the sample volume must be measured. With a small “pencil” beam, this is accomplished by translation and rotation of the sample. (Kral et al., 2004)

2.3 Three-Dimensional (3D) Reconstruction via Serial Sectioning

The behavior of materials is controlled by their microstructure. The characteristics of a material's microstructure, such as size, distribution, and morphology, control the mechanical and thermal behavior and properties of the material. Thus, establishing a link between microstructure and properties is vital to fully understanding and predicting material behavior. (Wunsch et al., 2003)

A serial sectioning process has been developed to visualize and model the behavior of a material by using a computer reconstructed 3D microstructure. Two-dimensional microstructures were acquired and used to develop 3D solids for visualization and finite-element modeling (FEM). Visualization and modeling of the 3D composite microstructure aided in the understanding of microstructure morphology and provided the means to make the connection between material structure and performance. (Wunsch et al., 2003)

Below are the brief descriptions of the experimental parameters involved in serial sectioning method.

2.3.1 Specimen Mounting

Samples are mounted primarily for ease in manipulation and for edge protection during preparation. There are many types of mounting that are available to be used in this project such as compression mounting, cold mounting and vacuum impregnation. However, cold mounting is the best technique of specimen mounting for this project.

Three most common types of materials used in cold mounting are epoxide, polyesters and acrylics. These systems are all two component types which consist of a resin and hardener. Since an exothermic reaction during polymerization is involved, the mixing by volume or weight ratios of each system is critical. The epoxides are pale yellow and transparent, same goes to the polyesters which are transparent. However, the polyesters are also available in water clear or a slight pink hue while the acrylics are opaque. (Johnson, 1997)

2.3.2 Polishing and Etching

In basic serial-sectioning material-removal method, manual or semiautomated polishing are involve which it can remove between 0.05 to 1.0 micron/section. In this project, the author decided to use 0.5 to 1.0 micron/section of interval for the removal rates of the material. In order to avoid and prevent pitting from continuing or even accelerating in the material, all pits are essentially removes during the subsequent polishing steps. (Kral et al., 2004)

As for etching, this process may need to be performed to some materials and may not be to the others. Etching is required for some materials in order to obtain its sufficient contrast between phases subsequent to the removal of each layer. Problems may occur during this process such as inconsistent etching between layers, boundaries that do not respond due to their orientation and etching artifacts. (Kral et al., 2004)

2.3.3 Applying Fiducial Marks

Fiducial marks used in this project are microhardness indents which performed by using microhardness testing machines. Fiducial marks are used to align or register the images in the x-y plane and to track the actual material removal rate. Prior to the commencement of actual image acquisition, the material-removal rate may be calibrated by measuring the change in the diagonal length of an indent when the indent-to-depth ration is known. (Kral et al., 2004)

2.3.4 Image Recording

Digital optical micrographs can be obtained by using optical microscope. There are a number of digital cameras now available specifically for optical microscopy from manufacturers such as Olympus, Zeiss and Diagnostic Instrument. Scanning Electron Microscope (SEM) may also be used, although with a considerable increase in the time required to remove and insert the sample into a vacuum chamber for each section. Noted that pixels in a SEM are not square and unless there is a calibration and correction for the pixel aspect ratio, the sample must be placed into the SEM

chamber in the same orientation for each section to make subsequent registration more convenient. (Kral et al., 2004)

2.3.5 Registration and Number of Sections Required.

Alignment or registry of the serial sections can be manually performed by overlaying the fiducial marks in subsequent images. This process can be done through the use of image-processing software such as Adobe Photoshop and NIH Image. It may be faster to align automatically using microstructural features of individual cross section when the depth between sections is known and it can be determined from the fiducial marks, in this case the microhadness indents. (Kral et al, 2004)

For the number of sections required, the scale of the features being studied and the limitations of the material-removal technique being used must be considered. The resolution of 3D presentation in every serial sectioning project has been limited by the thickness of each serial section layer. Thus, for this project, it is advisable to take from 50 to 100 sections of images. (Kral et al., 2004)

2.4 Three-Dimensional (3D) Reconstruction Software

Characterization of materials by analysis of 3D microstructures is placing a strong demand for visualization tools and techniques. Nowadays, there are many computer software packages currently available for 3D reconstruction and visualization. Some of the programs are “shareware” and “freeware” while others are commercially available. **Table 1** illustrates some of the tools from the on-line sources. (Kral et al., 1999)

Table 1: List of on-line sources for 3D visualization and techniques

Website name	URL	Note
Portable Pixel Map (PPM)	sourceforge.net/projects/netpbm	Image conversion
NIH Image	rsb.ibfo.nih.gov/nih-image	Public domain preprocessing
Aphelion	Hallogram.com/apheliondev	Commercial
Noesis Images	www.norpix.com/visilog.htm	Commercial
WorkSpace	www.fakespacesystems.com/index.htm	Virtual reality
CAVE,NCSA	www.vrco.com/	Virtual reality
Juggle, Iowa State	www.vrjuggler.org	Virtual reality
Amira, Template Graphics, Inc. (TGS)	www.amiravis.com/	Commercial algorithm
SCIRun, University of Utah	software.sci.utah.edu/scirun.html	Public domain ray tracing
Volpack, Stanford University	graphics.stanford.edu/software/volpack	Public domain ray tracing
Gnu Image Manipulation Program (GIMP)	www.gimp.org	Image processing
Paint.NET	http://www.getpaint.net/	Image processing
ImageJ	http://rsbweb.nih.gov/ij/	Image processing

2.4.1 Gnu Image Manipulation Program (GIMP)

GIMP is an acronym for GNU Image Manipulation Program. It is a freely distributed program for such tasks as photo retouching, image composition and image authoring. In the free software world, there is generally no distinction between users and developers. It has many capabilities. It can be used as a simple paint program, an expert quality photo retouching program, an online batch processing system, a mass production image renderer, an image format converter, etc.

GIMP is expandable and extensible. It is designed to be augmented with plug-ins and extensions to do just about anything. The advanced scripting interface allows everything from the simplest task to the most complex image manipulation procedures to be easily scripted.

GIMP is written and developed under X11 on UNIX platforms. But basically the same code also runs on MS Windows and Mac OS X.

2.4.2 Paint.NET

Paint.NET is a free image and photo editing software for computers that run Microsoft Windows, developed on the .NET Framework. Originally created as a Washington State University student project, Paint.NET has evolved from a simple replacement for the Microsoft Paint program, which is included with Windows, into a powerful editor with support for layers, blending, transparency, and plug-in. It is often used as a free alternative to Adobe Photoshop.

It features an intuitive and innovative user interface with support for layers, unlimited undo, special effects, and a wide variety of useful and powerful tools. An active and growing online community provides friendly help, tutorials, and plug-in.

2.4.3 ImageJ

ImageJ is a public domain Java image processing program inspired by NIH Image for the Macintosh. It runs, either as an online applet or as a downloadable application, on any computer with a Java 1.4 or later virtual machine. Downloadable distributions are available for Windows, Mac OS, Mac OS X and Linux.

It can display, edit, analyze, process, save and print 8-bit, 16-bit and 32-bit images. It can read many image formats including TIFF, GIF, JPEG, BMP, DICOM, FITS and "raw". It supports "stacks", a series of images that share a single window. It is multithreaded, so time-consuming operations such as image file reading can be performed in parallel with other operations.

It can calculate area and pixel value statistics of user-defined selections. It can measure distances and angles as well. Besides, it can create density histograms and

line profile plots. It also supports standard image processing functions such as contrast manipulation, sharpening, smoothing, edge detection and median filtering.

It does geometric transformations such as scaling, rotation and flips. Image can be zoomed up to 32:1 and down to 1:32. All analysis and processing functions are available at any magnification factor. The program supports any number of windows (images) simultaneously, limited only by available memory. Spatial calibration is available to provide real world dimensional measurements in units such as millimeters. Density or gray scale calibration is also available.

ImageJ was designed with an open architecture that provides extensibility via Java plugins. Custom acquisition, analysis and processing plugins can be developed using ImageJ's built in editor and Java compiler. User-written plugins make it possible to solve almost any image processing or analysis problem.

CHAPTER 3

METHODOLOGY

3.1 Flow Chart

Figure 1 summarizes the serial section process flow for CFRP.

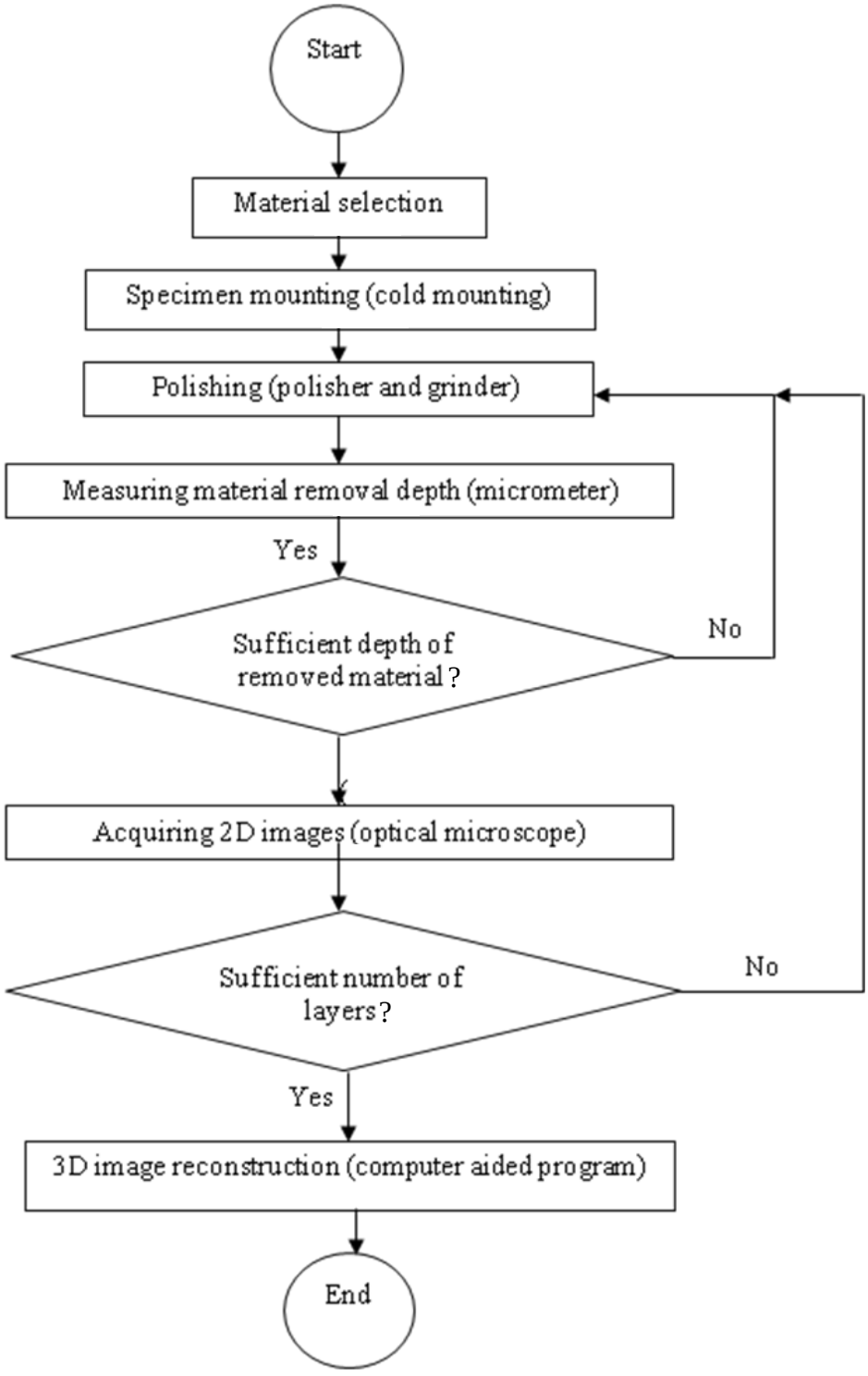

Figure 1: The serial sectioning process flow chart for CFRP

The project started with the selection of material which is the Carbon Fiber Reinforced Polymer (CFRP). Then, it is continued with specimen mounting, where cold mounting is selected to be used instead of hot mounting. Next, the most crucial step is the polishing process. About one to one and half hour are needed to prepare a single layer of the material. After that, the specimen is measured by using micrometer. If there is insufficient depth of removed material, polishing process need to be repeated until the desired depth is removed. Once the sufficient depth is obtained, 2D images are acquired by using optical microscope. Sufficient numbers of layers need to be obtained so this stage must be repeated. The last stage of the project work is the 3D image reconstruction. This process requires the use of computer software program which is ImageJ. The project is ended once the final stage is completed.

3.2 Project Activities

3.2.1 Material Selection

The material used in this project is Carbon Fiber Reinforced Polymer (CFRP). Carbon Fiber Reinforced Polymer is a very strong, light, and expensive composite material or fiber-reinforced polymer. The composite material is commonly referred to by the name of its reinforcing fibers (carbon fiber). The polymer is most often epoxy, but other polymers, such as polyester, vinyl ester or nylon are sometimes used. Some composites contain both carbon fiber and other fibers such as Kevlar, aluminum and fiberglass reinforcement.

It has many applications in aerospace and automotive fields, as well as in sailboats, and notably in modern bicycles and motorcycles, where its high strength-to-weight ratio is of importance. Improved manufacturing techniques are reducing the costs and time to manufacture, making it increasingly common in small consumer goods as well, such as laptops, tripod, fishing rods, paintball equipment, archery equipment, racquet frames, stringed instrument bodies, classical guitar string, drum shells, golf clubs, and pool/billiard/snooker cues.

3.2.2 Specimen Mounting

There are three types of common materials used in cold mounting which are polyesters, epoxides and acrylics. In this project, epoxide is the material chosen for cold mounting of a sample. Below are the procedures of mounting a specimen by using Epo-Kwick Fast Cure Epoxy Kit.

i. A scale mix by weight must be used which is five parts Epo-Kwick Resin to one part Epo-Kwick Hardener.
ii. The samples are cleaned and dried thoroughly before encapsulation
iii. The inside of the mounting cup is coated with Release Agent (20-8185) to ensure easy removal of the mount from the mold.
iv. The specimen is placed inside the center of the mounting cup with the surface of interest facing down.
v. The mixture is blended thoroughly for approximately 1 – 1.5 minutes.
    - For best result, the cup containing the resin and hardener is tipped slightly and by using a stirring stick, the resin and hardener are gently work together using a lift and stir motion until the mixture is thoroughly blended.
    - The mix will start out cloudy as the resin and hardener are blended together. The mixture is kept blended until it becomes clear, indicating it is thoroughly mixed.
    - Violent stirring must be avoided in order to prevent the formation of air bubbles.

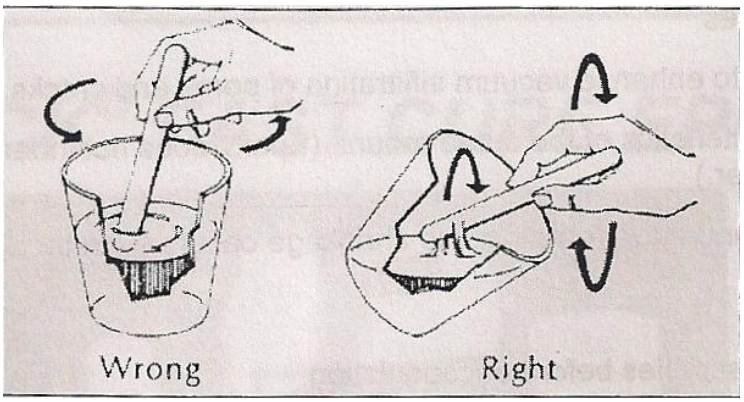

Figure 2: Technique of stirring the mixture.

vi. Once the mixture is clear, it is poured into the mounting cup to near capacity of best result.

vii. The mold is allowed to cure at room temperature for approximately 12 hours.

viii. After curing, the mount is removed from the mounting cup.

Figure 3: Epo-Kwick Fast Cure Epoxy Kit.

3.2.3 Polishing

For this project purposes, METASERV 2000 Grinder and Polisher are used and there are procedures of grinding and polishing that need to be followed. The procedures are as stated below:

i. The mounted sample must be grinded by using 240 grit of Silicon Carbide (SiC) with water as lubricant for the first step.

ii. The mount is cleaned thoroughly and dried.

iii. Step i is repeated by using 320, 400 and 600 grit of SiC with water as lubricant and sample is rotated 90º during the process.

iv. The mount is cleaned thoroughly by using cotton swab saturated with alcohol and dried.

v. Step i is repeated by using precondition synthetic velvet cloth with six micron diamond paste and a water soluble extender as lubricant.

vi. Polishing continued by using three micron diamond paste and one micron diamond paste.

vii. If the removal depth is not achieved, the polishing process is repeated with P1200 grade of SiC, followed by P2400, P4000, three micron diamond paste and one micron diamond paste.

viii. Step vii is continued until the desired removal depth is removed.

ix. Sample must be rotated 90º during each grade of polishing processes.

Figure 4: METASERV 2000 Grinder and Polisher.

3.2.4 Measuring Removal Depth

In order to measure the depth or removed material, Mitutoyo Micrometer is used. Below are the steps in using the micrometer.

i. The sample is located between anvil and spindle of the micrometer.

ii. The micrometer is closed by rotating its thimble and make sure that the interested surface is situated between the anvil and spindle surface.

iii. The ratchet is spin until the spindle meets the sample.

iv. The ratchet is spin until 3 clicks are heard.

v. Both the anvil and spindle are verified to touch the object evenly.

vi. The thimble lock is set while the micrometer is still on the object.

vii. The micrometer is removed from the object once it's been locked.

viii. The initial reading of micrometer is taken.

ix. After the sample has been polished for the next layer, step i to vii are repeated.

x. The current reading is taken.

xi. The current data must be deducted from the initial reading in order to get the depth of removed material

xii. Step ix to xi is repeated for the next number of layers.

Figure 5: Mitutoyo Micrometer (103-137 M110-25).

3.2.5 Acquiring 2D Images

In this project, Leica DMLM Optical Microscope is employed in order to capture the 2D images of the sample. Here are the steps and procedures to use the optical microscope;

i. The optical microscope is set as per settings below;
   - A = 2.25
   - F = 1.75
   - No polarizer
   - Optimum exposed light = between 10 and 11
   - DLF = Up
   - BG20 and gwin = Down

ii. The computer software, DinoCapture is set as per settings below;
   - Image mirror = Untick (X)
   - Image Flip = Untick (X)
   - Low Light = Tick (/)
   - Brightness = 126
   - Contrast =1.45
   - Gamma = 0.70

- Hue = 35
- Saturation = 2.20
- Sharpness = 4.50
- Exposure = 80
- Red = 1.00
- Blue = 1.00

iii. The sample is placed on the microscope stage, with the specimen directly over the center of the glass circle on the stage (directly over the light).

iv. If the image is on low power (unfocused), the position of diaphragm is adjusted by raising it to the objective lens

v. It is focused by using first the coarse knob, then the fine focus knob until the image appeared

vi. Once the image is appeared, the "capture" button is clicked at the DinoCapture software.

vii. Step iii-vi is repeated for the other desired area of the sample.

viii. Step iii-vi is also repeated for 50X magnification objective lens.

Figure 6: Leica DMLM Optical Microscope

3.2.6 3D Reconstruction

3D volume reconstruction of the material is fully done by using ImageJ computer program. Below are the steps taken in order to develop the volumes.

i. Open all the 2D images as an image sequence (File > Import > Image Sequence)
ii. Make sure to tick the "Convert to 8-bit Grayscale" box.
iii. Align all the images by using ImageJ plugins. Make sure to install the StackReg plugin first. (Plugins > Stackreg > StackReg)
iv. Crop the aligned images. (Image > Crop)
v. Set the threshold of the images. Make sure the colours of the images turn to black and white. (Image > Adjust > Threshold)
vi. Invert the colours (Edit > Invert)
vii. Set the properties of the images (Image > Properties)
viii. Finally, reconstruct those 2D images by using ImageJ 3D Volume Viewer plugin (Plugins > 3D > ImageJ 3D Volume Viewer > Select the white colour in appeared box)

3.3 Equipments and Computer Software

The equipments and computer software that are used for this project are as below.

Table 2: List of equipments and computer software used in this project

Equipments	Computer softwares
Epo-Kwick Fast Cure Epoxy Kit.	DinoCapture
METASERV 2000 Grinder and Polisher.	ImageJ
Mitutoyo Micrometer (103-137 M110-25)	
Leica DMLM Optical Microscope	

3.4 Gannt Chart

Detail / Week	1	2	3	4	5	6	7		8	9	10	11	12	13	14
Project continues on polishing and grinding for layers.															
Submission of Progress Report 1						◆									
Project continues on Computer Aided program for reconstruction.															
Submission of Progress Report 2									◆						
Seminar									◆						
Poster Exhibition											◆				
Submission of Dissertation Final Draft															◆
Oral Presentation															◆
Submission of Dissertation (hard bound)									7 days after oral presentation						

MID-SEMESTER BREAK

Figure 7: Gantt chart for Three-Dimensional (3D) Reconstruction of Microstructures via Serial Sectioning project.

CHAPTER 4
RESULTS AND DISCUSSIONS

4.1 Work completed and Data Presentation

Nine sections of images from the specimen need to be taken with 5X magnification and a section with 50 X magnification for each layer. Also, around 30 to 50 layers of specimens in 2D images with 20 to 40 micron interval are needed in this project. Time taken is about one and a half hour for the process of polishing and grinding and also including the process of acquiring 2D images to be completed.

Figures below show the layout of nine sections of images from specimen that would be taken with 5X magnification and a section with 50X magnification.

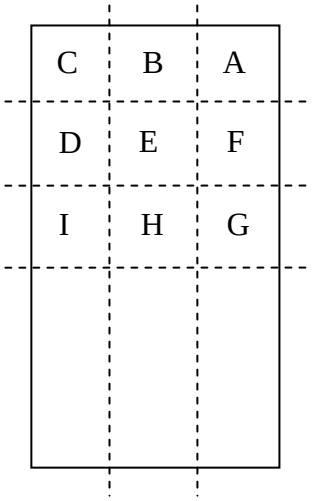

Figure 8: Nine sections of images of specimen with 5X magnification.

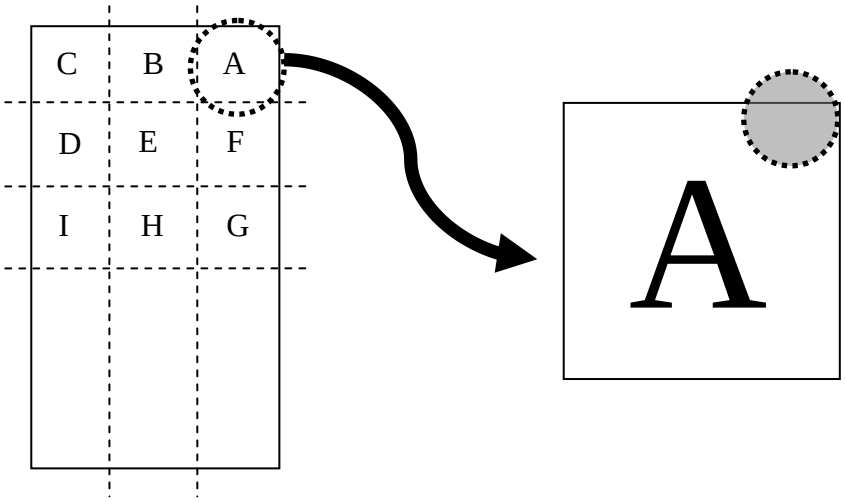

Figure 9: Area of a section with 50X magnification.

There are four locations need to be measured by micrometer in order to calculate the average material removal rate of the specimen after the polishing and grinding process. **Figure 6** and **Table 2** below show the location of measurement and the data gathered.

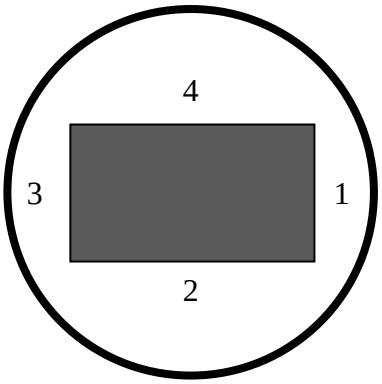

Figure 10: Four locations of measurement.

Table 3: Data gathered for average material removal rate.

No. of layer	Specimen Thickness (mm)				Average Material Removal Rate (mm)
	1	2	3	4	
1	11.98	11.97	11.96	11.94	0.000
2	11.91	11.92	11.93	11.92	0.043
3	11.86	11.88	11.88	11.87	0.047
4	11.82	11.84	11.84	11.82	0.043
5	11.78	11.80	11.81	11.78	0.037
6	11.74	11.76	11.79	11.74	0.035
7	11.70	11.70	11.77	11.70	0.040
8	11.31	11.33	11.33	11.33	0.093
9	11.27	11.29	11.29	11.29	0.041
10	11.23	11.27	11.28	11.26	0.026
11	11.20	11.24	11.24	11.23	0.030
12	11.08	11.12	11.11	11.10	0.126
13	11.01	11.04	11.05	11.04	0.069
14	10.97	11.01	11.03	11.01	0.029
15	10.92	10.97	10.98	10.96	0.049
16	10.90	10.93	10.94	10.92	0.033
17	10.88	10.90	10.91	10.90	0.025
18	10.86	10.88	10.89	10.80	0.040
19	10.84	10.87	10.87	10.85	0.013
20	10.81	10.84	10.83	10.82	0.020
21	10.78	10.81	10.80	10.78	0.032
22	10.75	10.78	10.78	10.76	0.025
23	10.72	10.76	10.76	10.73	0.025
24	10.70	10.74	10.74	10.70	0.023
25	10.66	10.72	10.72	10.65	0.032
26	10.62	10.68	10.68	10.61	0.040
27	10.58	10.65	10.66	10.58	0.030
28	10.54	10.63	10.62	10.54	0.035
29	10.51	10.61	10.60	10.50	0.027
30	10.48	10.58	10.58	10.47	0.027

There are nine sections of 2D images that need to be taken with 5X magnification and a section with 50X magnification. Here are the sample images from the second layer of the specimen with specified magnification.

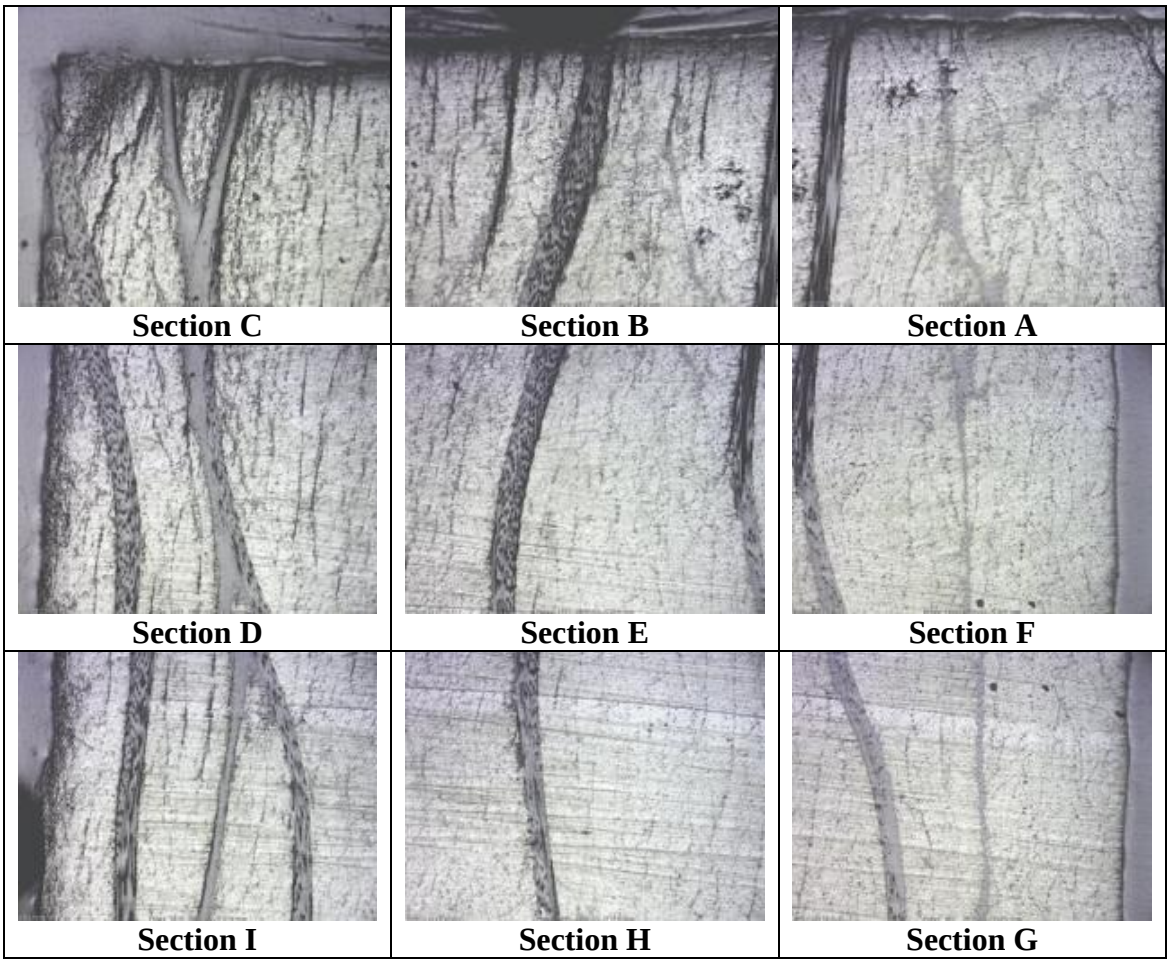

Figure 11: Nine sections of 2D images from the specimen with 5X magnification (second layer)

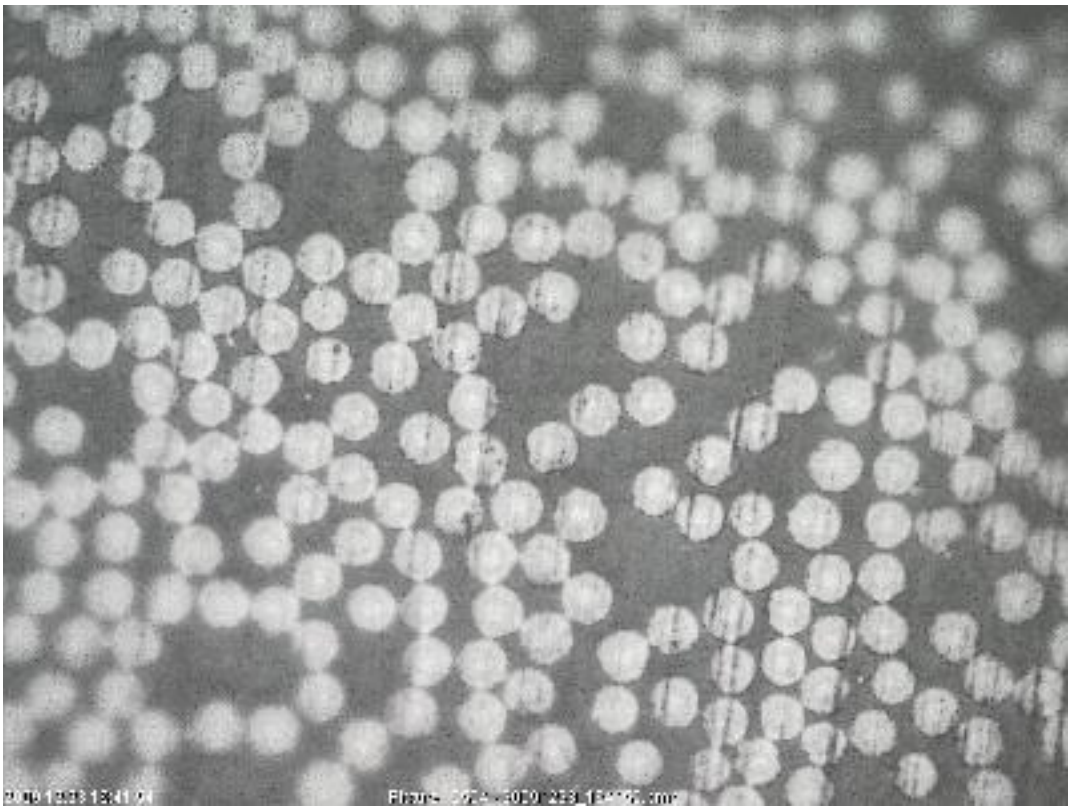

Figure 12: A 2D image from the specimen with 50X magnification.

There are 261 2D images for 5X magnification and 30 2D images of 50X magnification in total. For 5X magnification 2D images, they will be reconstructed to 3D volume by each section and same goes to 50X magnification. All 2D images are reconstructed by using computer software which is ImageJ.

The steps to develop those 3D volumes of CFRP have been described in **Project Activities Section 3.2.6**. Some characteristics of the CFRP can be seen in these 3D images in which, very useful in the study of this material. The importance of those characteristics will be discussed later in the Discussion section. Here are some figures that show the 3D volume reconstructed by this software.

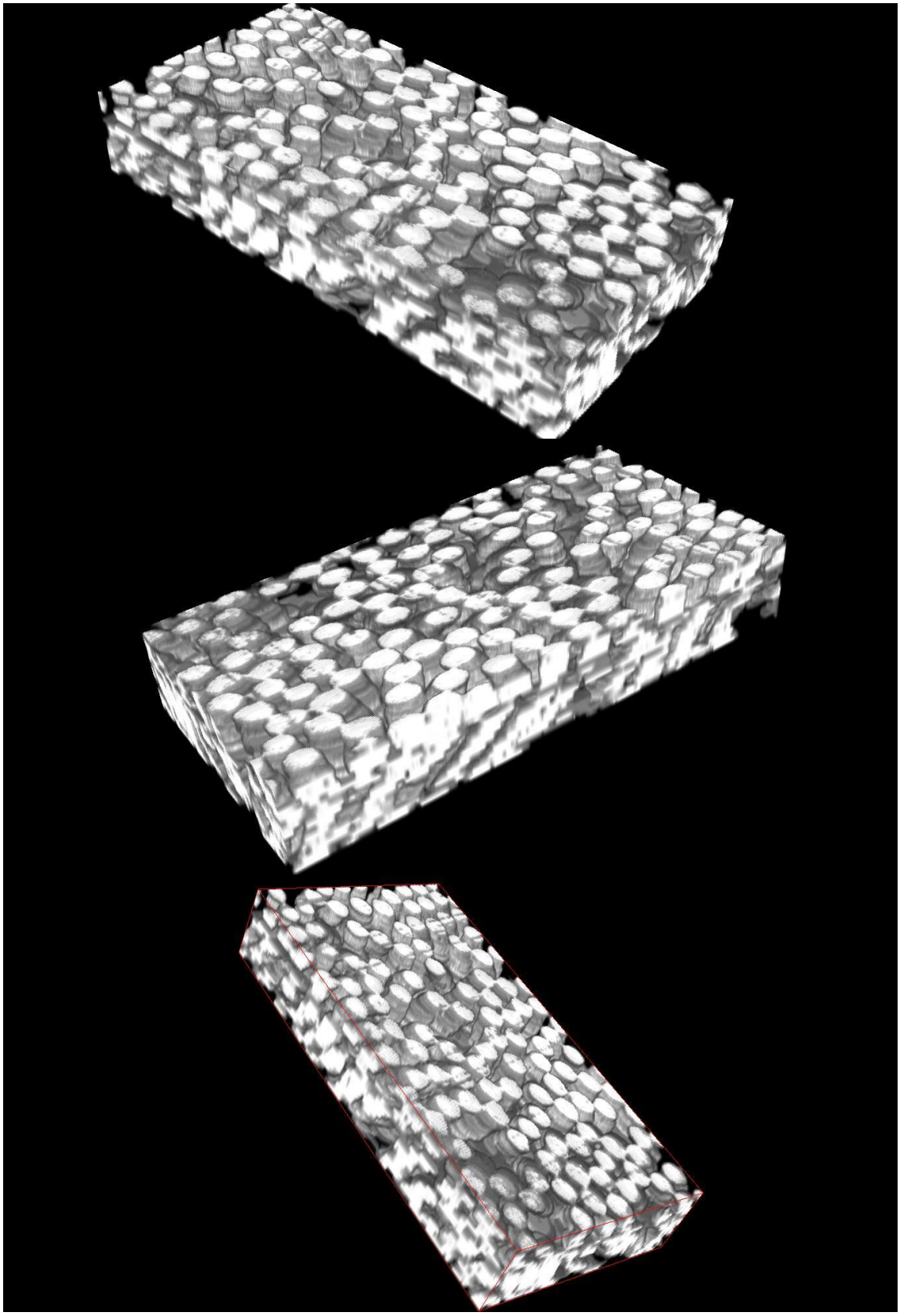

Figure 13: 3D (2394 x 1043 x 380 micron) volume of CFRP that are reconstructed from 50X magnification.

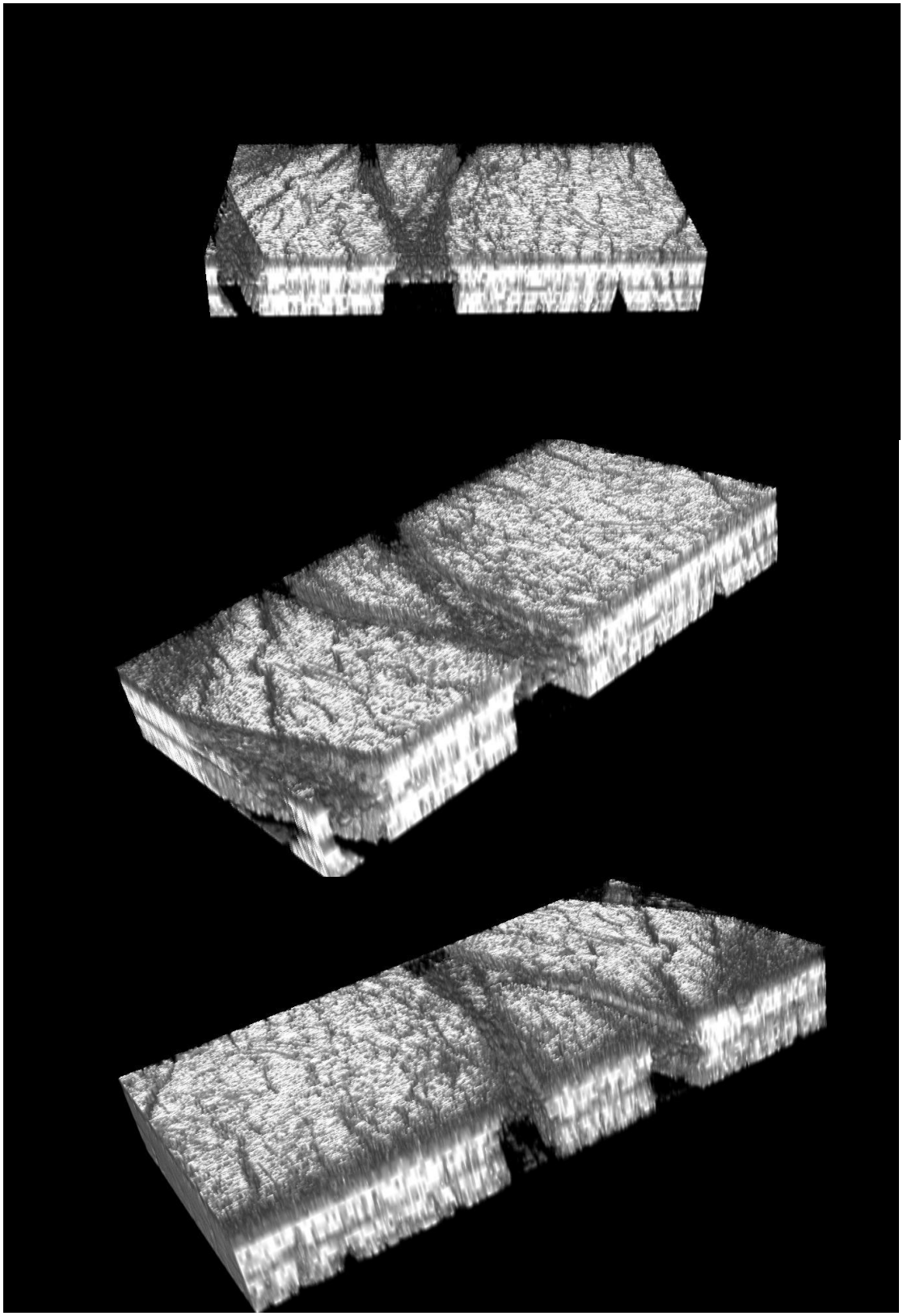

Figure 14: 3D (7094 x 2981 x 1100 micron) volume of CFRP that are reconstructed from Section C of 5X magnification.

4.2 Data Analysis

4.2.1 Angle Measurement by ImageJ

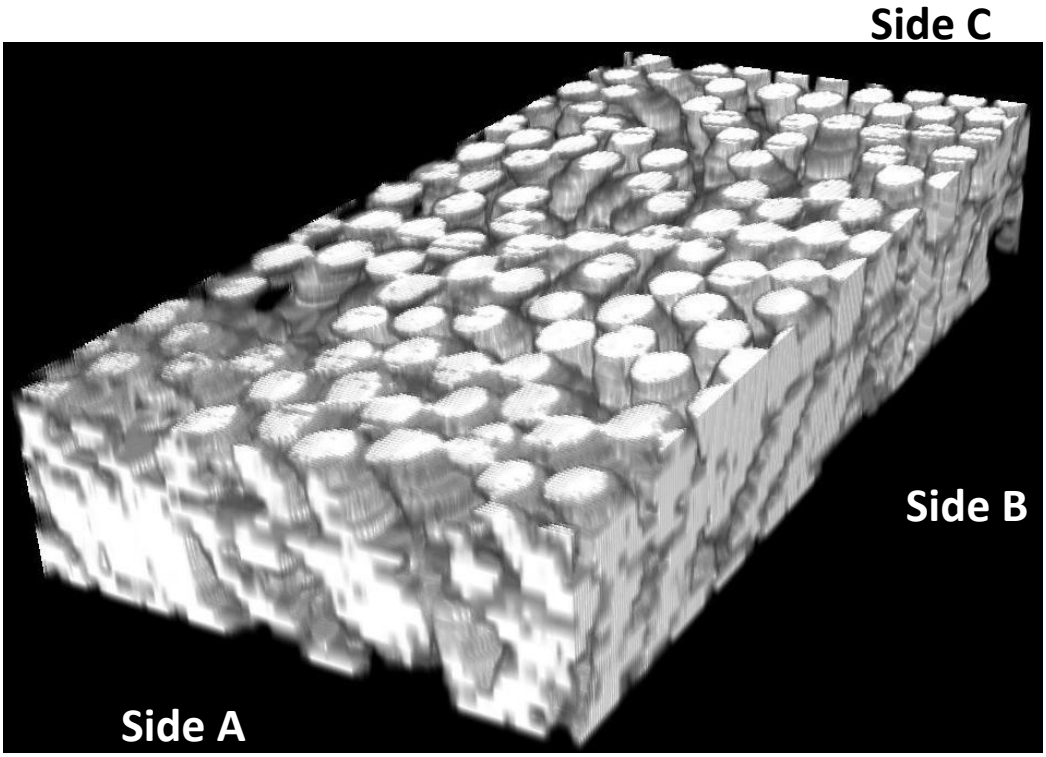

Figure 15: Three sides of sample for angle measurement purpose (2394 x 1043 x 380 micron).

For this project purpose, three sides as indicated in figure above are selected in order to measure some angles of the fibers. All measurements of angles are performed by using ImageJ computer software and angle measurement steps are as follows.

i. Go to File, and open samples.
ii. Take Angle Tool and click on one length of the open angle.
iii. Draw the line down to the apex and then out the other length.
iv. Go up to Analyze, click on Measure.
v. A set of result should be appeared including the angle of the line drawn.

Several positions of fibers are selected and their results are shown in figures and tables below.

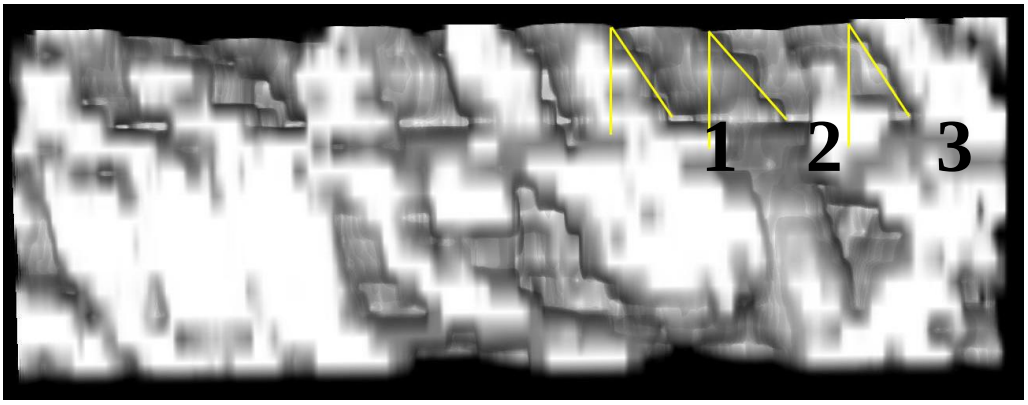

Figure 16: Side A of fibers angle measurement.

Table 4: Angle of fibers calculated by ImageJ for Side A

Position	Angle (°)
1	35.12
2	39.71
3	35.10

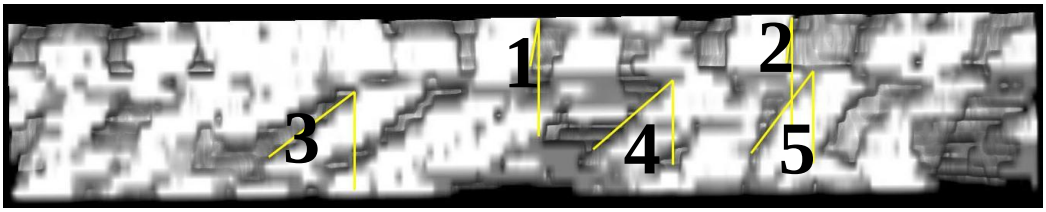

Figure 17: Side B of fibers angle measurement.

Table 5: Angle of fibers calculated by ImageJ for Side B

Position	Angle (°)
1	11.31
2	7.72
3	49.31
4	48.30
5	36.06

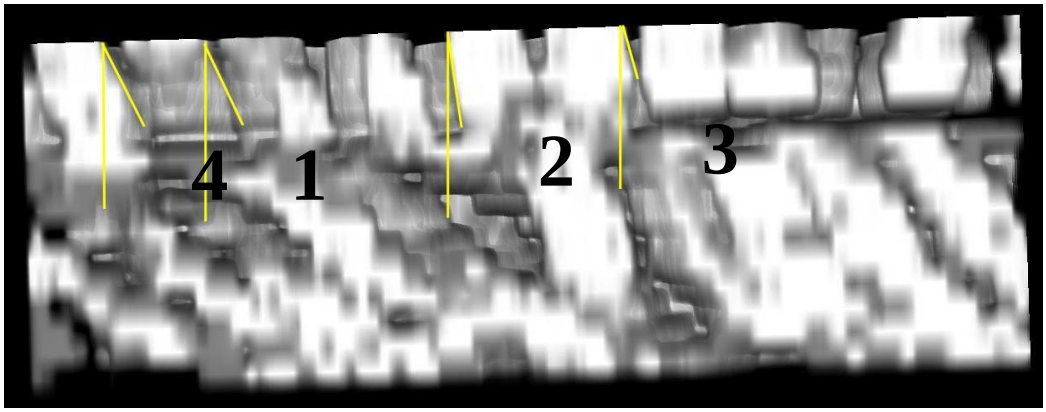

Figure 18: Side C of fibers angle measurement.

Table 6: Angle of fibers calculated by ImageJ for Side C

Position	Angle (°)
1	12.01
2	8.12
3	10.97
4	18.79

4.2.2 Angle Measurement by Tracking a Fiber

This technique of angle measurement requires both of computer software feed and simple calculation based on Pythagorean Theorem.

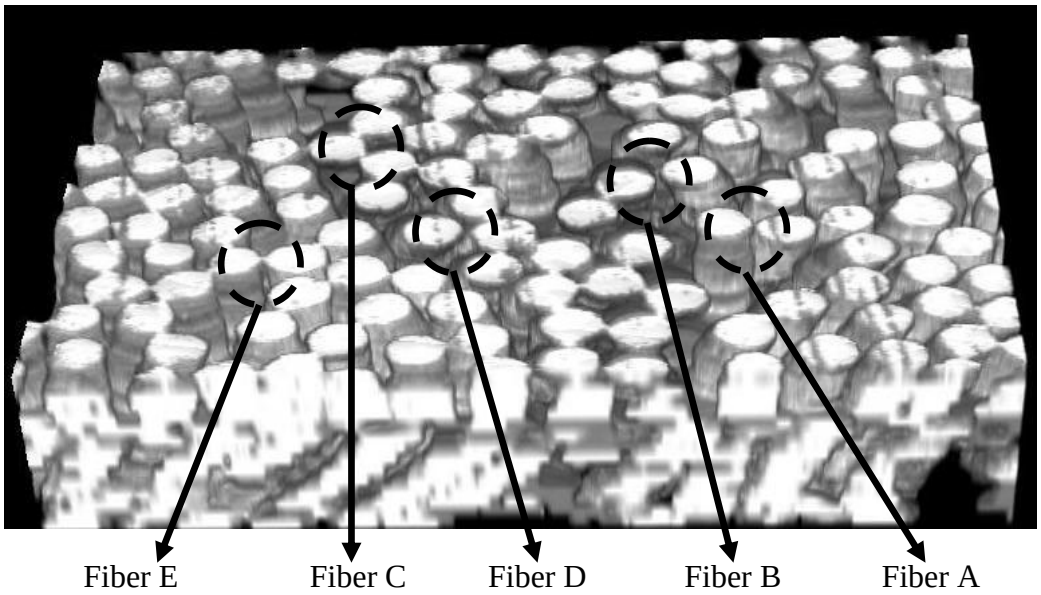

Figure 19: Five selected fibers to be tracked

As for this project purpose, five carbon fibers are selected as shown in **Figure 14**. Then by using ImageJ, each fiber is tracked down up to nine layers to see their

orientation. The steps involved in tracking down the fibers and necessary information gathered are explained in set of procedures below.

i. The aligned of 2D images of 50X magnification is opened. (File > Open)
ii. Preferred fiber is cropped out form the image by using rectangle tool. (Rectangle Tool > Select the area of preferred fiber > Image > Crop)
iii. Separate the image sequence into a set of image files to create a new image sequence. (Image > Stacks > Stacks to Image)
iv. Save all the 9 first layers in a folder by alphabetical order.
v. Create a new image sequence. (Open > Image Sequence > Select one of the 9 layers saved)
vi. Select a point on the fiber. Create a line from the point of the first layer to the same point of second layer.
vii. Measure the length of the line. (Analyze > Measure)
viii. Repeat step vii to viii up to 9 layers.

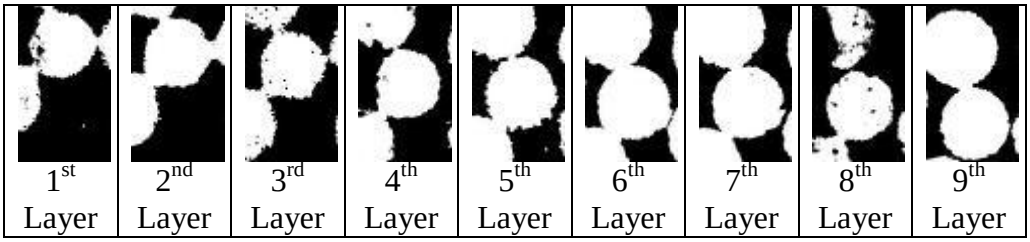

Figure 20: Set of tracking images for Fiber E.

From the length measured and depth removed between layers, Pythagoras Theorem is employed in order to determine the angle of the fibers. A picture of this calculation concept is shown in Figure 16 for better understanding.

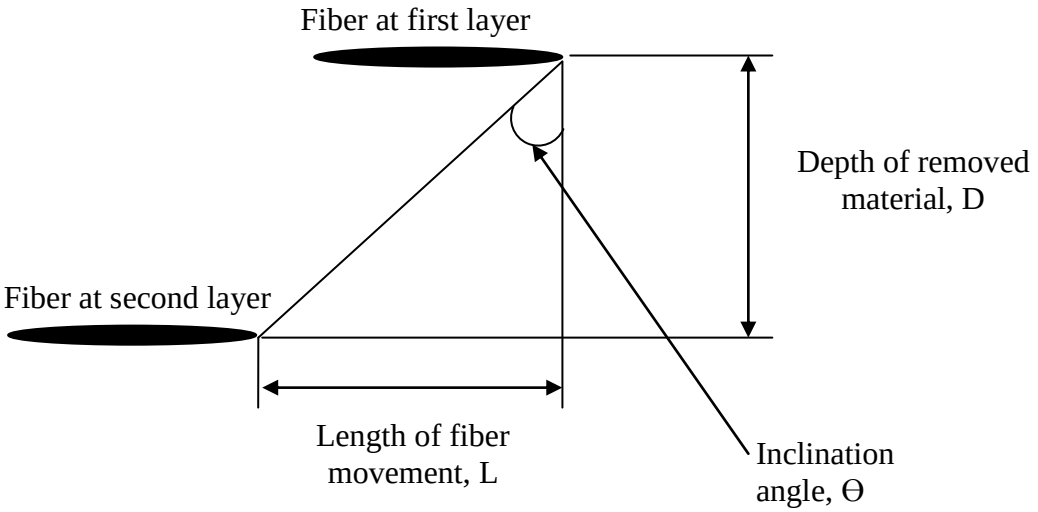

Figure 21: Pythagoras Theorem principle in measuring inclination angle.

Thus, in order to calculate the inclination angle, Θ the following equation are used.

$$\Theta = \tan^{-1}(L / D)$$

Where; Θ = Inclination angle

L = Length of fiber movement

D = Depth of removed material

Assumptions: Diameter of a fiber = 2 μm

Sample calculation for second layer of Fiber A;

$$\Theta = \tan^{-1}(L / D)$$
$$= \tan^{-1}(0.2371 / 43)$$
$$= \tan^{-1}(0.0055)$$
$$= 0.32^{O}$$

Table 7: Data gathered for angle measurement by using tracking fiber method.

Carbon Fiber	Layer	L (μm)	D (μm)	L / D	θ (^{o})
Fiber A	1	0.00	0.00	0.00	0.00
	2	0.24	43.00	0.01	0.32
	3	0.34	47.00	0.0072	0.41
	4	0.37	43.00	0.0086	0.49
	5	0.19	37.00	0.0052	0.30
	6	0.19	35.00	0.0055	0.32
	7	0.00	4.00	0.0000	0.00
	8	0.24	393.00	0.0006	0.03
	9	0.499	41.00	0.0119	0.68
Fiber B	1	0.00	0.00	0.0000	0.00
	2	0.40	43.00	0.0093	0.53
	3	0.33	47.00	0.0071	0.41
	4	0.64	43.00	0.0148	0.85
	5	0.33	37.00	0.0090	0.52
	6	0.37	35.00	0.0107	0.61
	7	0.00	4.00	0.0000	0.00
	8	0.00	393.00	0.0000	0.00
	9	0.59	41.00	0.0145	0.83
Fiber C	1	0.00	0.00	0.0000	0.00
	2	0.36	43.00	0.0084	0.48
	3	0.37	47.00	0.0079	0.45
	4	0.65	43.00	0.0151	0.87
	5	0.59	37.00	0.0159	0.91
	6	0.38	35.00	0.0108	0.62
	7	0.00	4.00	0.0000	0.00
	8	0.00	393.00	0.0000	0.00
	9	0.39	41.00	0.0096	0.55
Fiber D	1	0.00	0.00	0.0000	0.00
	2	0.24	43.00	0.0056	0.32
	3	0.24	47.00	0.0050	0.29
	4	0.41	43.00	0.0095	0.54
	5	0.26	37.00	0.0070	0.40
	6	0.24	35.00	0.0069	0.40
	7	0.00	4.00	0.0000	0.00
	8	0.00	393.00	0.0000	0.00
	9	0.47	41.00	0.0115	0.66
Fiber E	1	0.00	0.00	0.0000	0.00
	2	0.24	43.00	0.0055	0.32
	3	0.34	47.00	0.0072	0.42
	4	0.50	43.00	0.0117	0.67
	5	0.34	37.00	0.0091	0.52
	6	0.30	35.00	0.0087	0.50
	7	0.00	4.00	0.0000	0.00
	8	0.00	393.00	0.0000	0.00
	9	0.54	41.00	0.0132	0.76

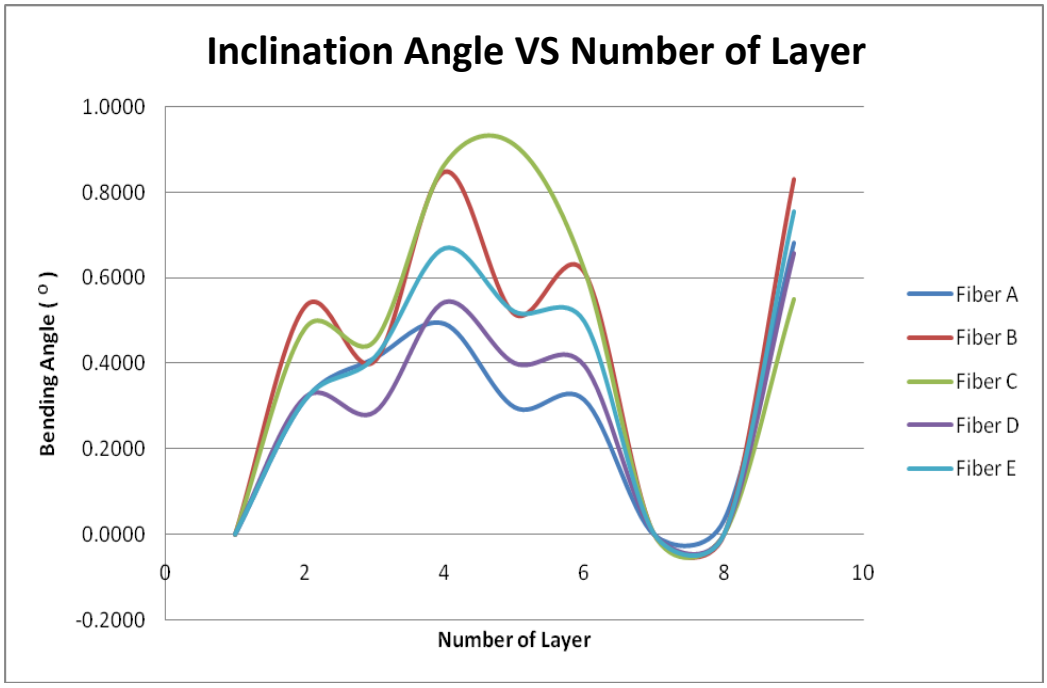

Figure 22: Graph of Inclination Angle vs Number of Layers

The inclination angle of fiber is an important characteristic of a material. With 2^{O} of inclination angle, it will give effect of 30% of compression strength reduction of CFRP. Also, with the increase of fiber inclination angle, fiber apparent strength will decrease.

Up to 9 layers are used for this project as the tenth layer of the sample is misaligned thus disturbing the orientation of the fibers. However, the 3D volume is continued to be developed for the next number of layers since all of them are properly aligned by using the computer software, ImageJ.

From the data gathered, all the inclination angles of the fibers for this CFRP sample is less than 1^{O}. The highest inclination angle is 0.9109^{O} and the lowest is 0.0343^{O}. Thus, it can be considered that this sample is still strong enough to be used in industry.

4.2.3 Fiber-Rich Area and Resin-Rich Area

After developing the 3D volume of the material, there are some important features that need to be considered. Two of these features are the fiber-rich and resin-rich areas.

It is always assumed that the fibers will evenly distribute in the whole composite. However, based on the 3D images developed through serial sectioning method, there are some areas full of fibers and other parts that are rich with resin. This condition will affect the strength of the material as there is no reinforcement in the resin rich area. It may become a weak location of the material and this condition is critical, since CFRP will be used in wide application such as in automotive, aircraft and also in military applications.

These features can be seen clearly using 3D reconstructed image whereas 2D images might not be as convincing. **Figures 23 - 25** are attached together in this report that shows the fiber-rich area and resin-rich area from some sections of CFRP sample.

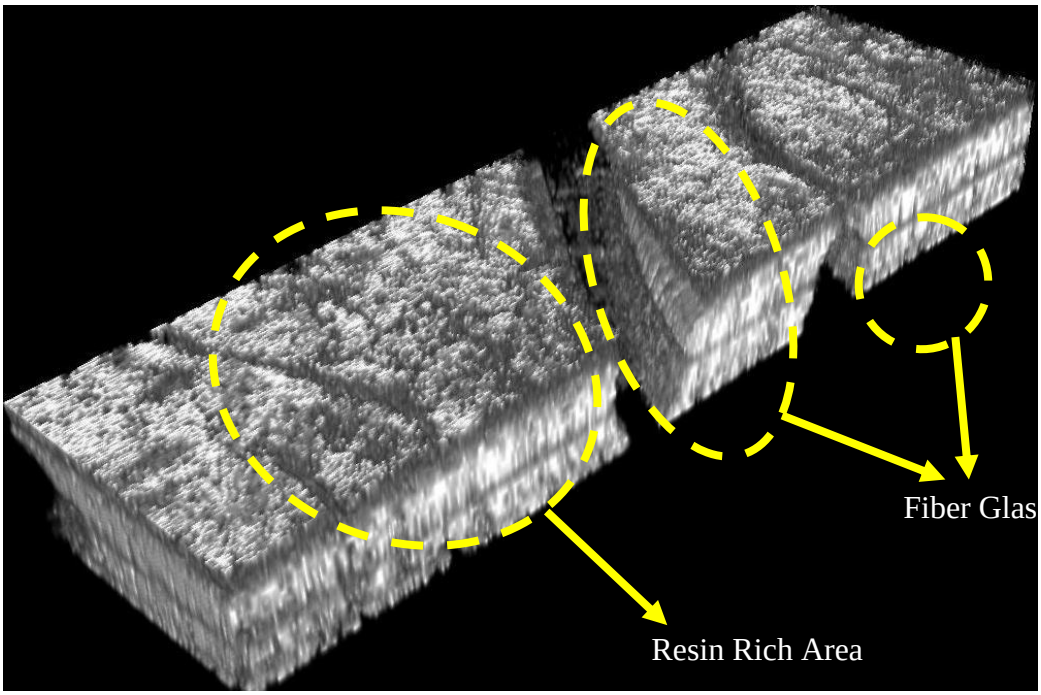

Figure 23: Resin-rich area from 3D (8479 x 2644 x 1100 miccron) volume of Section-B

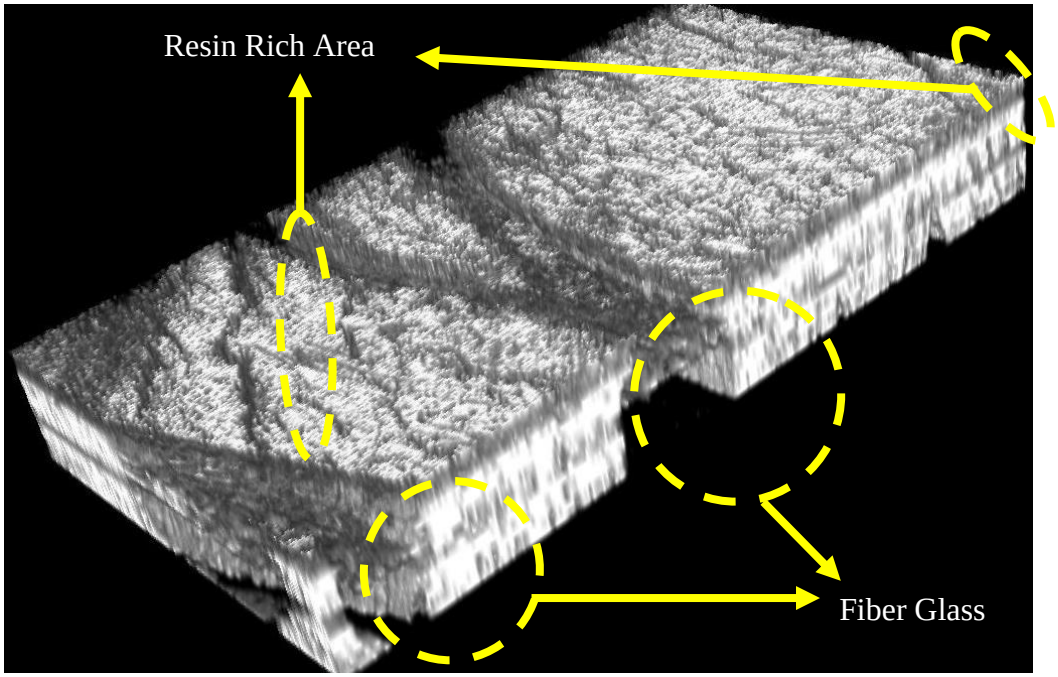

Figure 24: Resin-rich area from 3D (7094 x 2981 x 1100 micron) volume of Section-C

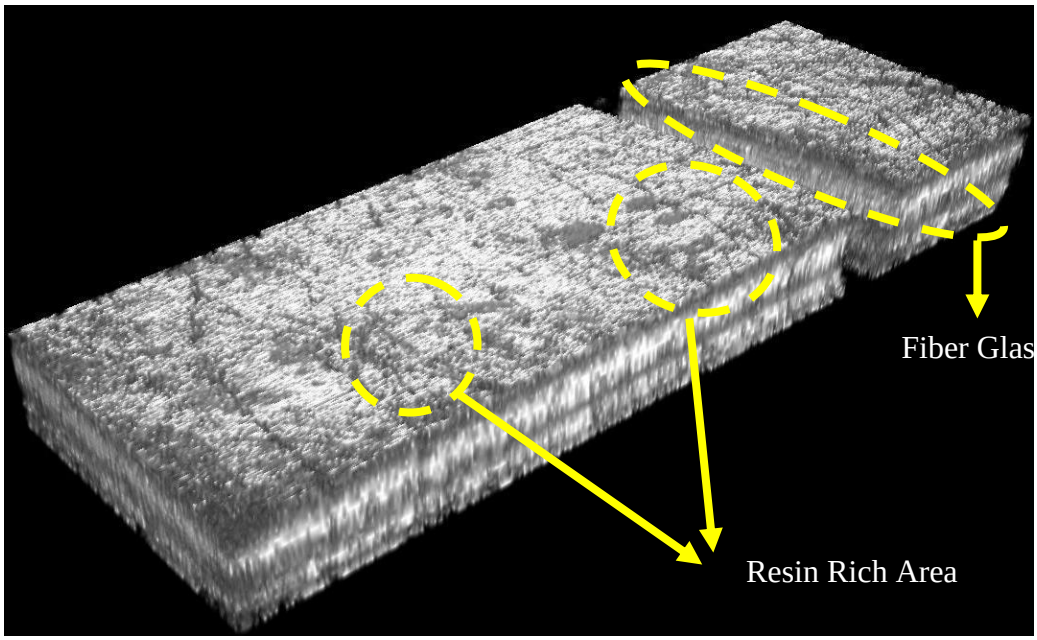

Figure 25: Resin-rich area from 3D (8325 x 2600x 1100 micron) volume of Section-H

CHAPTER 5
CONCLUSION AND RECOMMENDATIONS

As for the conclusion, the main objective of this project have been achieved which is to generate the three dimensional image of microstructures. Both images from 5X magnification and 50X magnification have been successfully developed and reconstructed into 3D volume by using ImageJ computer software program.

Also, proper processes and procedures to generate these 3D volumes have been established by the author in **Methodology Section 3.2 Project Activities**. Besides, some features and characteristics of CFRP which are the inclination angle measurements and fiber-rich areas have also been discussed by the author in this report.

For mounting process, it is advised to blend the mixture of resin and hardener more gently in order to avoid air to be trapped inside the mounting. Otherwise, vacuum can be used to remove the entrapped air. The ratio of mixture must be followed correctly which is five parts resin to one part hardener and the mixture must be blended completely. This is to prevent defects such as cracking and soft mounts to occur. Last but not least, the container should be tightly sealed to divert discoloring.

During polishing, it is necessary to grind both surfaces until become flat surface in order to ensure the sample can manage to stand still. Thus, errors can be avoided during the measuring and acquiring image process by using optical microscope. For silicon carbide disk, steady stream of water will facilitate the polishing process and it is important to always ultrasonically clean samples between polishing steps to minimize contaminations.

As for measuring process, the zero error of the micrometer should be recorded and the value need to be deducted then with the readings obtained in order to get the actual depth of the removal rate. Also, the thimble should not be rotated more after its anvil and spindle have reached the surface of the material as this will damage the

device itself. It is just necessary to rotate the ratchet until 3 clicks are heard when the surface of material has touched the anvil and spindle surface.

Usually, the measurement of material removal rate is done based on fiducial marks. However, using fiducial marks on CFRP is not applicable due to the elasticity of this material. The fibers tend to get back to their earlier shape after the indenter is removed. The mark still can be seen but not in the desired shape which can be used to calculate the depth of material removed. Thus, micrometer is chosen in this project in order to measure the depth of removed material.

In acquiring 2D images, the optical microscope and the computer software are set with appropriate setting that is suitable with the material surface. All settings need to be saved and make sure to use the same settings when recording the next number of layers. All layers should be used in the same settings of optical microscope and computer software program in order to synchronize the colors and appearance of the images taken. Hence, the process of 3D reconstruction by ImageJ would be easier.

REFERENCES

1. M. V. Kral, M.A. Mangan, R.O. Rosenberg and G. Spanos, 1999, *THREE DIMENSIONAL ANALYSIS OF MICROSTRUCTURES,* University of Canterbury, Department of Mechanical Engineering, Christchurch, New Zealand, Naval Research Laboratory, Physical Metallurgy Branch, Washington, DC 20375, Naval Research Laboratory, Scientific Visualization Laboratory, Washington, DC 20375.

2. D. Kopeliovich, 1st June 2010, *Carbon Fiber Reinforced Polymer Composites,* http://www.substech.com/dokuwiki/doku.php?id=carbon_fiber_reinforced_polymer_composites

3. M.V. Kral, Gene Ice and M.K. Miller, M.D. Uchic, R.O. Rosenberg, 2004, *Three-Dimensional Microscopy*, University of Canterburry, Christchurch, New Zealand, Oak Ridge National Laboratory, Wright-Petterson Air Force Research Laboratory, Naval Research Laboratory.

4. B. Wunsch and N. Chawla, 2003, *Serial Sectioning for 3D Visualization and Modeling of SiC Particle Reinforced Aluminum Composites*, Department of Chemical and Material Engineering, Arizona State University, Tempe, AZ 85287-6006.

5. Cornelius A. Johnson, 1977, *Metallography Principles and Procedures Leco Corporation,* LECO CORPORATION, 3000 Lakeview Ave., St. Joseph, MI 49085,U.S.A.

APPENDICES

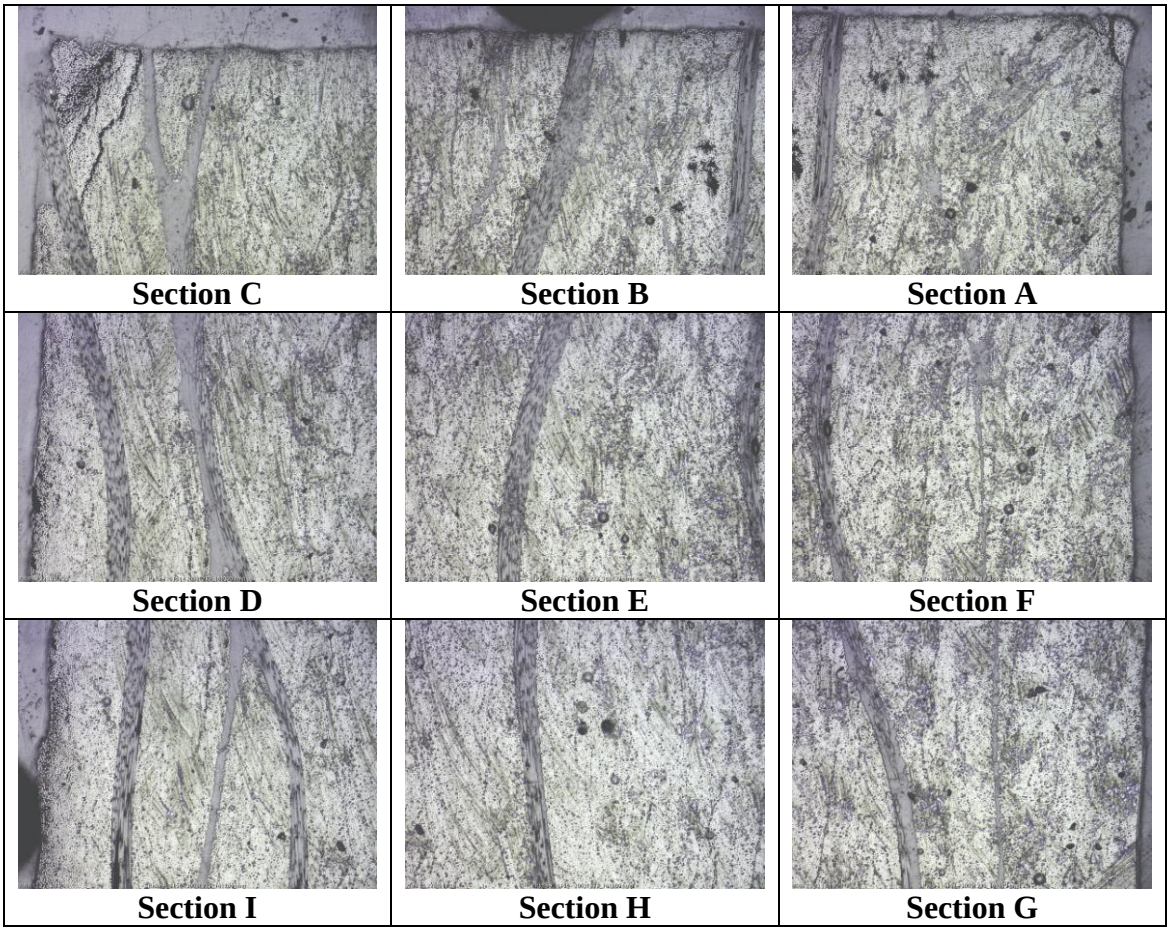

Figure 26: 9 sections of 2D images from the specimen with 5X magnification (1st layer)

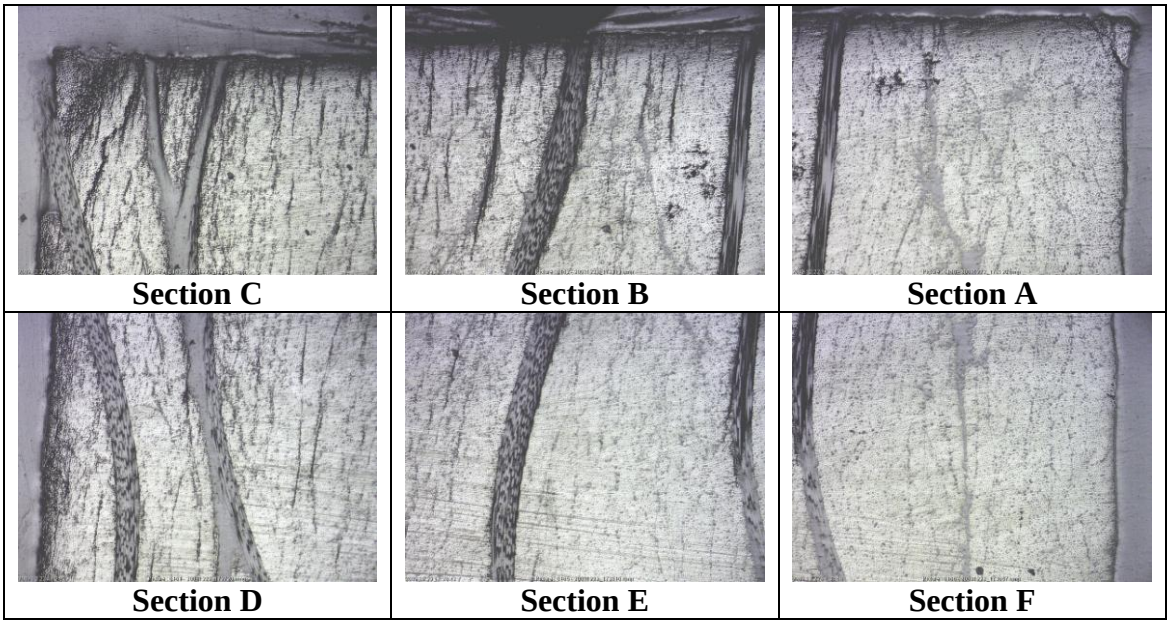

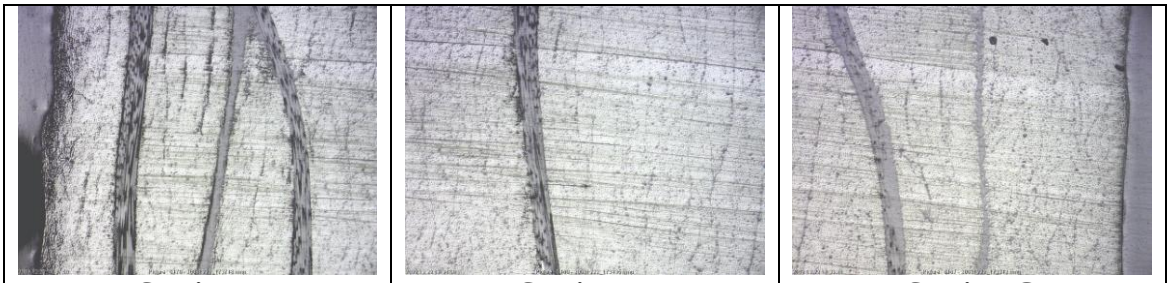

Section I	Section H	Section G

Figure 27: 9 sections of 2D images from the specimen with 5X magnification (2nd layer)

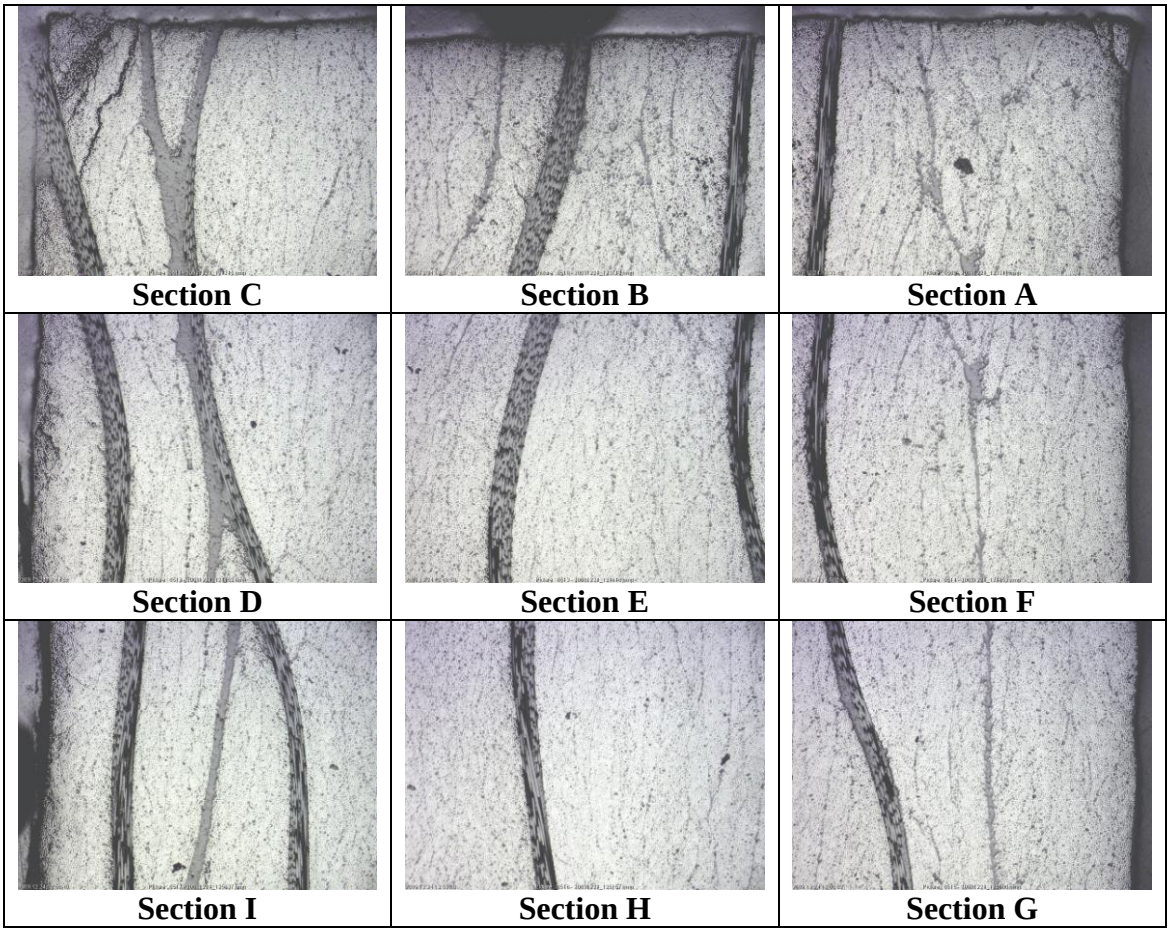

Section C	Section B	Section A
Section D	Section E	Section F
Section I	Section H	Section G

Figure 28: 9 sections of 2D images from the specimen with 5X magnification (3rd layer)

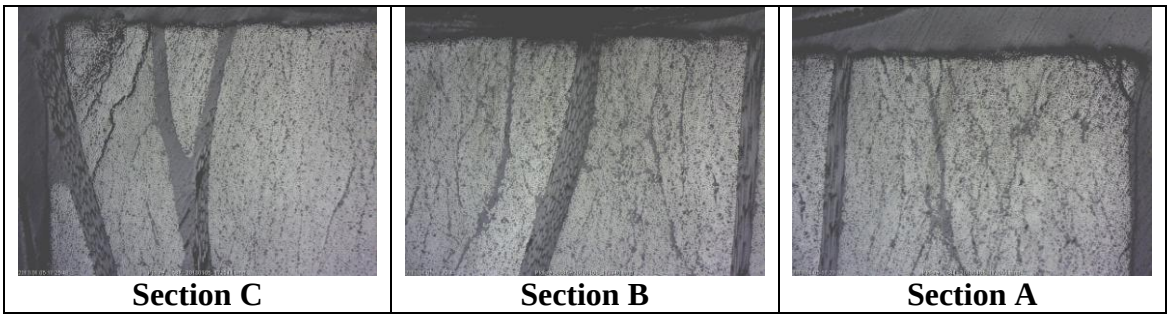

Section C	Section B	Section A

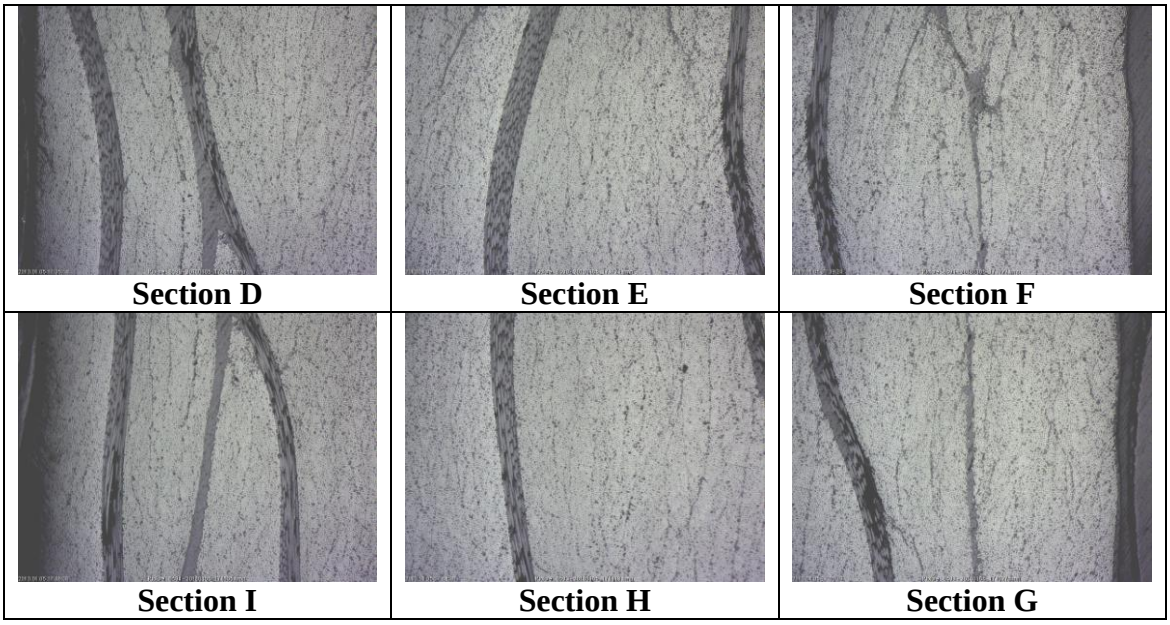

Figure 29: 9 sections of 2D images from the specimen with 5X magnification (4th layer)

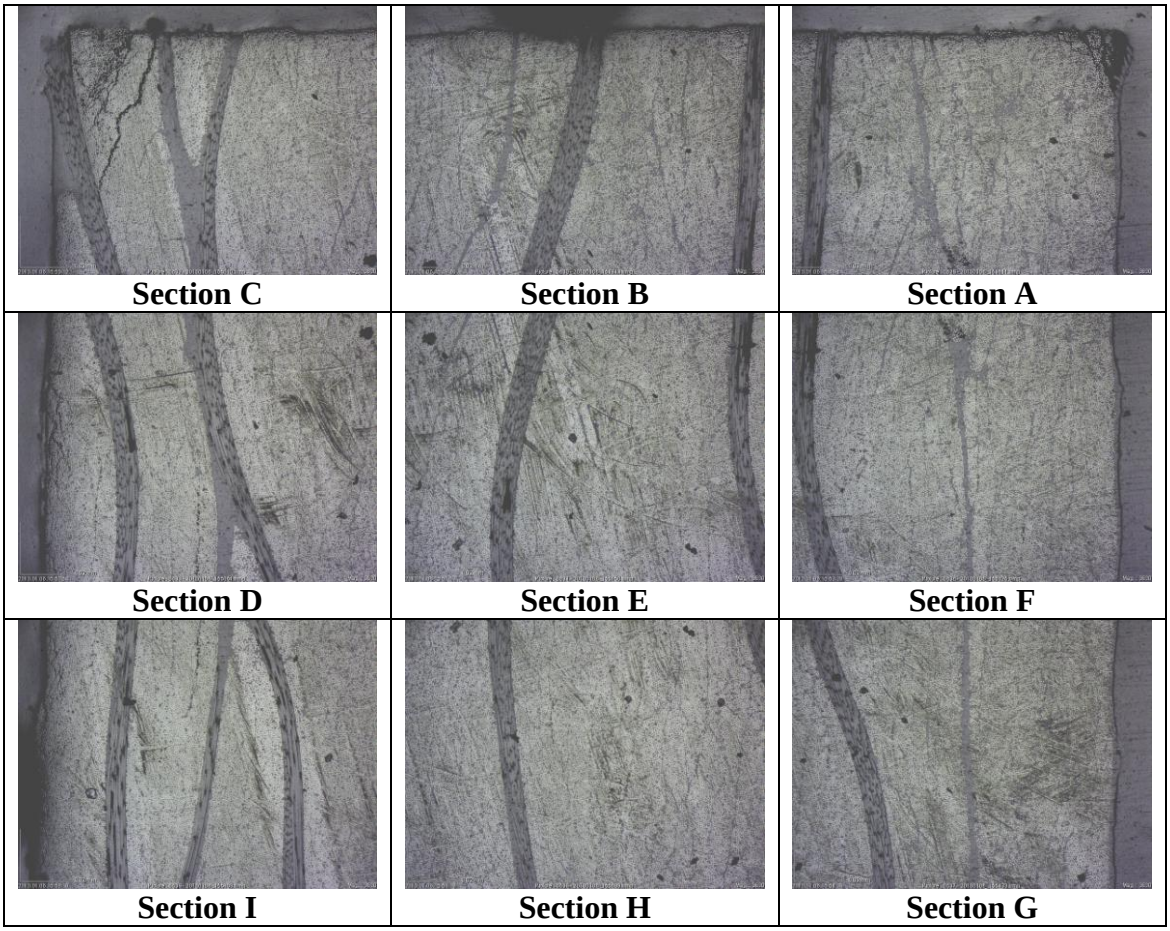

Figure 30: 9 sections of 2D images from the specimen with 5X magnification (5th layer)

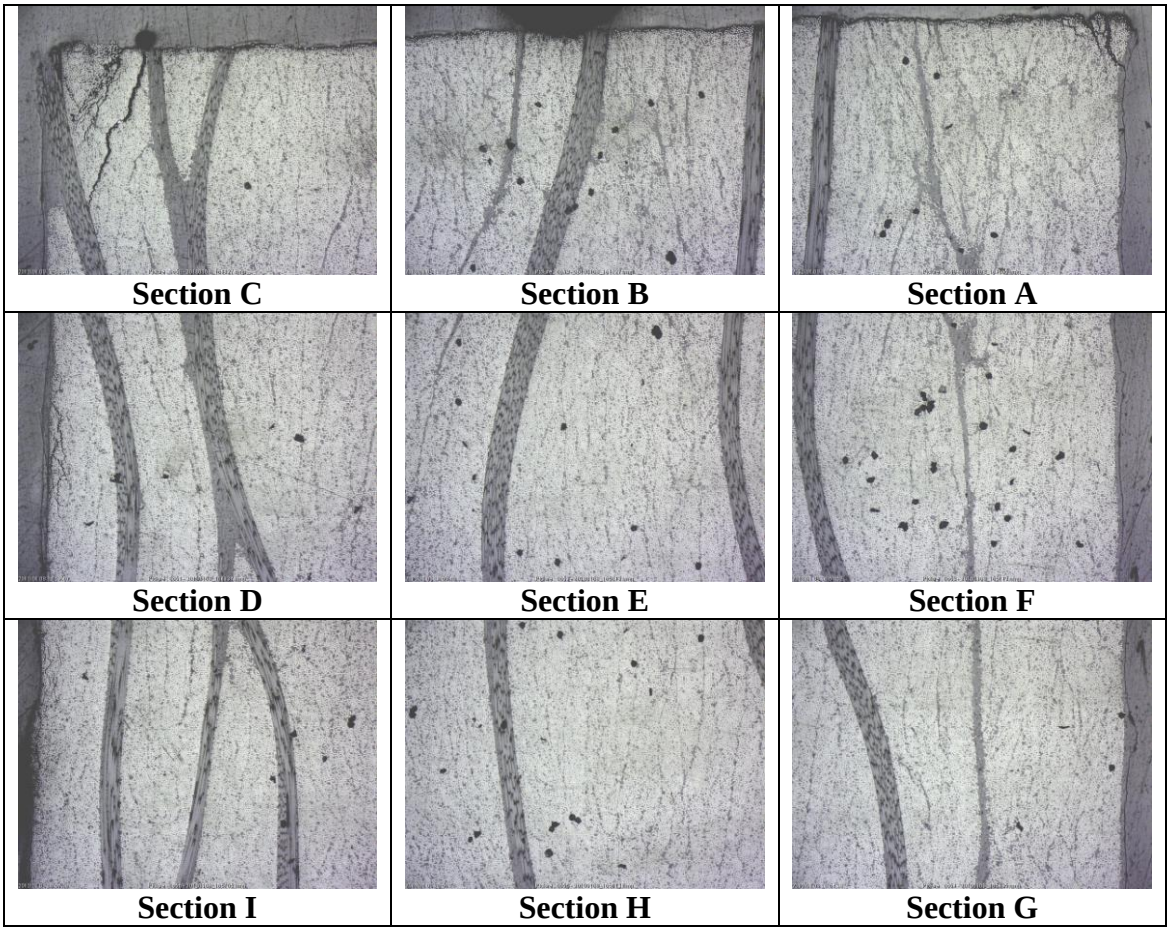

Figure 31: 9 sections of 2D images from the specimen with 5X magnification (6th layer)

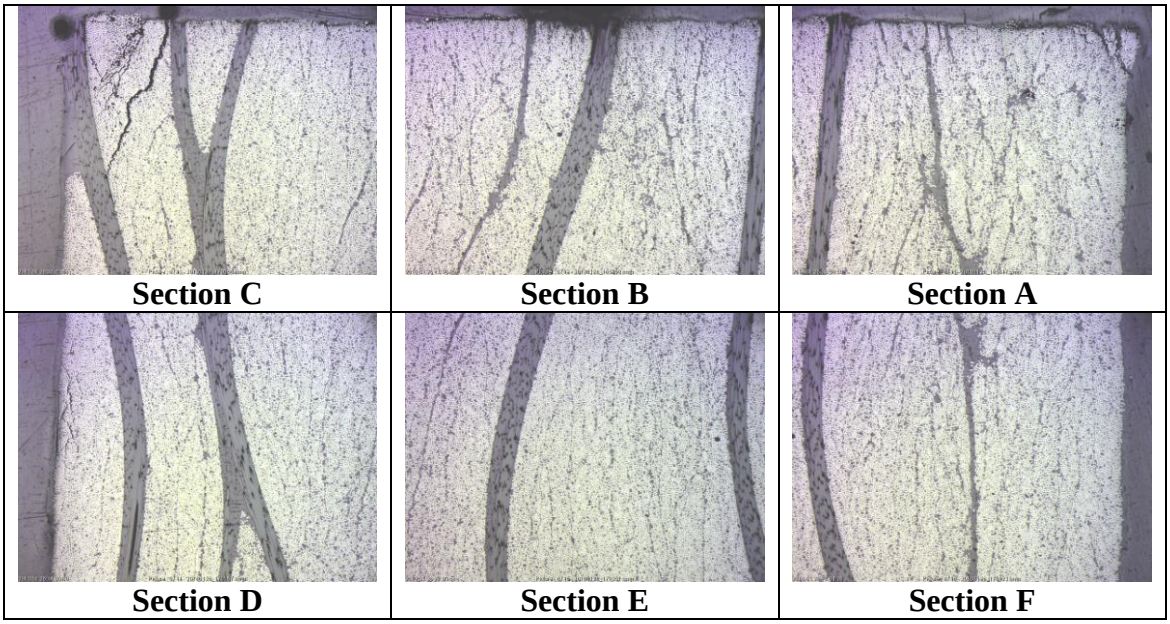

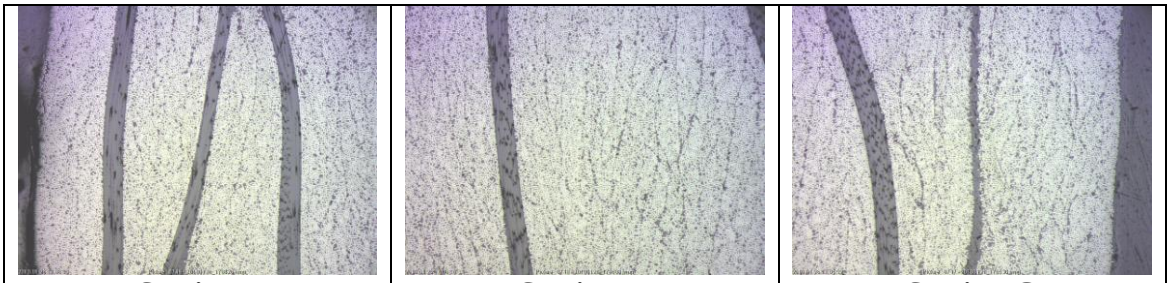

Section I	Section H	Section G

Figure 32: 9 sections of 2D images from the specimen with 5X magnification (7th layer)

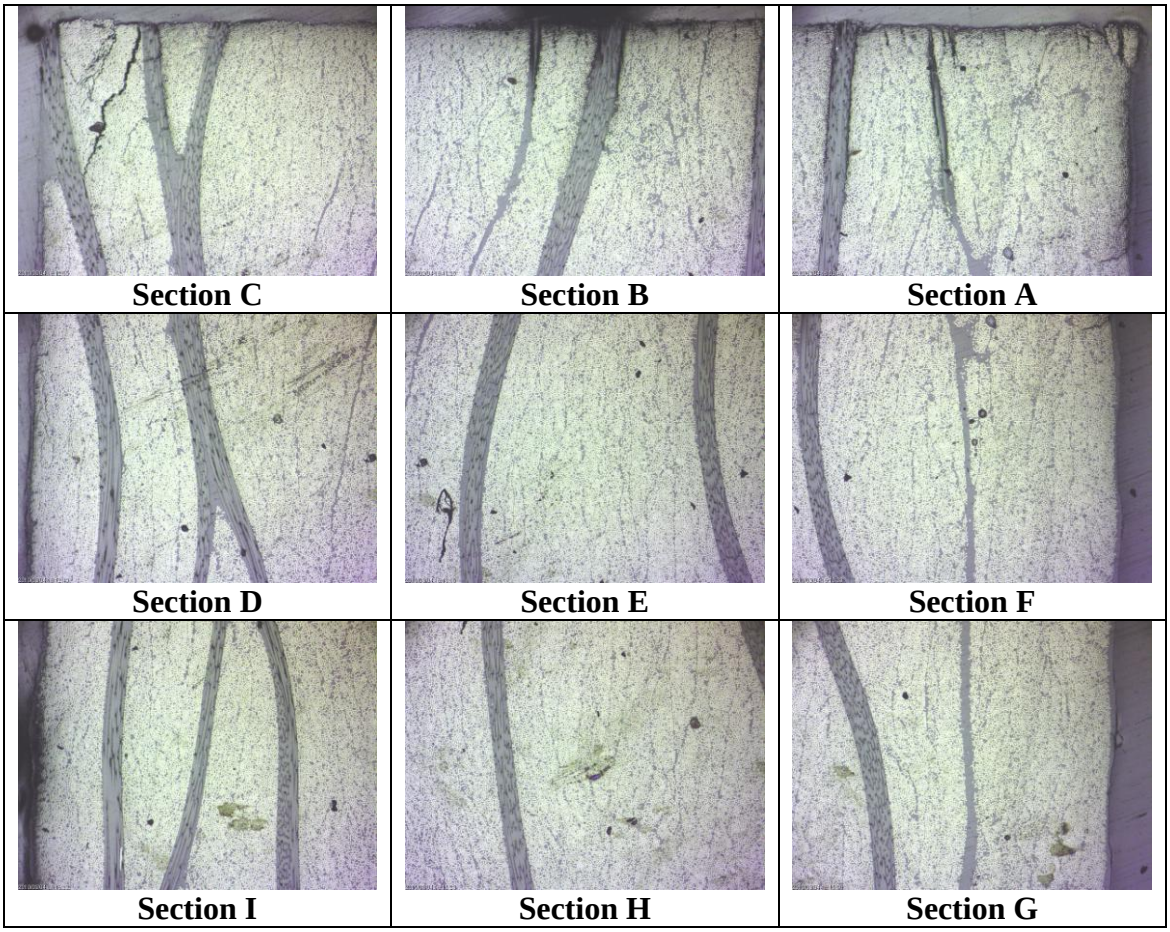

Section C	Section B	Section A
Section D	Section E	Section F
Section I	Section H	Section G

Figure 33: 9 sections of 2D images from the specimen with 5X magnification (9th layer)

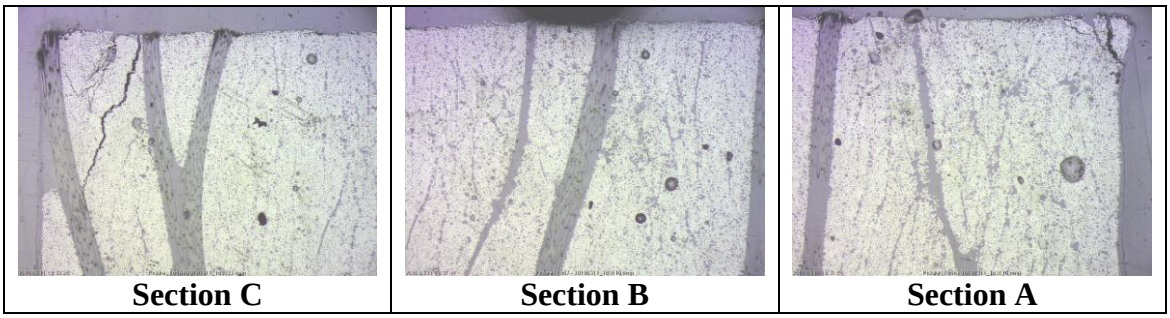

Section C	Section B	Section A

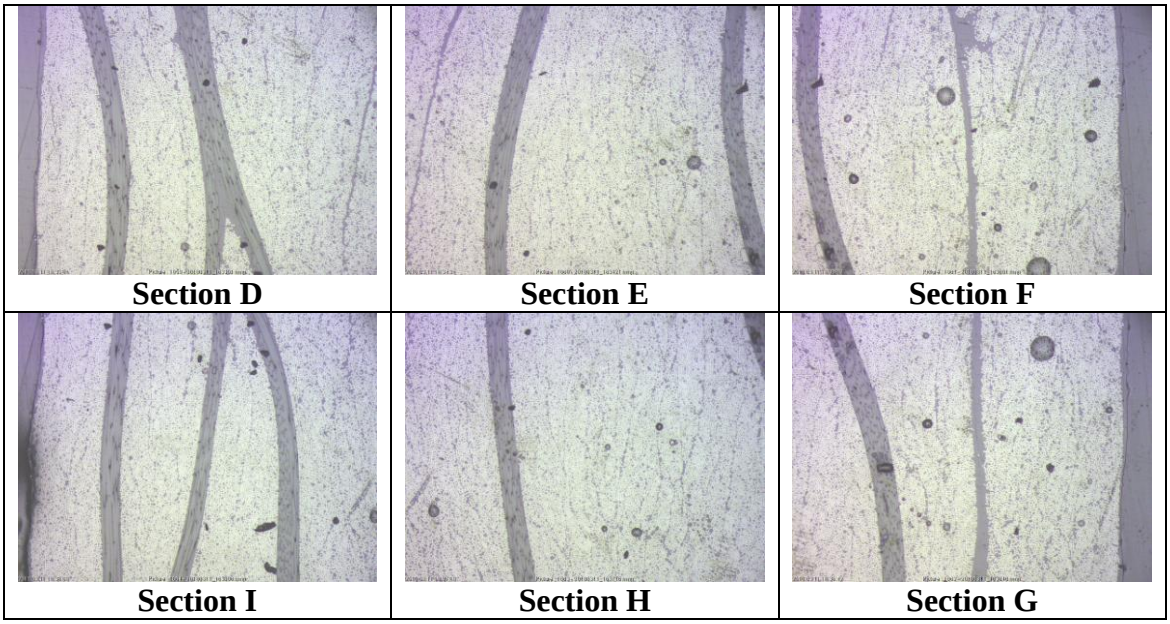

Figure 34: 9 sections of 2D images from the specimen with 5X magnification (11th layer)

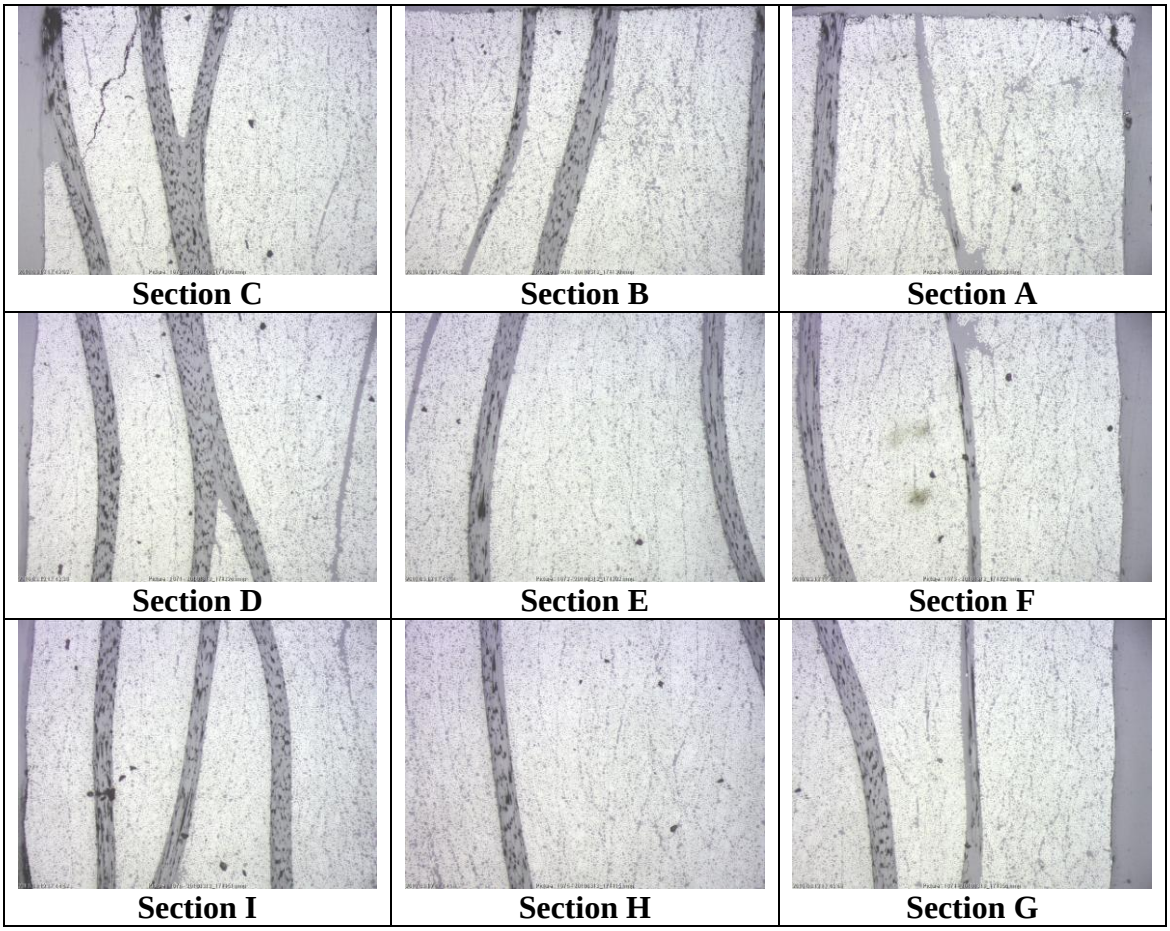

Figure 35: 9 sections of 2D images from the specimen with 5X magnification (12th layer)

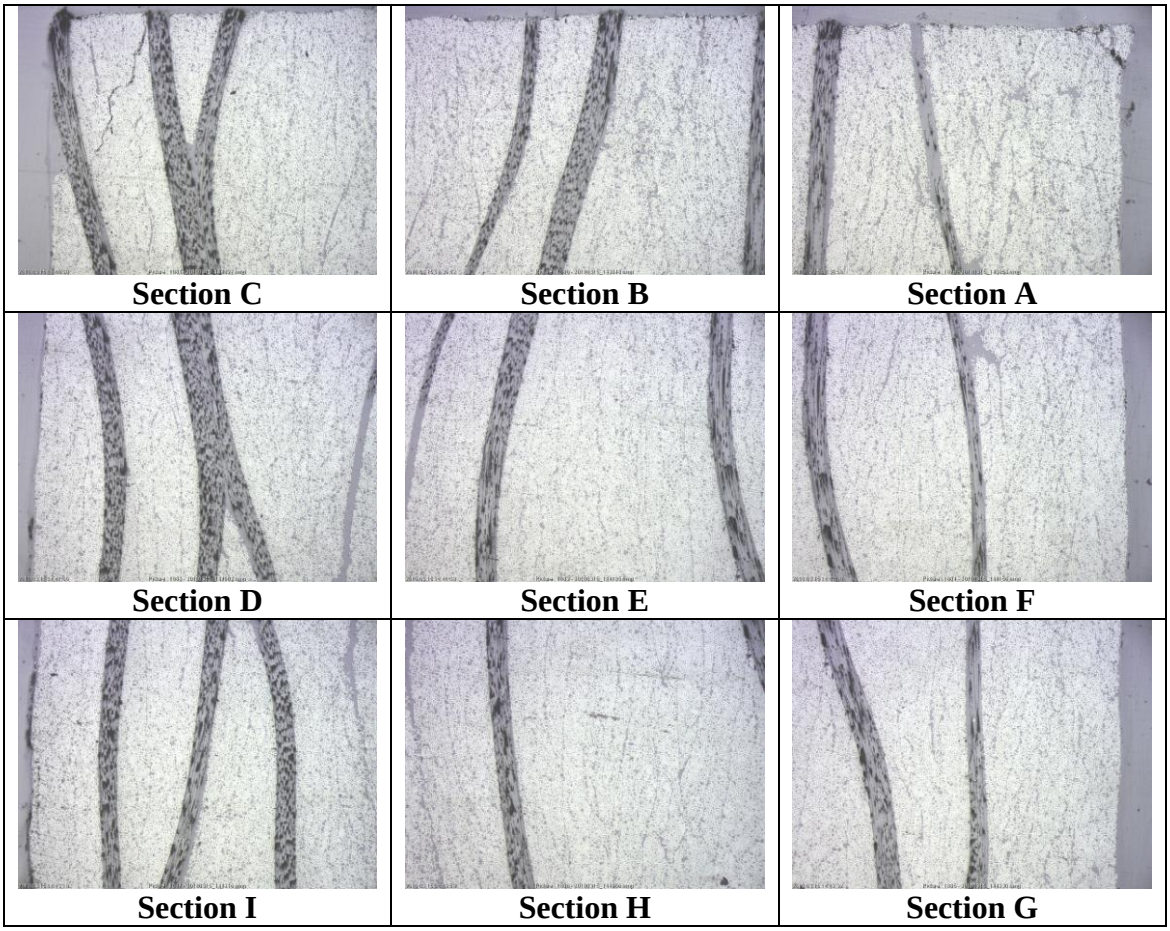

Figure 36: 9 sections of 2D images from the specimen with 5X magnification (13th layer)

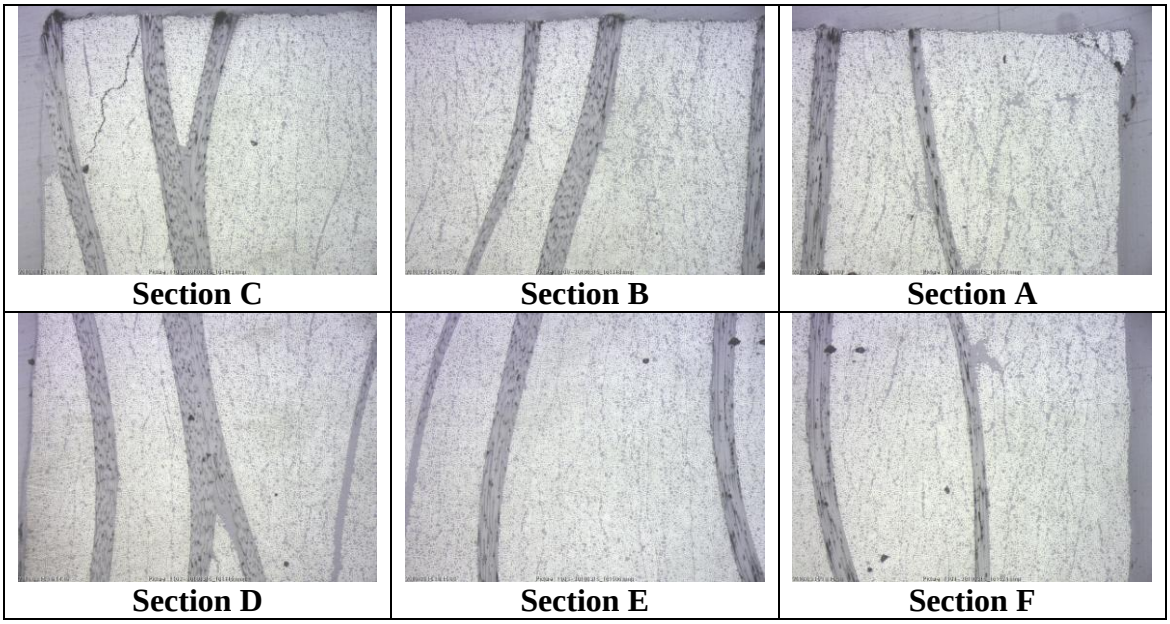

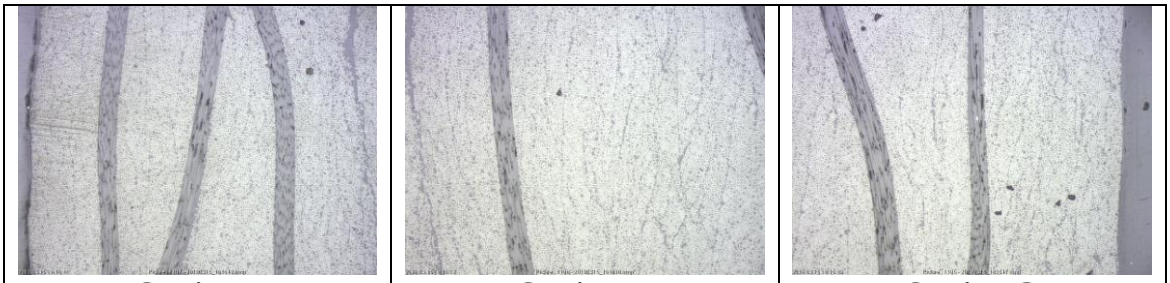

Section I	Section H	Section G

Figure 37: 9 sections of 2D images from the specimen with 5X magnification (14th layer)

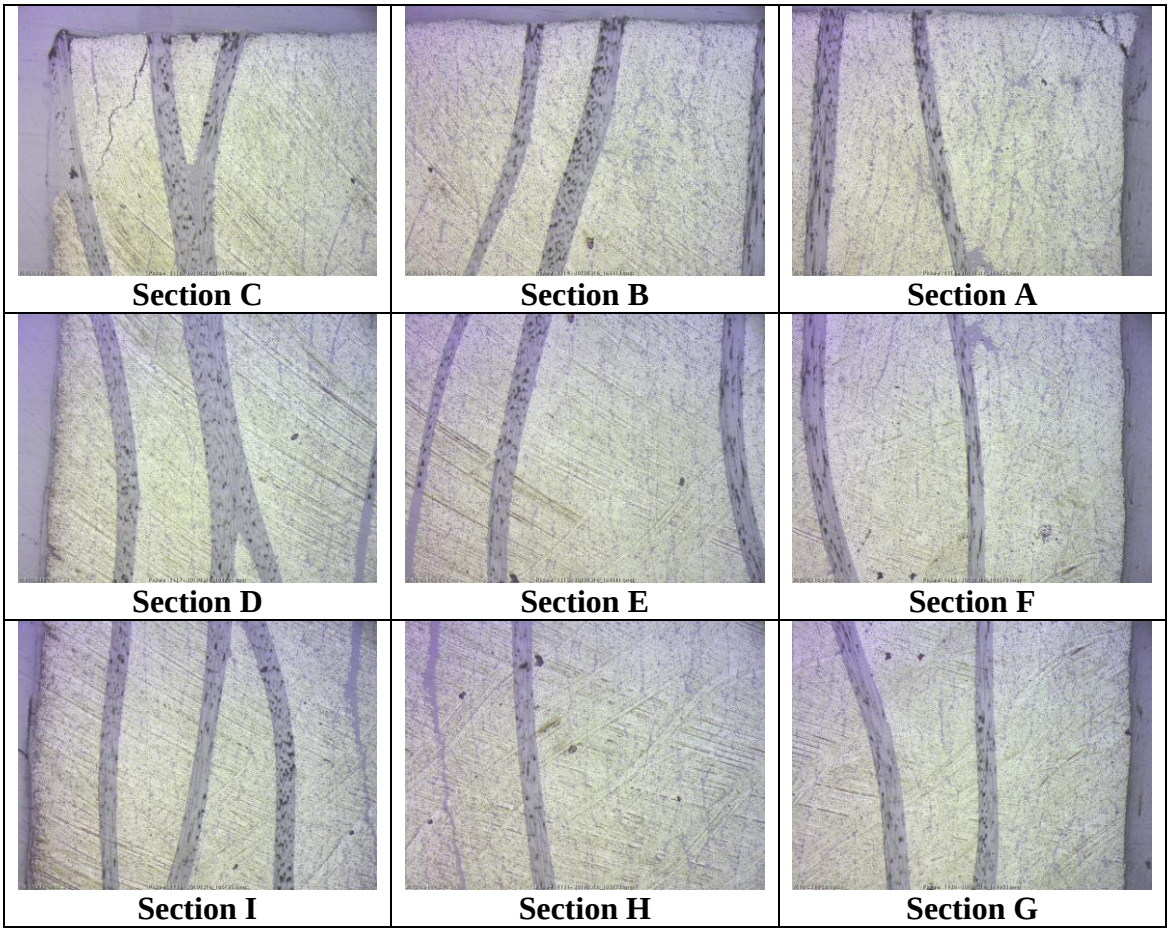

Section C	Section B	Section A
Section D	Section E	Section F
Section I	Section H	Section G

Figure 38: 9 sections of 2D images from the specimen with 5X magnification (15th layer)

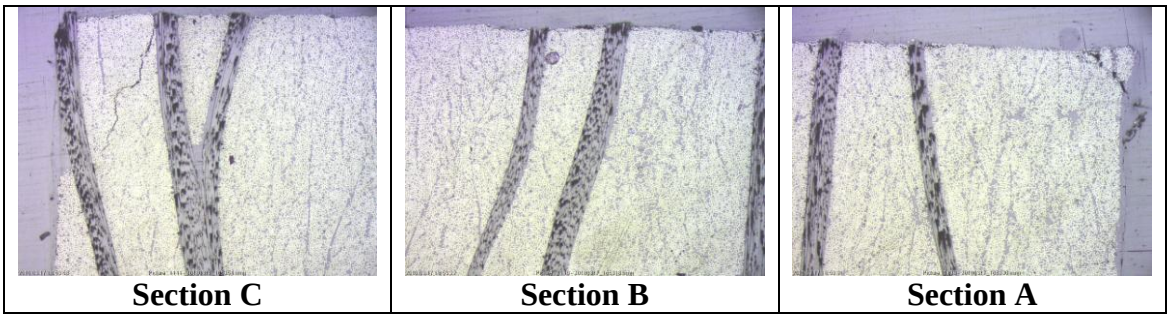

Section C	Section B	Section A

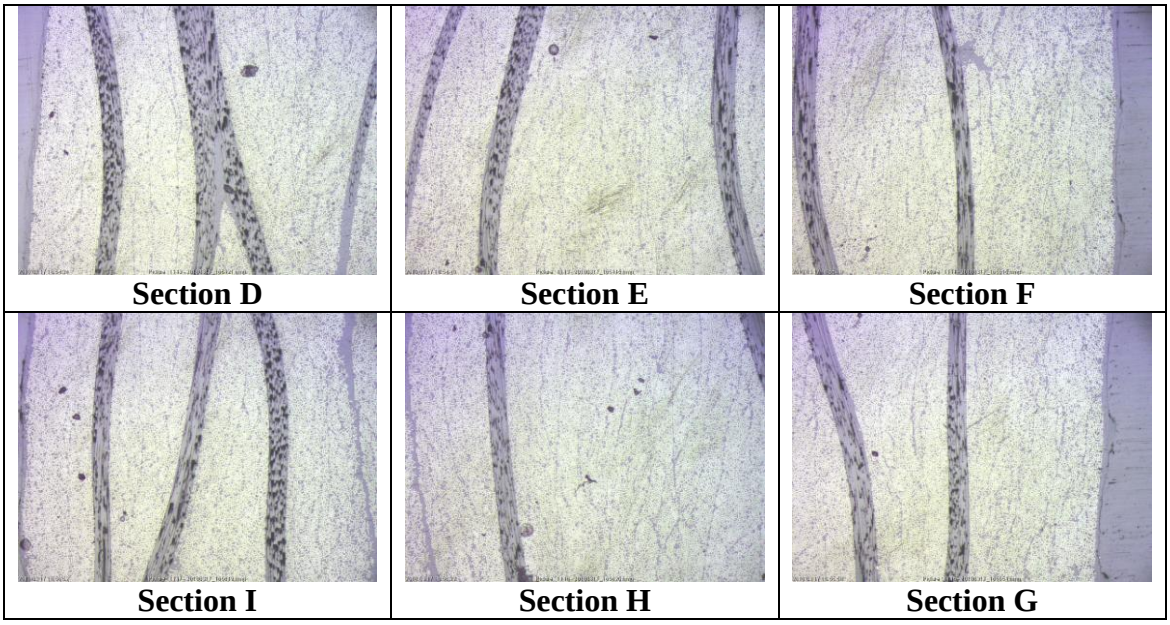

Figure 39: 9 sections of 2D images from the specimen with 5X magnification (second layer)

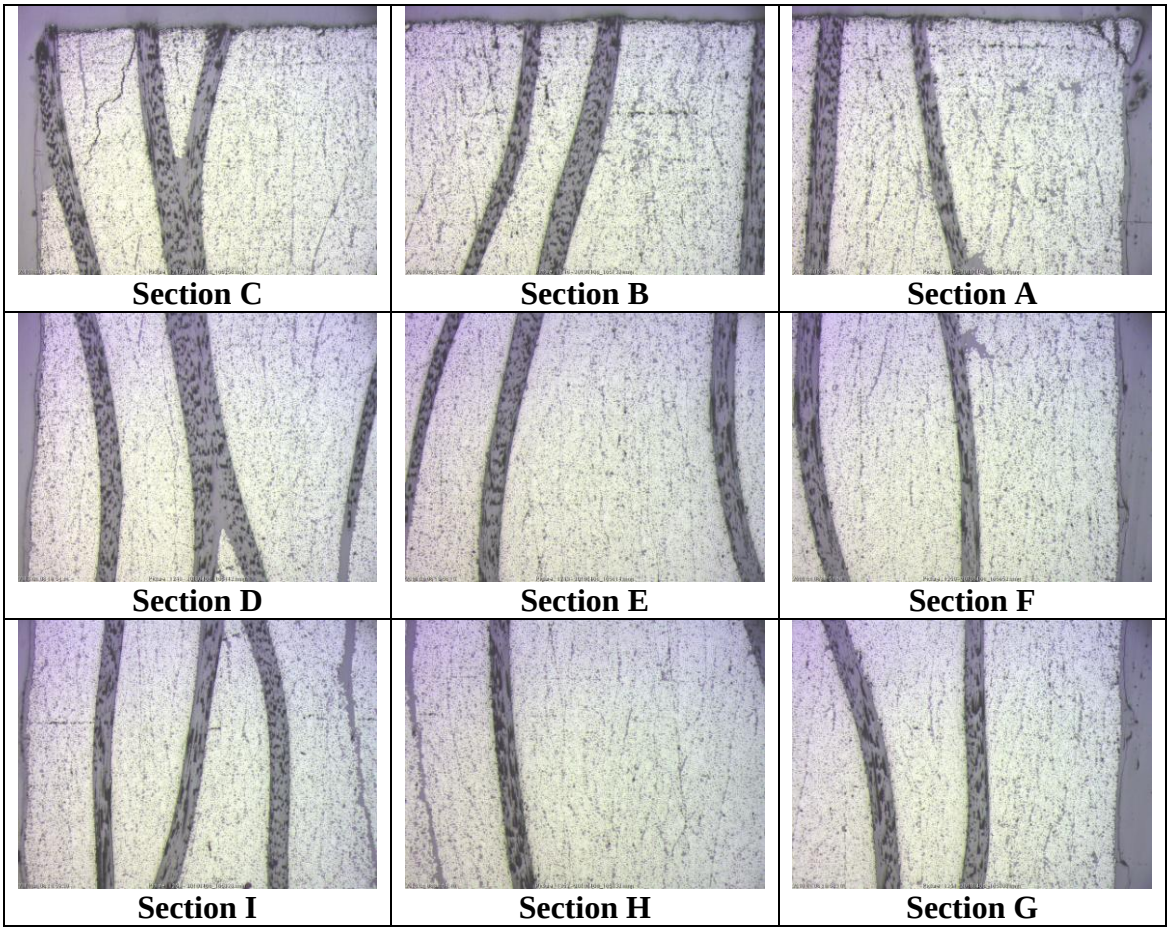

Figure 40: 9 sections of 2D images from the specimen with 5X magnification (17th layer)

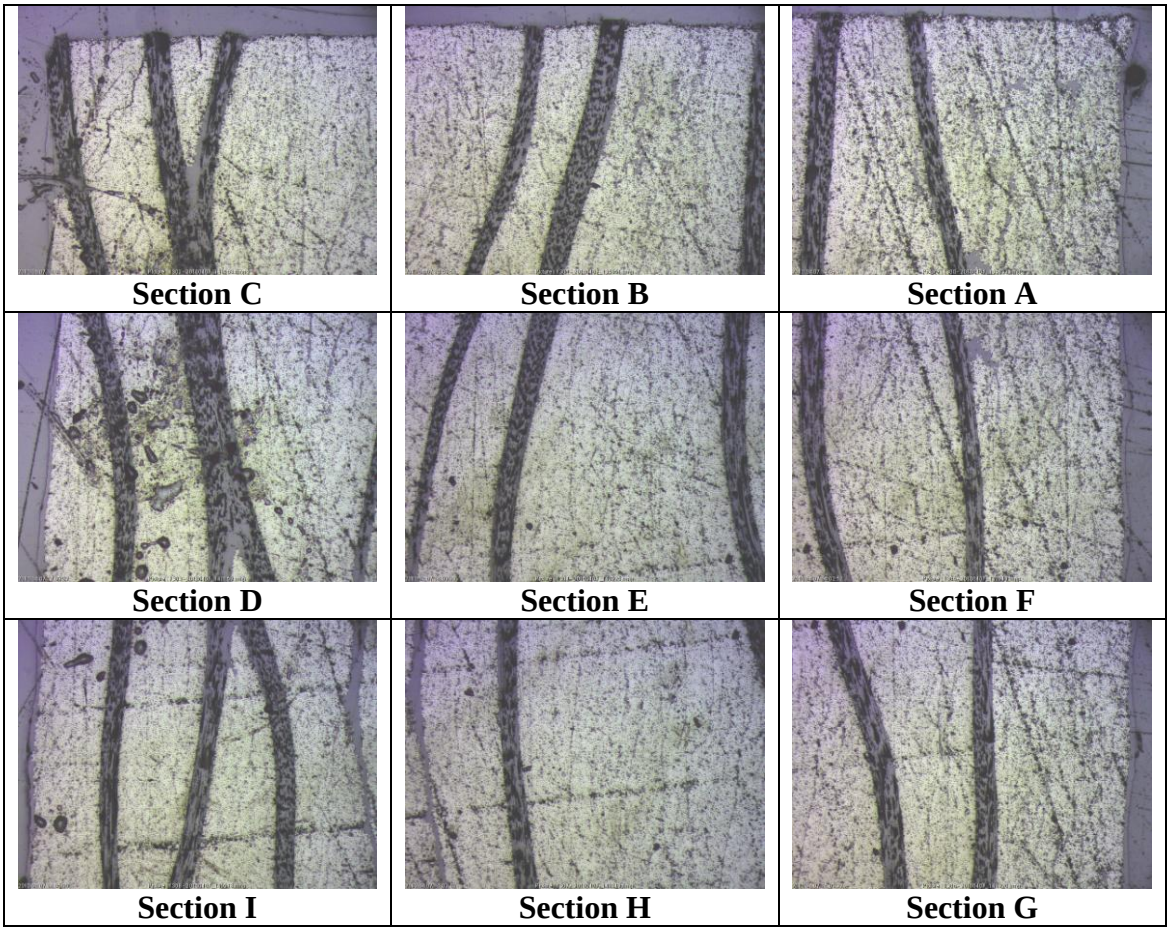

Figure 41: 9 sections of 2D images from the specimen with 5X magnification (18th layer)

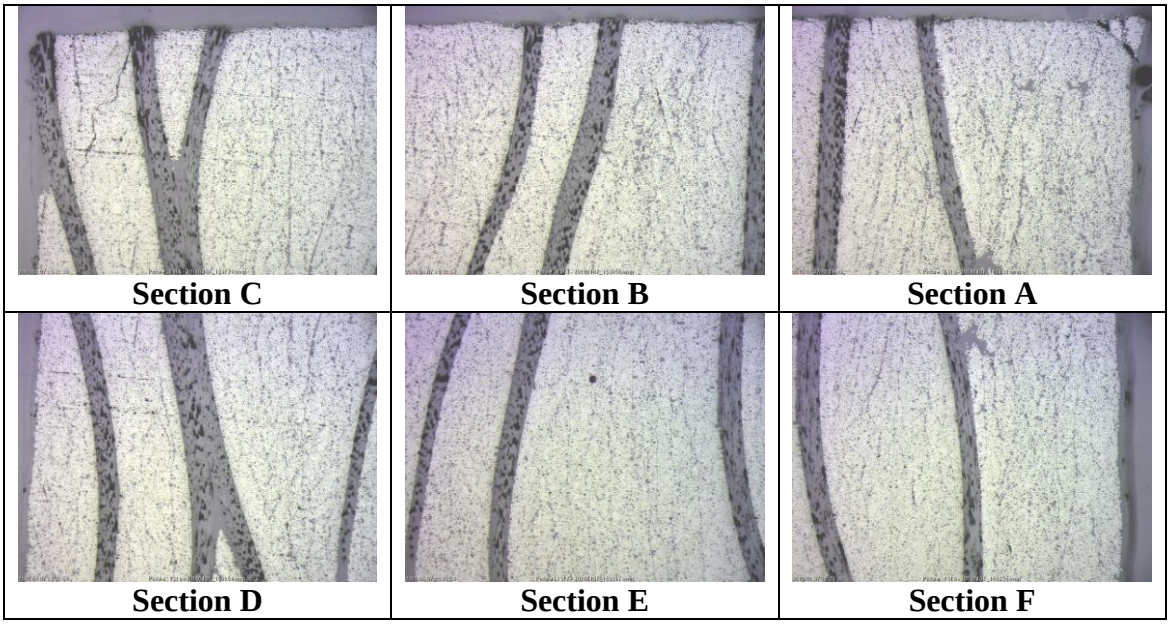

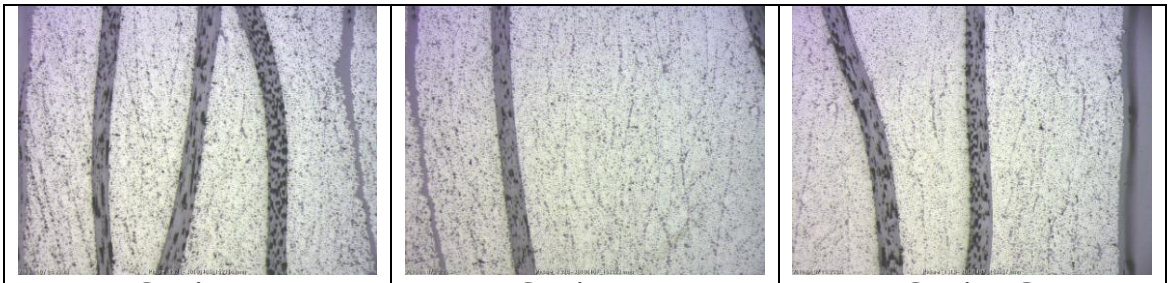

Section I	Section H	Section G

Figure 42: 9 sections of 2D images from the specimen with 5X magnification (19th layer)

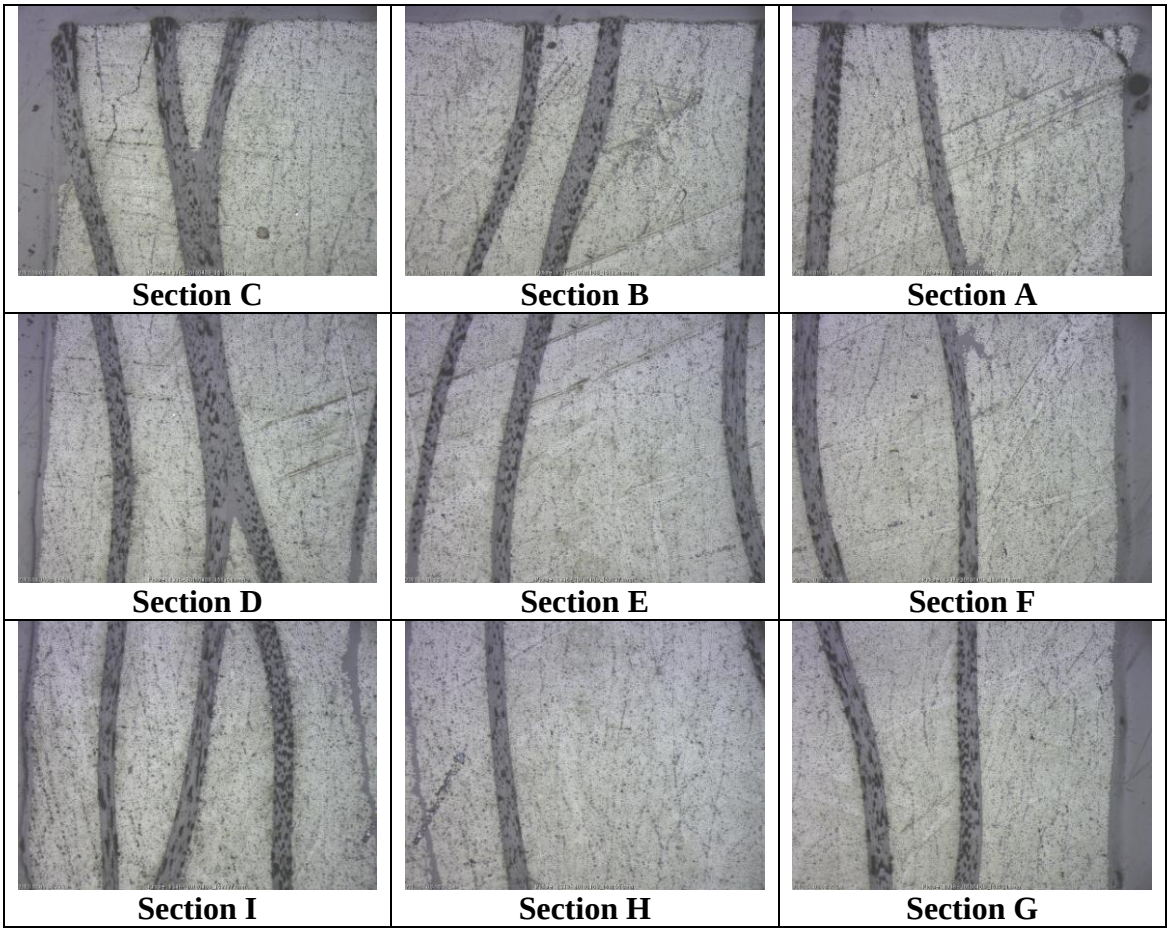

Section C	Section B	Section A
Section D	Section E	Section F
Section I	Section H	Section G

Figure 43: 9 sections of 2D images from the specimen with 5X magnification (20th layer)

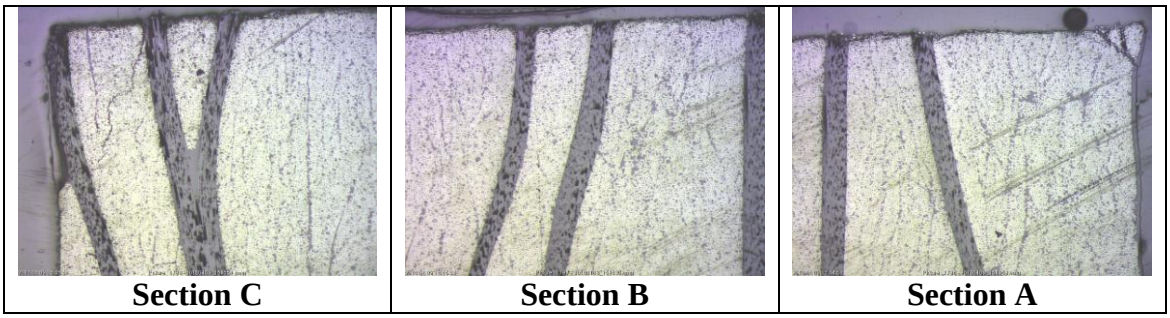

Section C	Section B	Section A

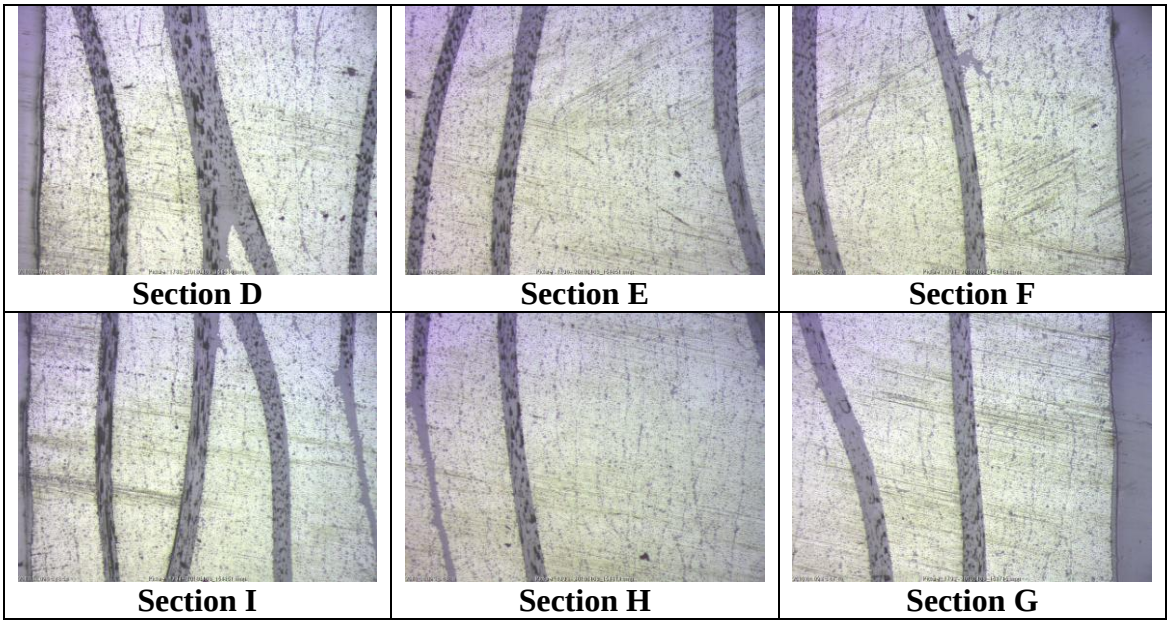

Figure 44: 9 sections of 2D images from the specimen with 5X magnification (21st layer)

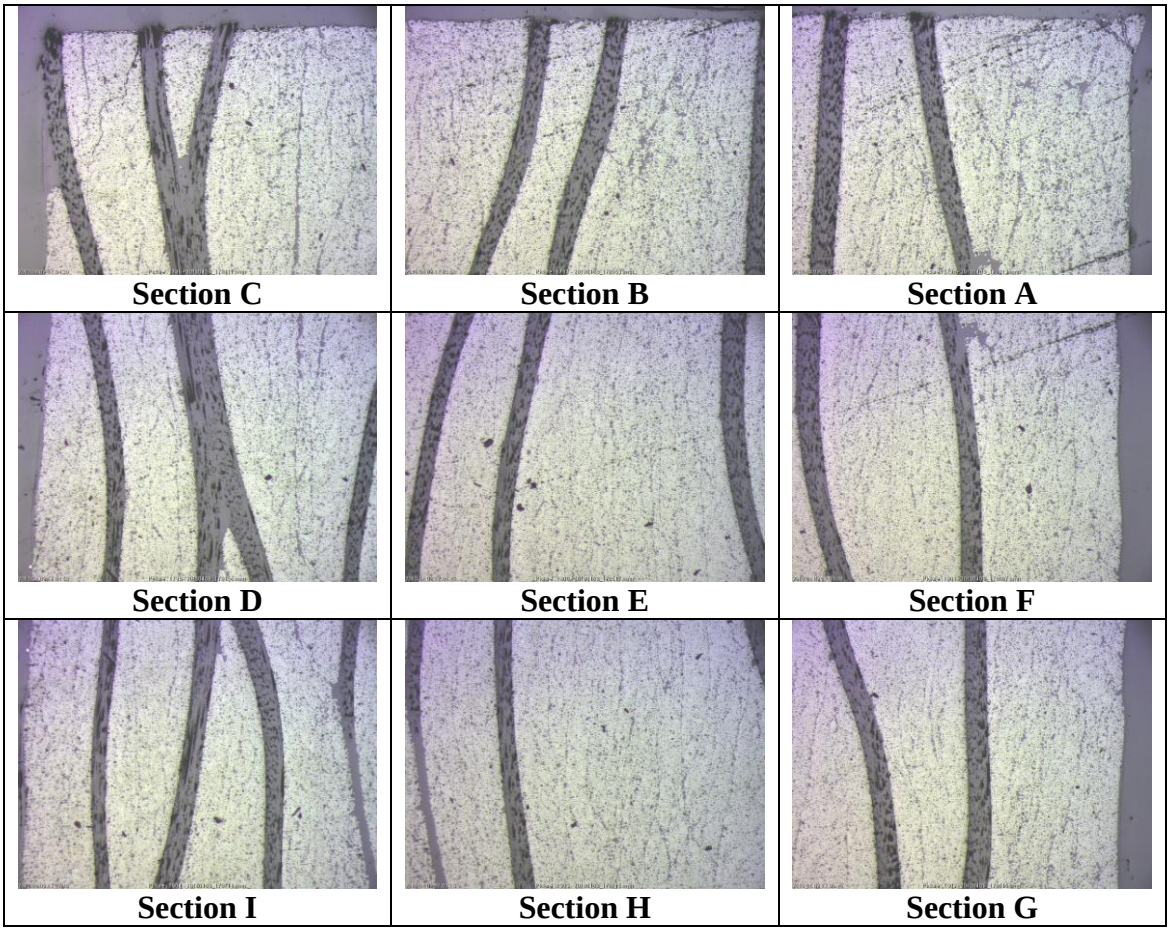

Figure 45: 9 sections of 2D images from the specimen with 5X magnification (22nd layer)

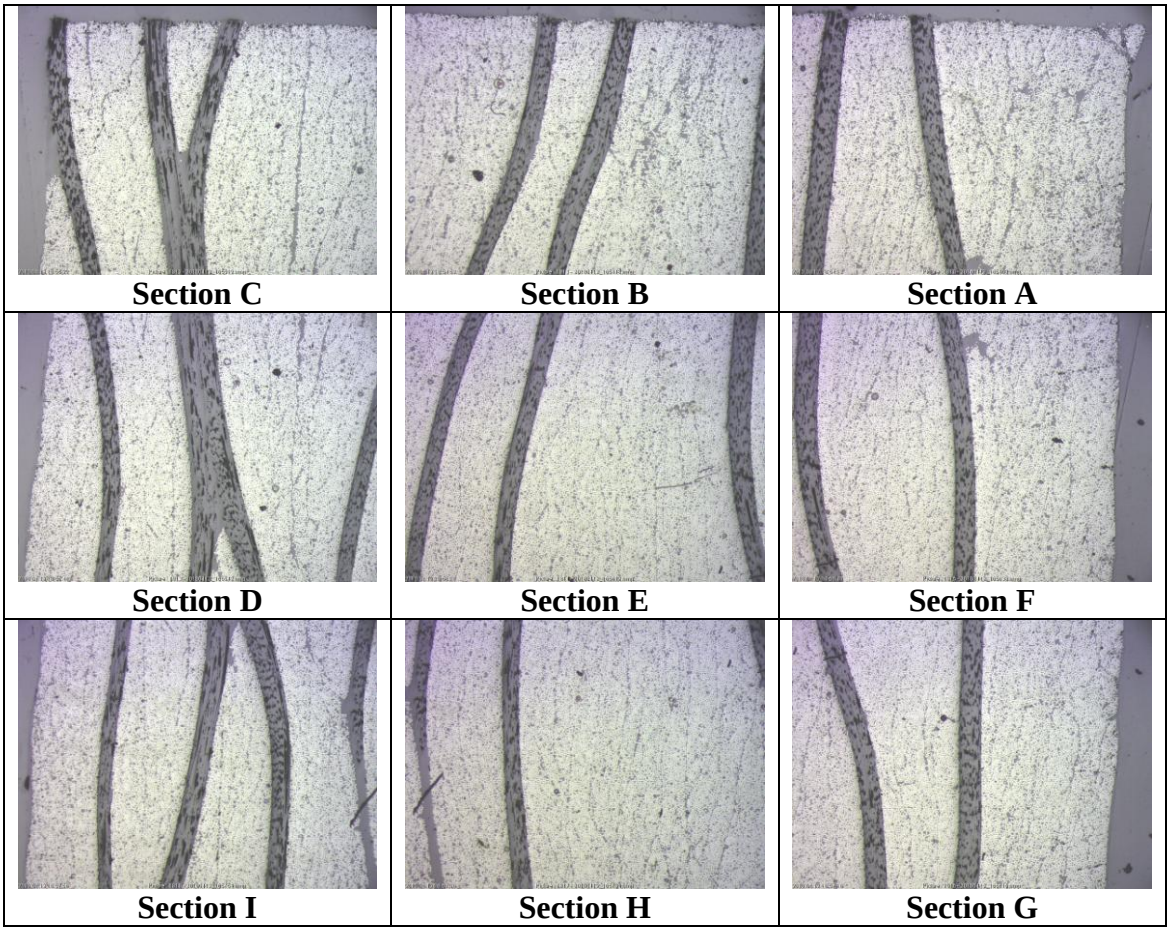

Figure 46: 9 sections of 2D images from the specimen with 5X magnification (23rd layer)

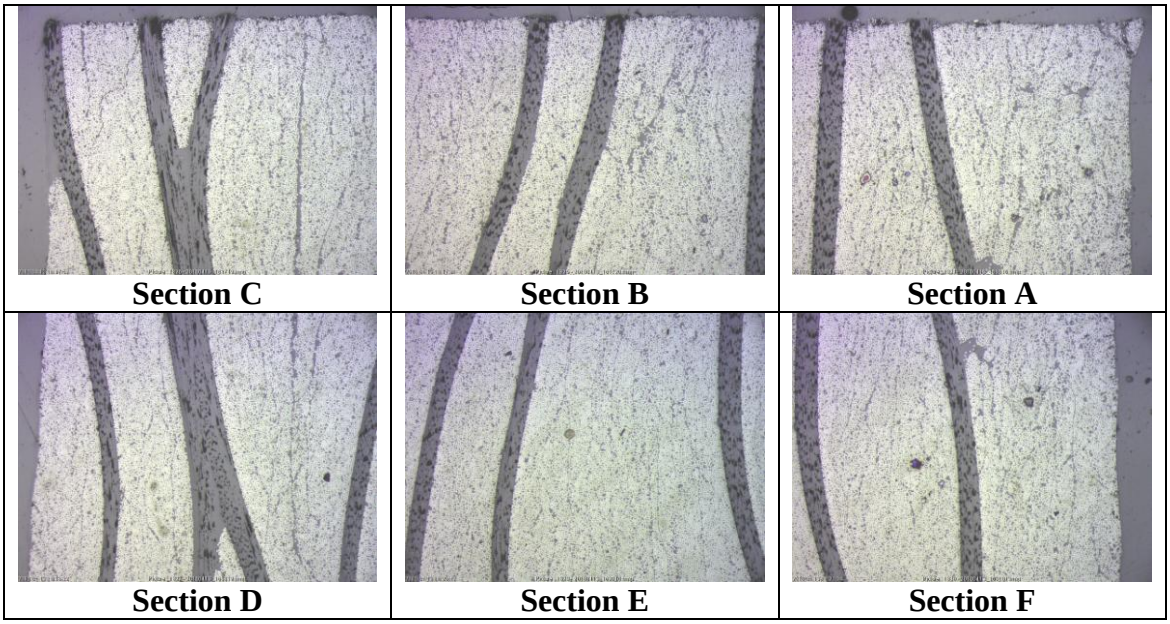

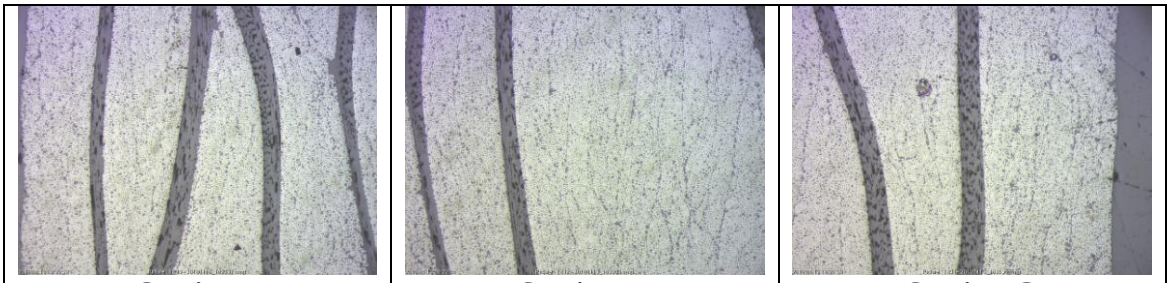

Section I	Section H	Section G

Figure 47: 9 sections of 2D images from the specimen with 5X magnification (24th layer)

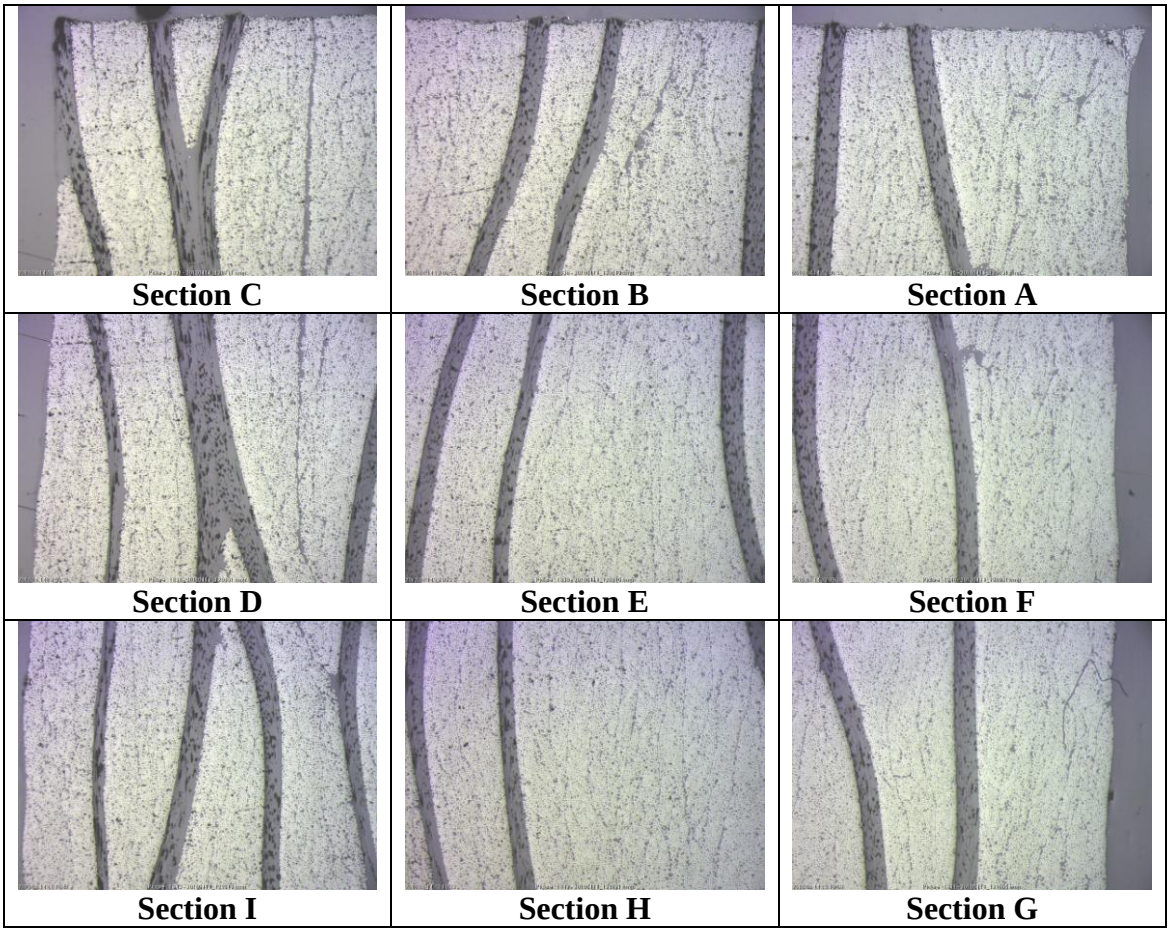

Section C	Section B	Section A
Section D	Section E	Section F
Section I	Section H	Section G

Figure 48: 9 sections of 2D images from the specimen with 5X magnification (25th layer)

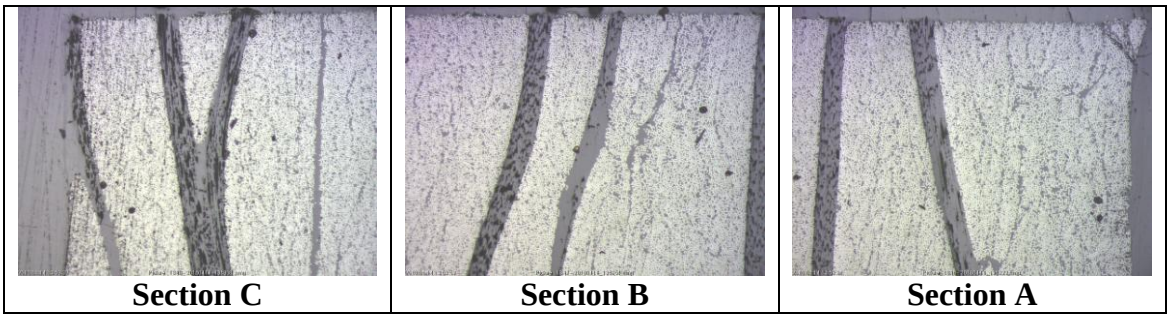

Section C	Section B	Section A

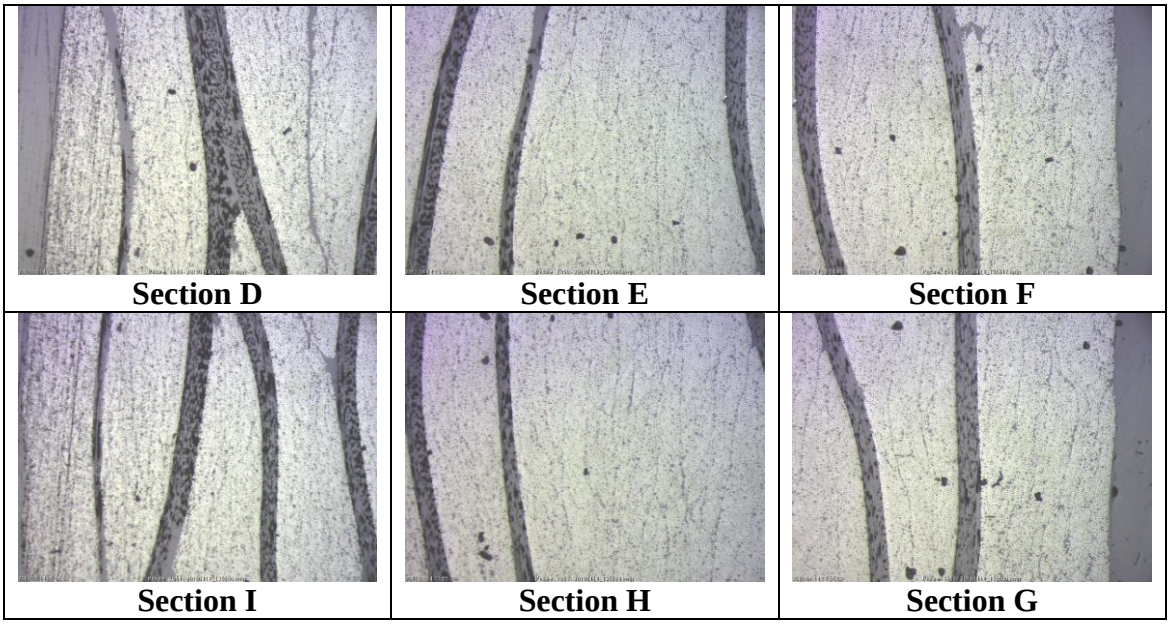

Figure 49: 9 sections of 2D images from the specimen with 5X magnification (26th layer)

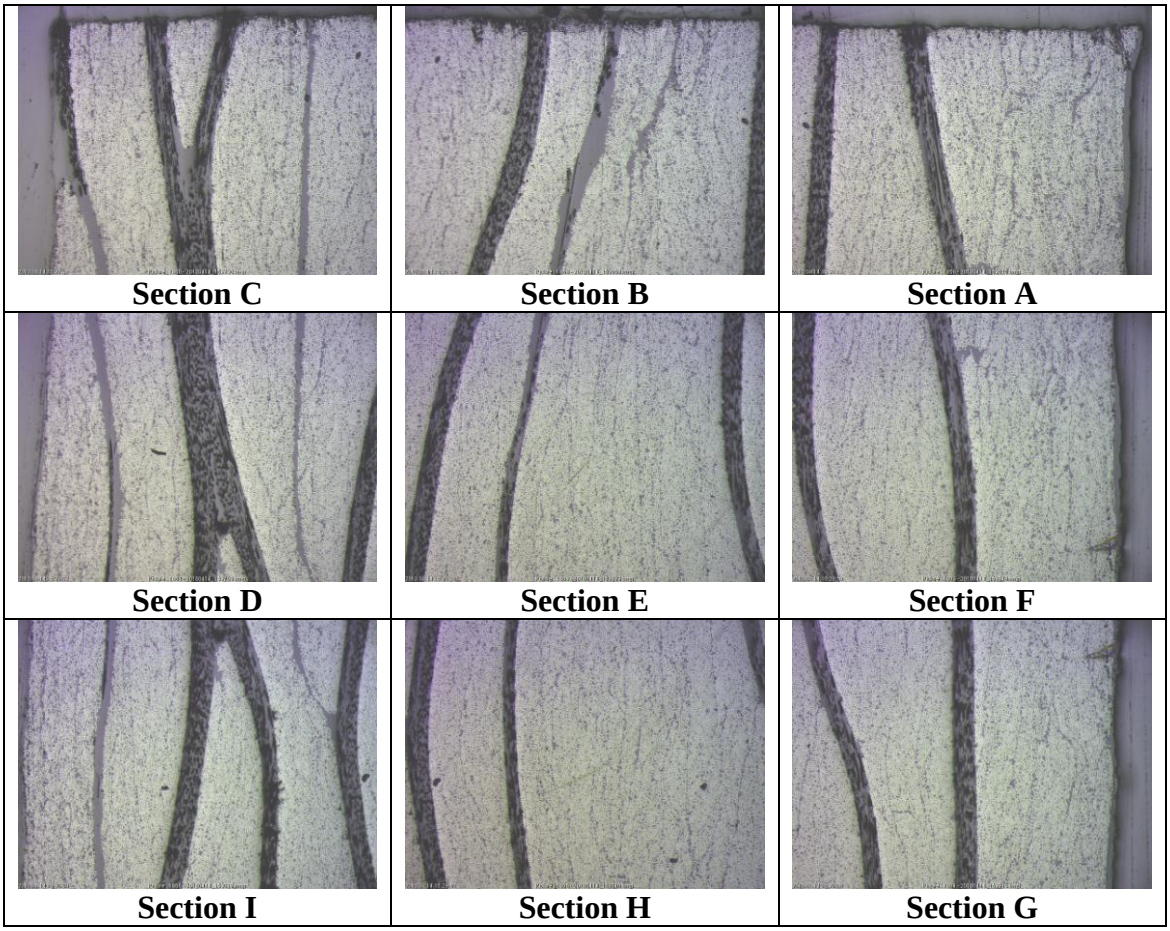

Figure 50: 9 sections of 2D images from the specimen with 5X magnification (27th layer)

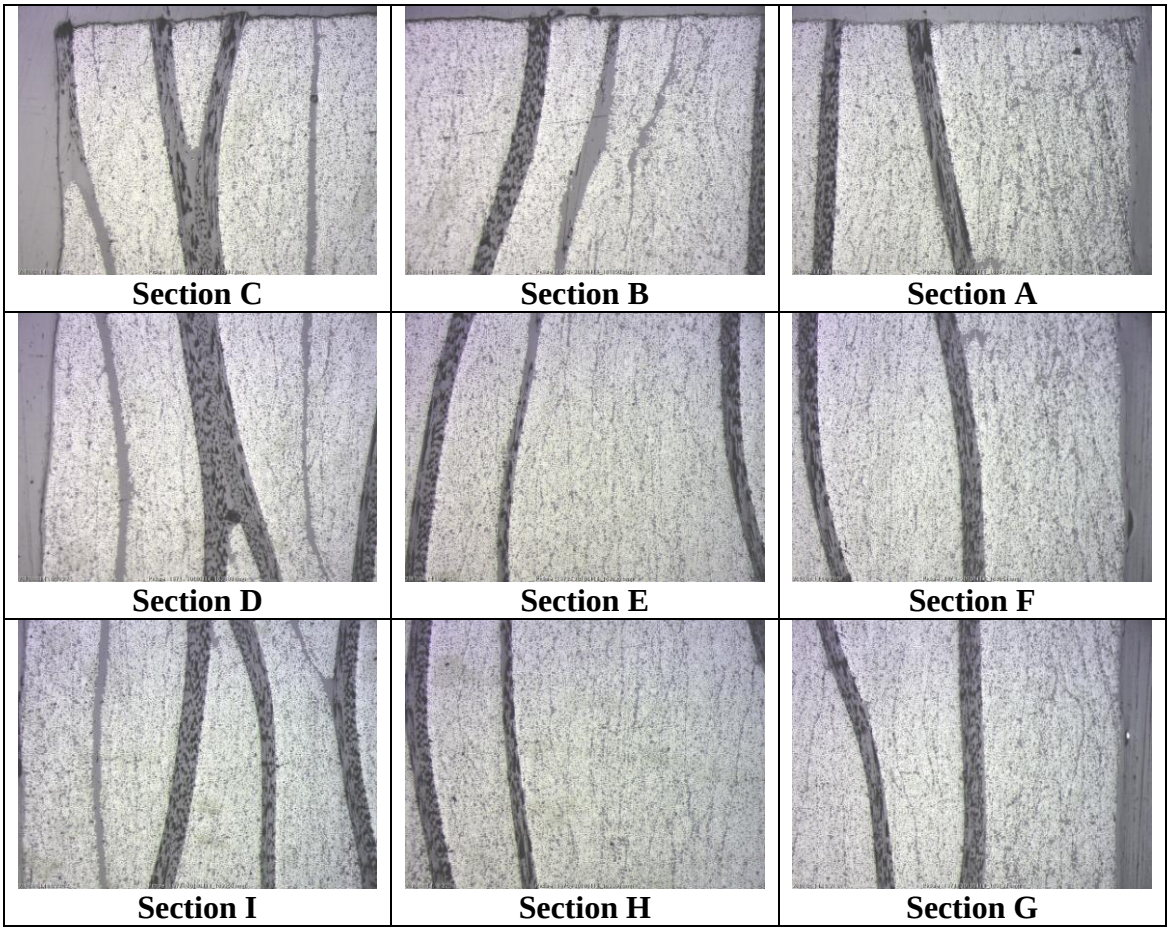

Figure 51: 9 sections of 2D images from the specimen with 5X magnification (28th layer)

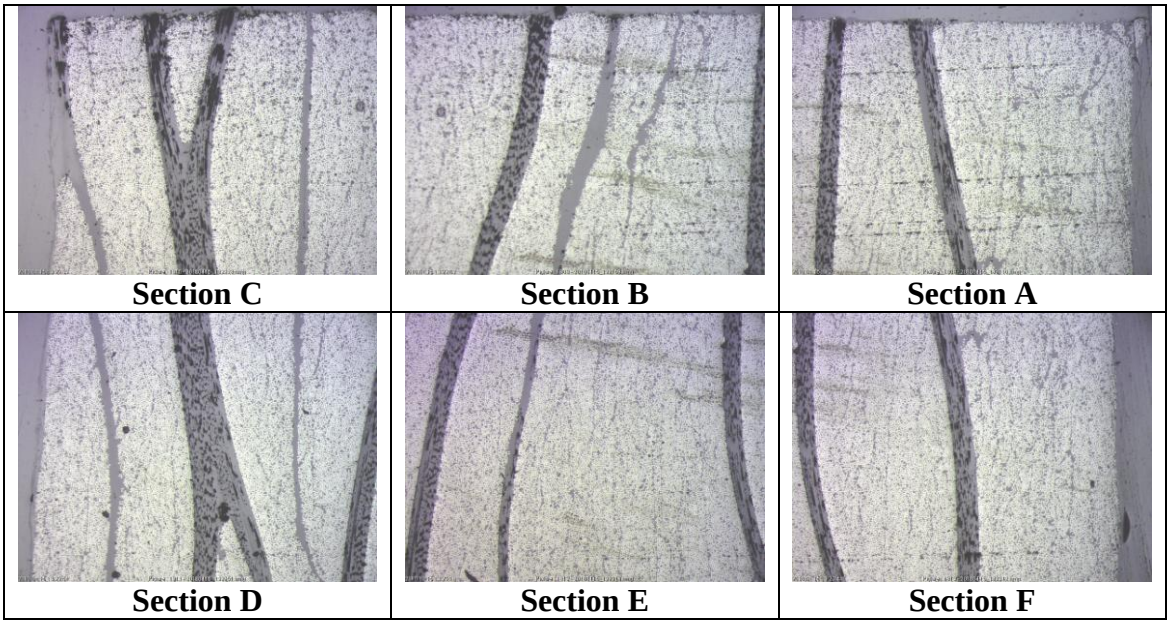

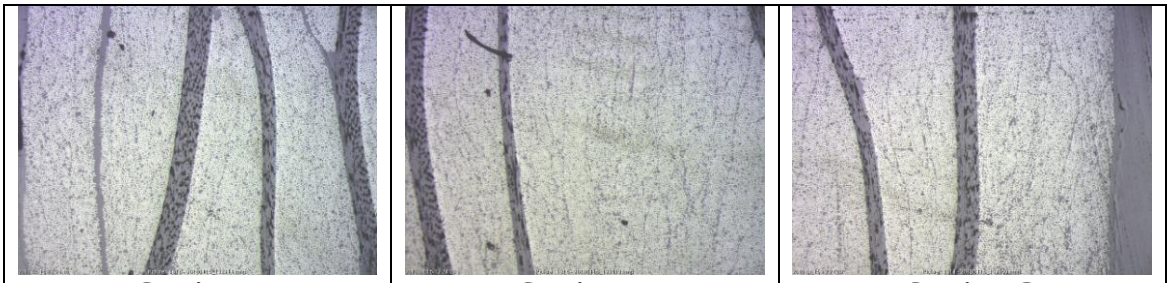

Section I	Section H	Section G

Figure 52: 9 sections of 2D images from the specimen with 5X magnification (29th layer)

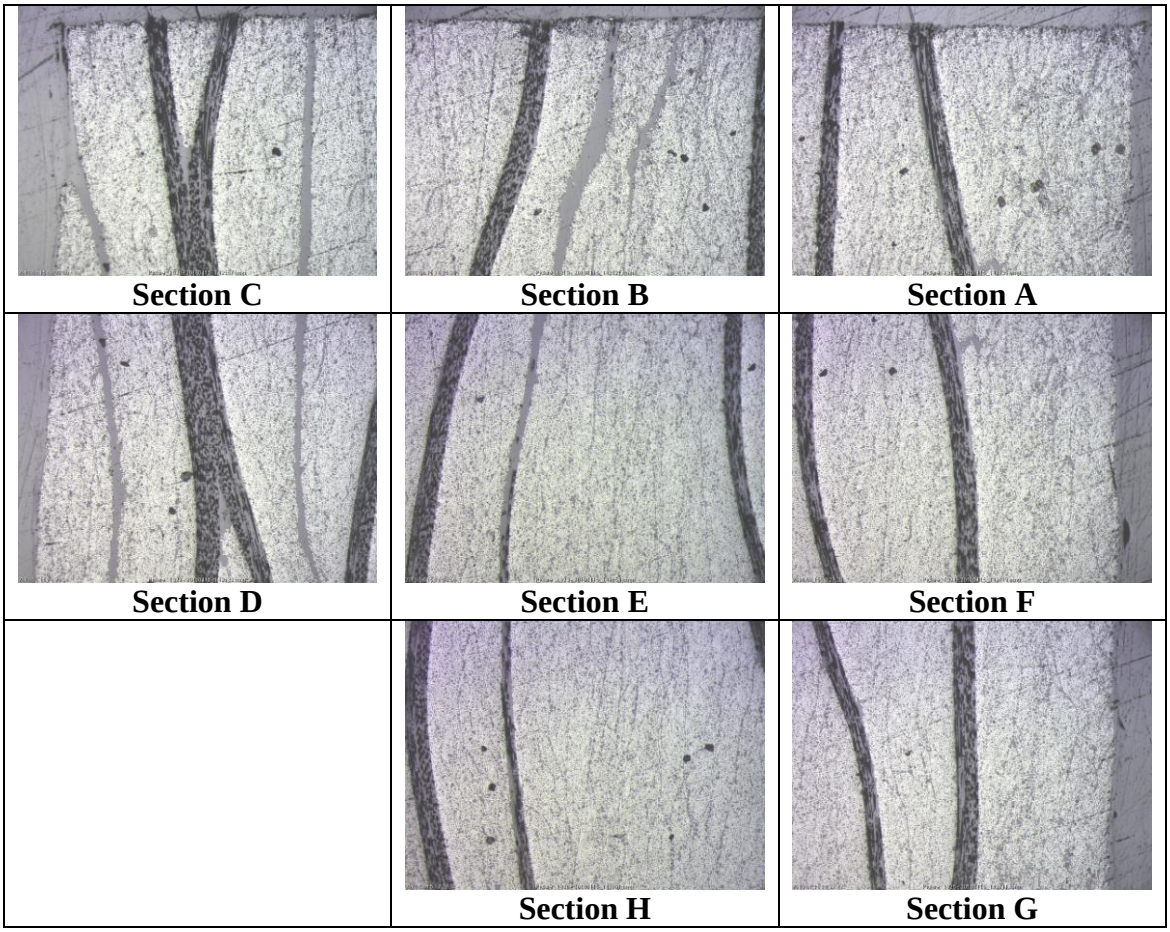

Section C	Section B	Section A
Section D	Section E	Section F
	Section H	Section G

Figure 53: 9 sections of 2D images from the specimen with 5X magnification (30th layer)

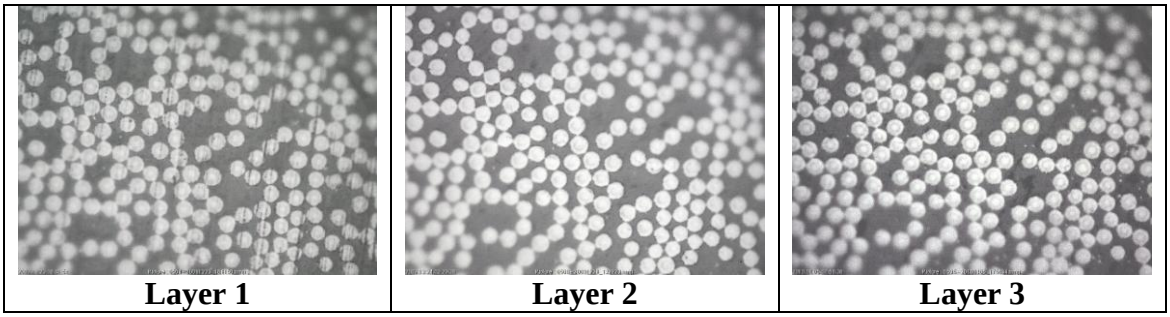

Layer 1	Layer 2	Layer 3

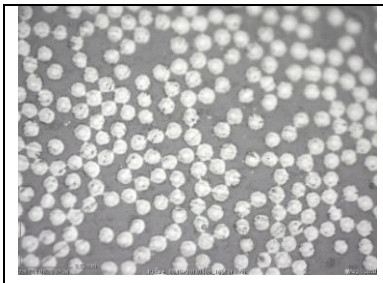	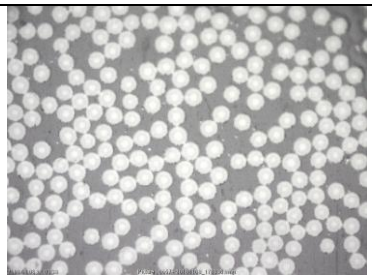	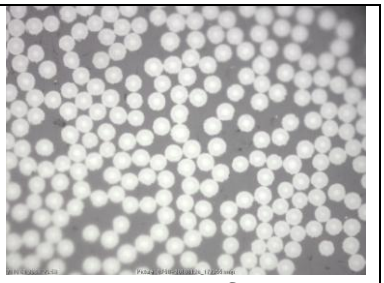
Layer 4	**Layer 5**	**Layer 6**
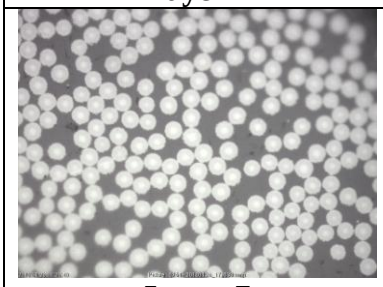	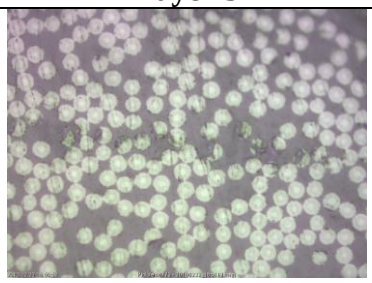	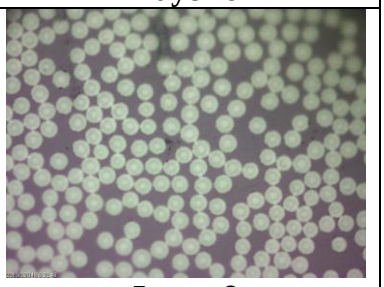
Layer 7	**Layer 8**	**Layer 9**
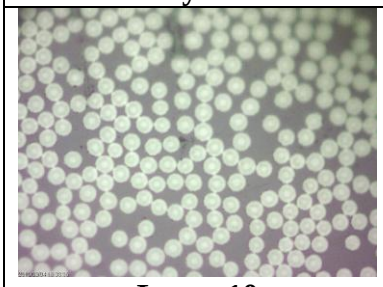	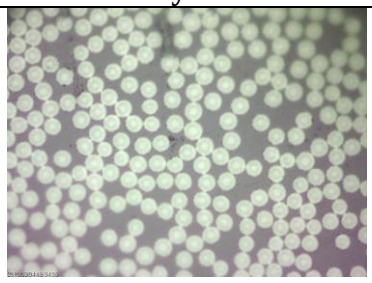	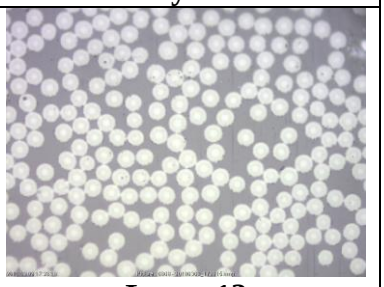
Layer 10	**Layer 11**	**Layer 12**
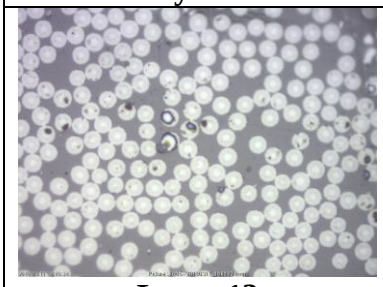	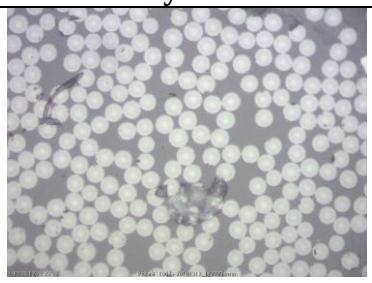	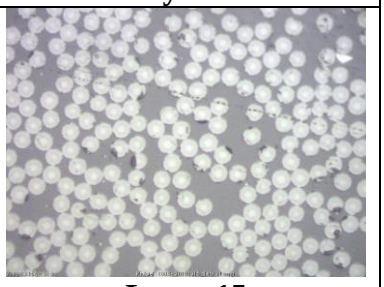
Layer 13	**Layer 14**	**Layer 15**
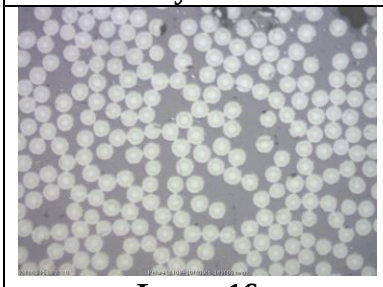	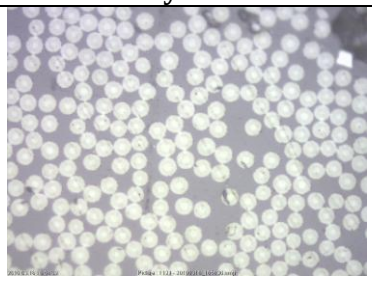	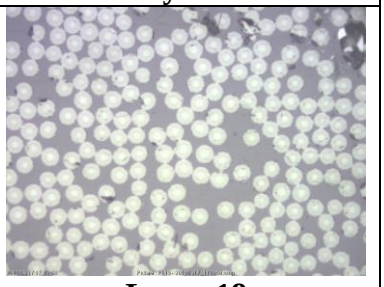
Layer 16	**Layer 17**	**Layer 18**
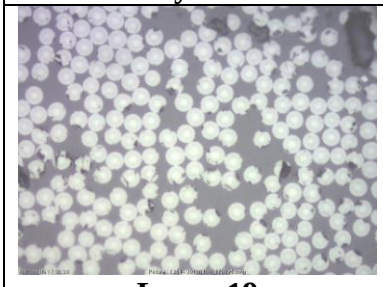	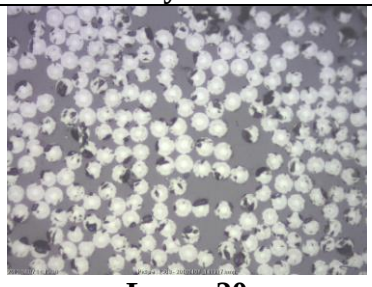	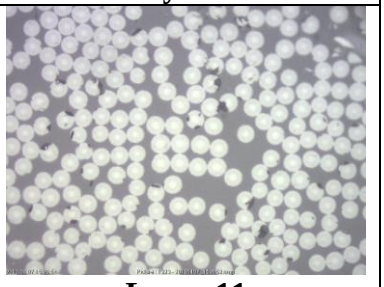
Layer 19	**Layer 20**	**Layer 11**

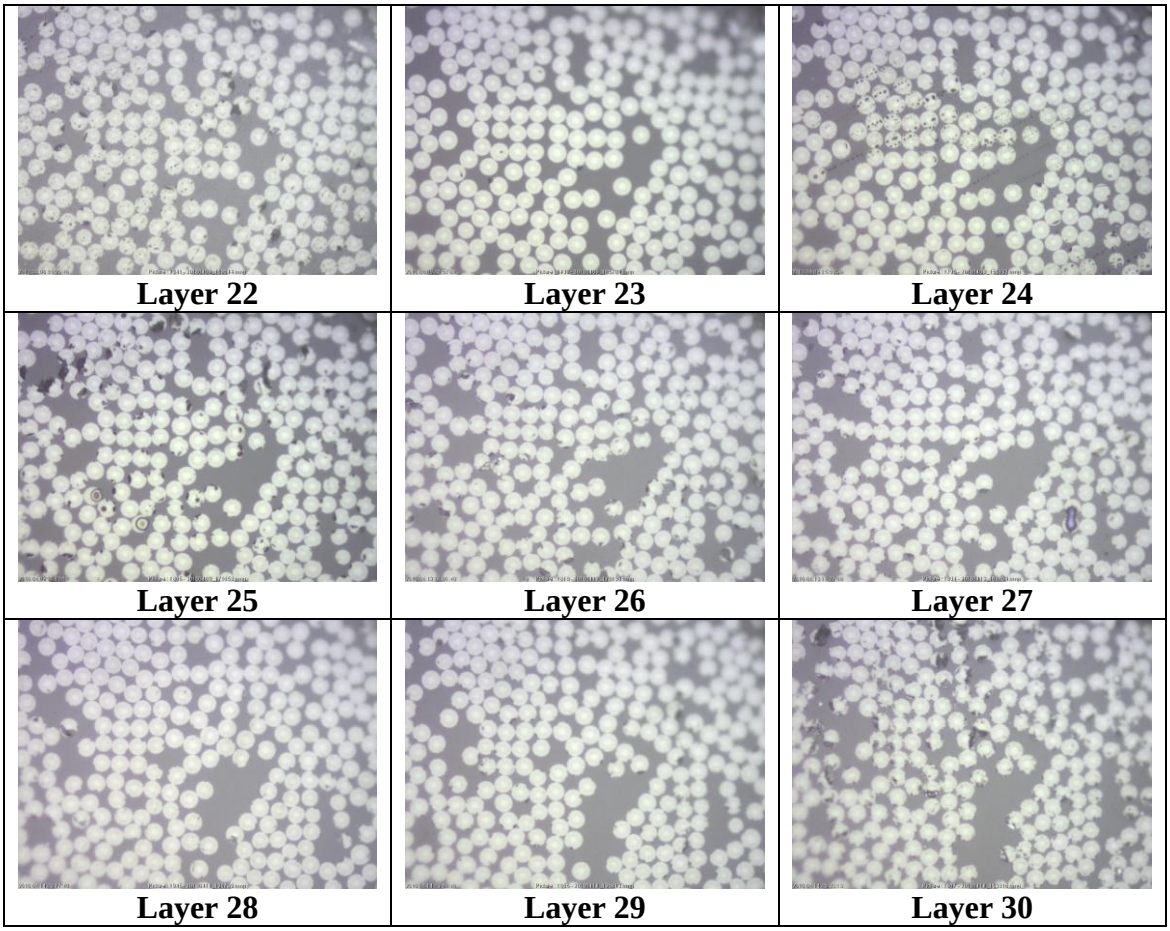

Figure 54: 28 layers of 2D images from the specimen with 50X magnification

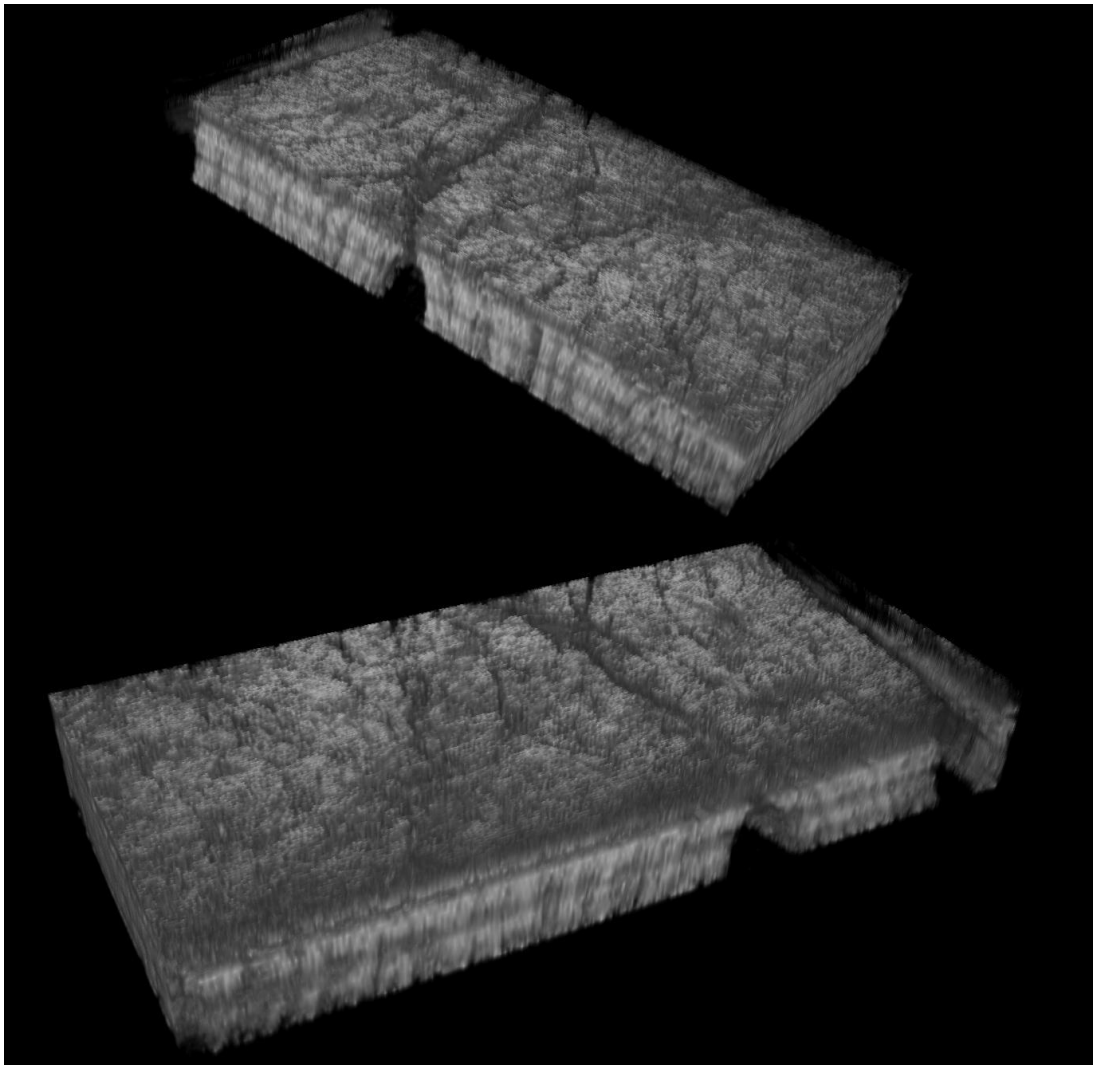

Figure 55: 3D volume of 5X magnification for Section A

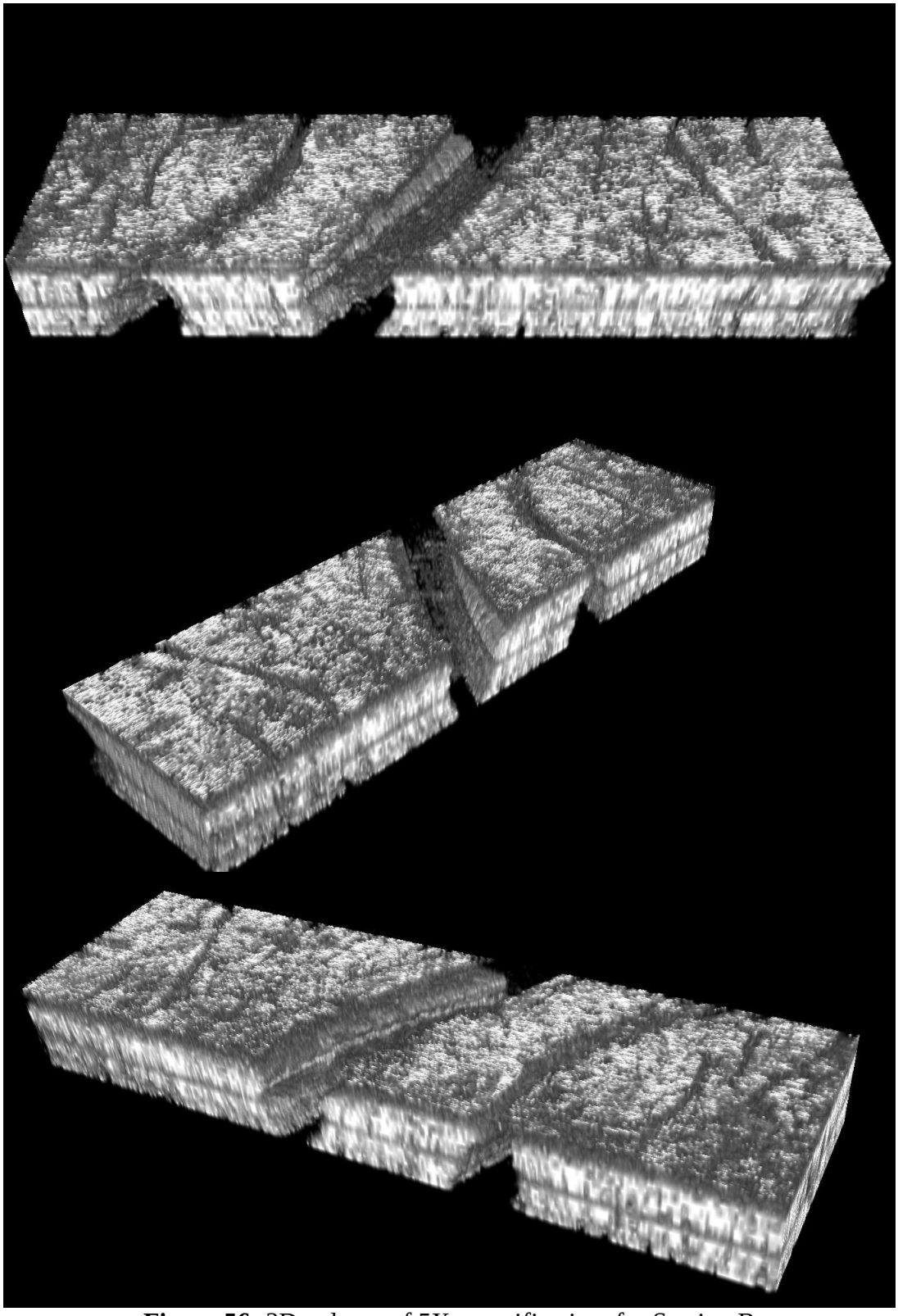

Figure 56: 3D volume of 5X magnification for Section B

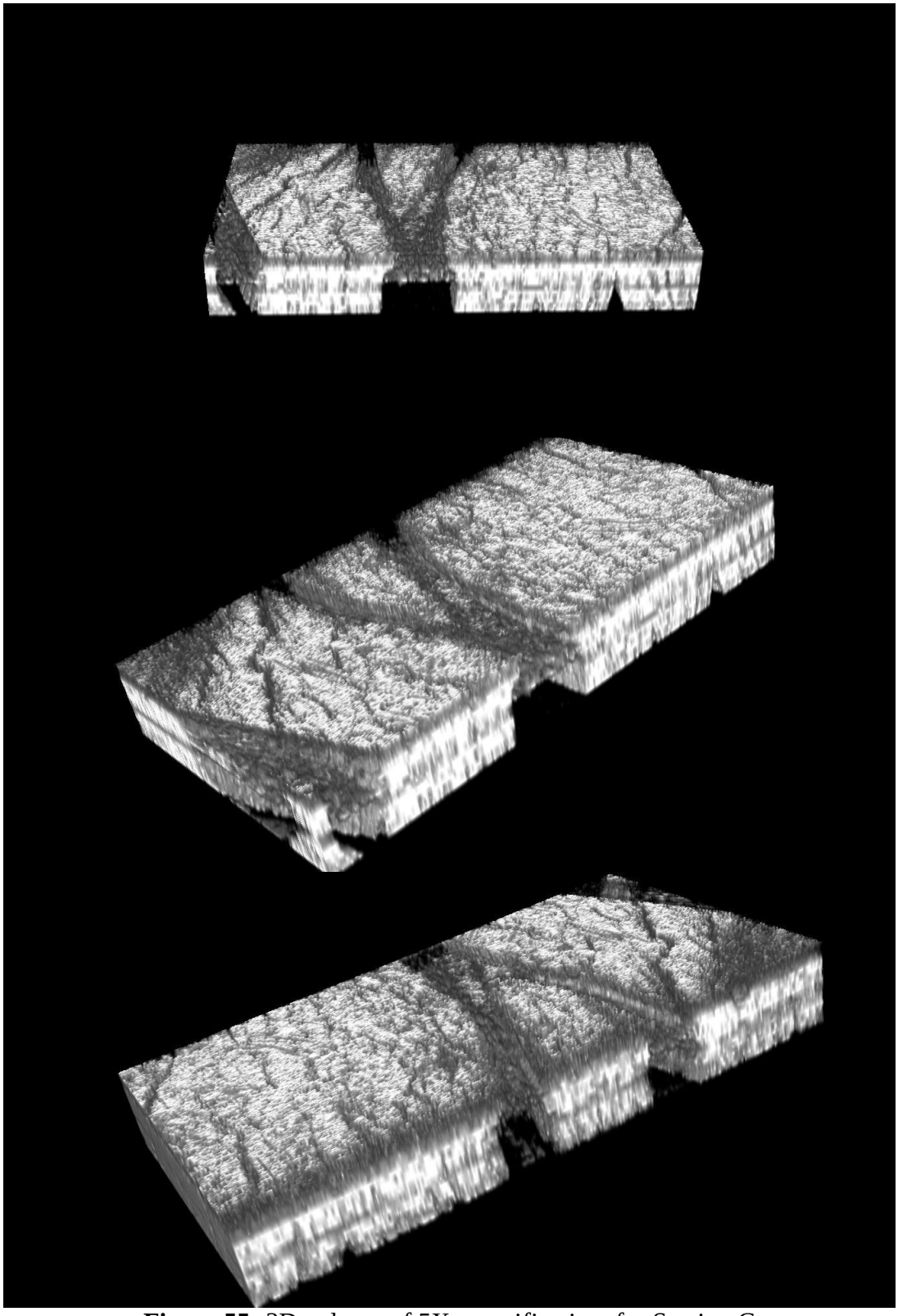

Figure 55: 3D volume of 5X magnification for Section C

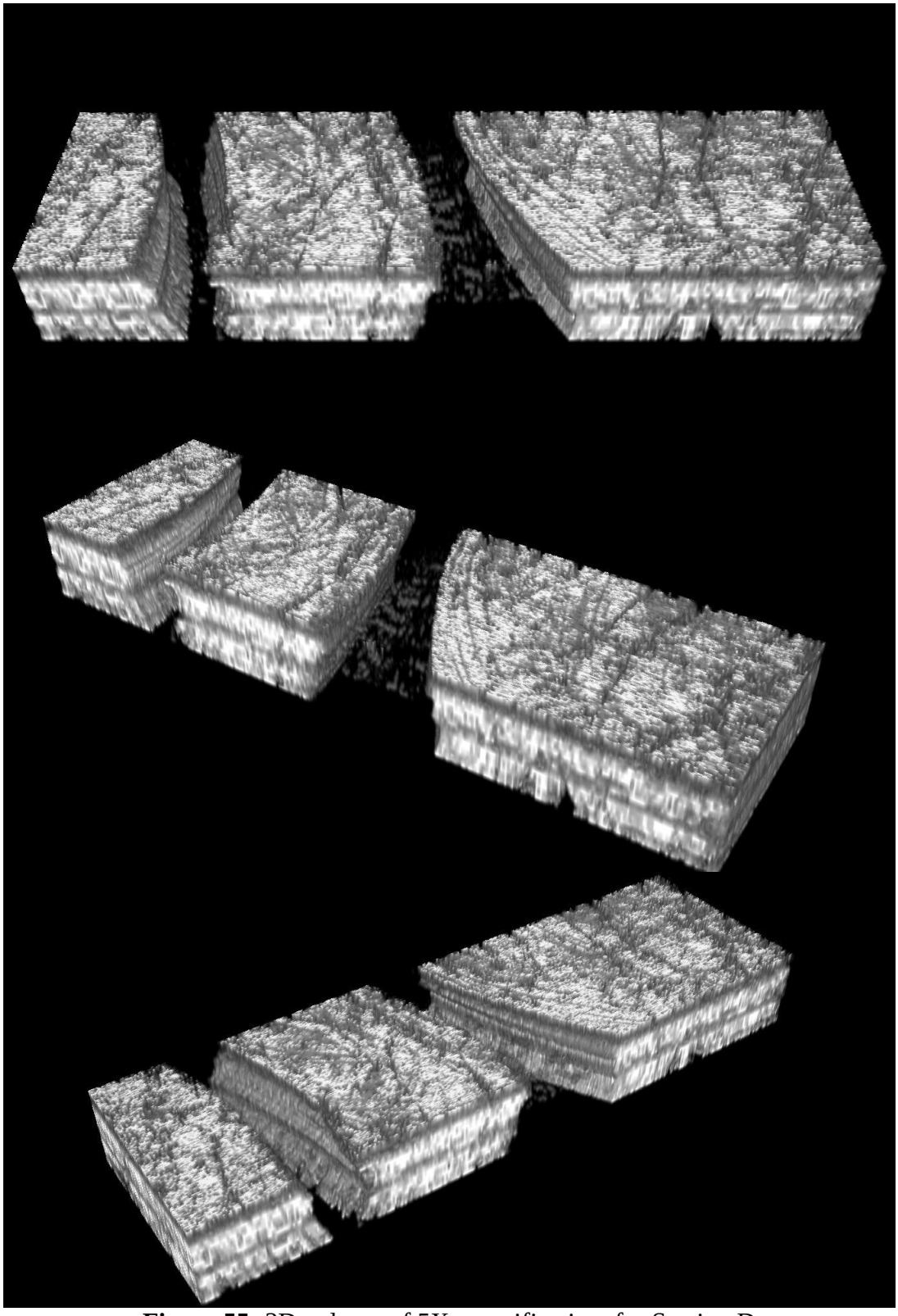

Figure 55: 3D volume of 5X magnification for Section D

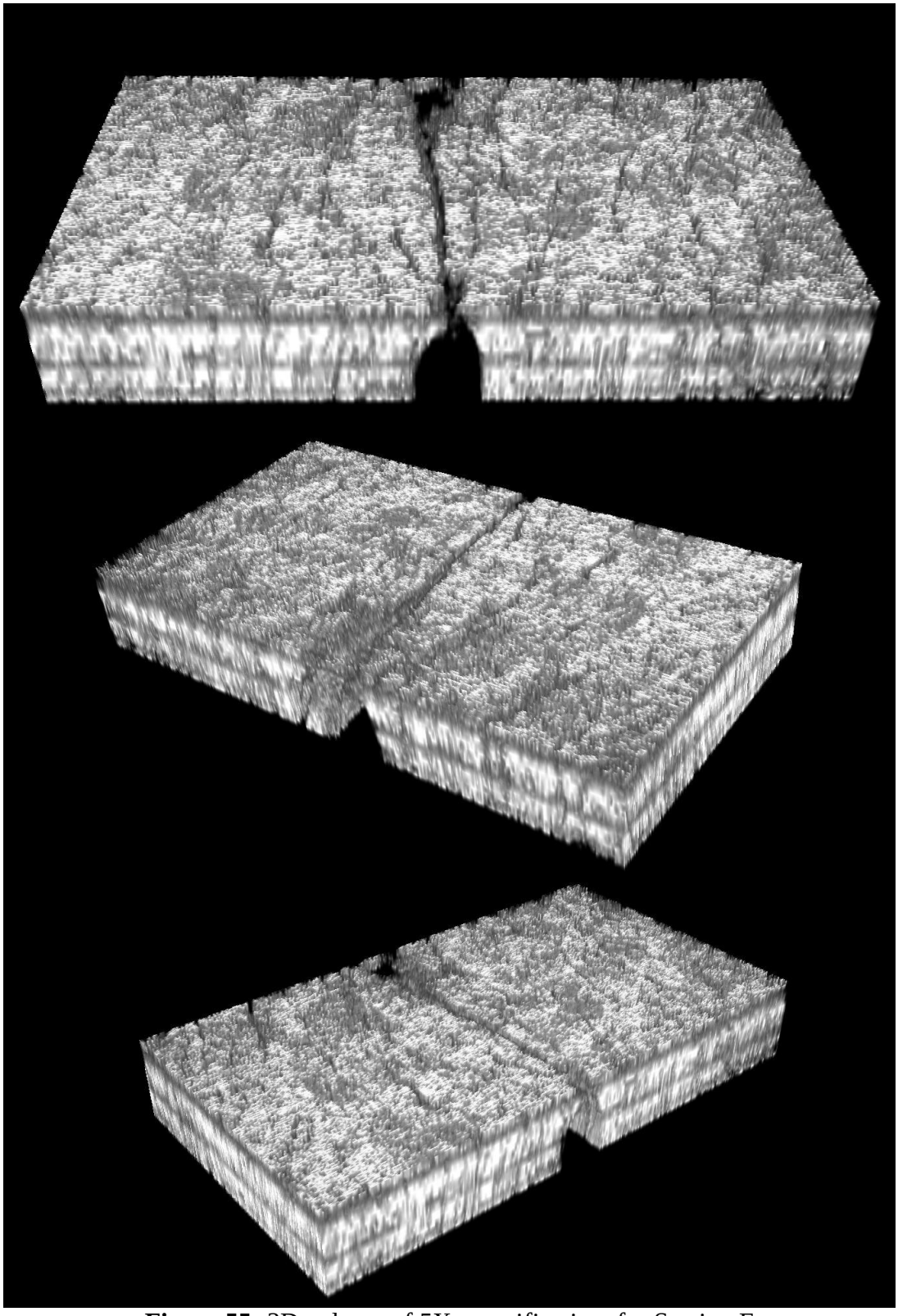

Figure 55: 3D volume of 5X magnification for Section F

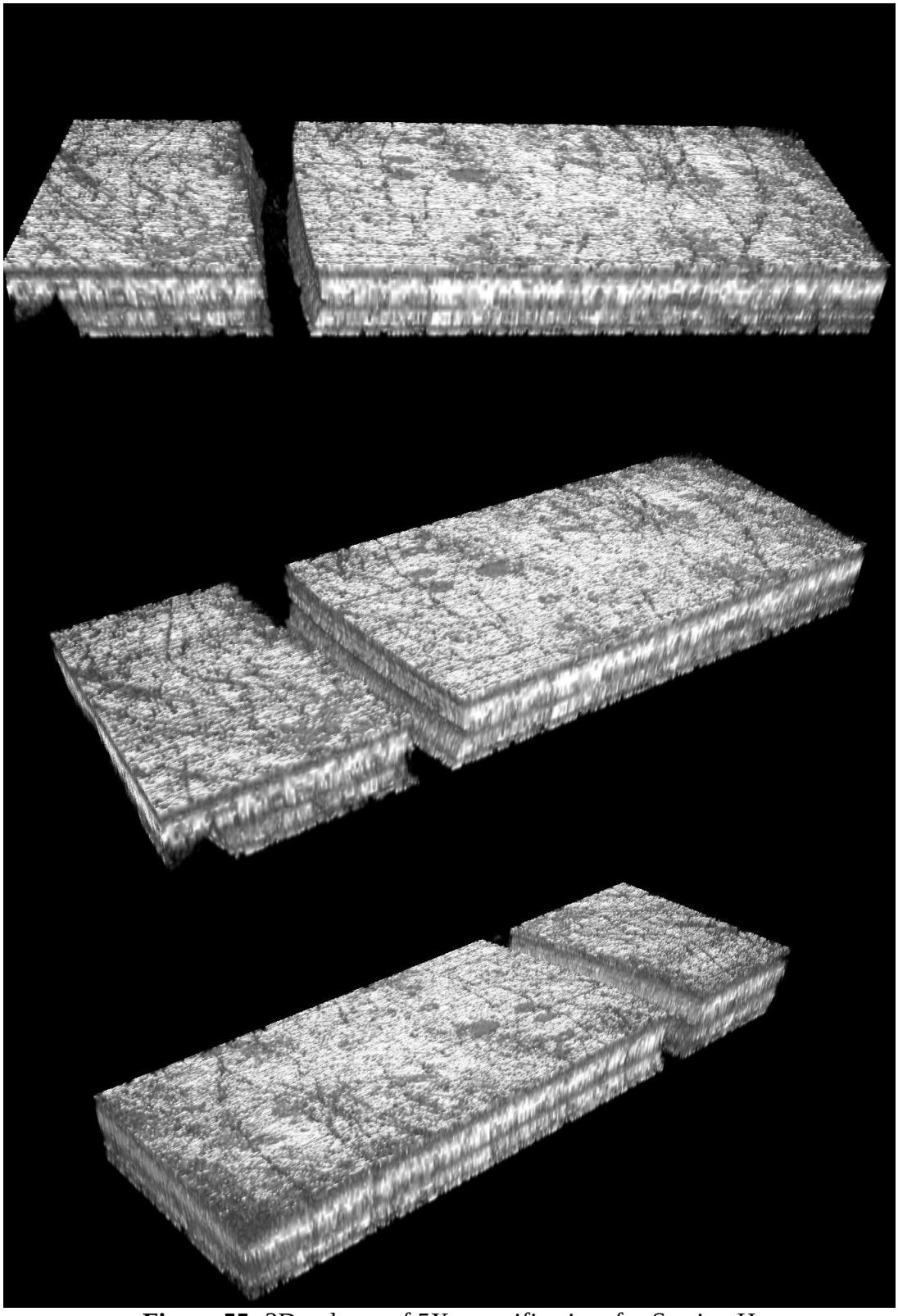

Figure 55: 3D volume of 5X magnification for Section H

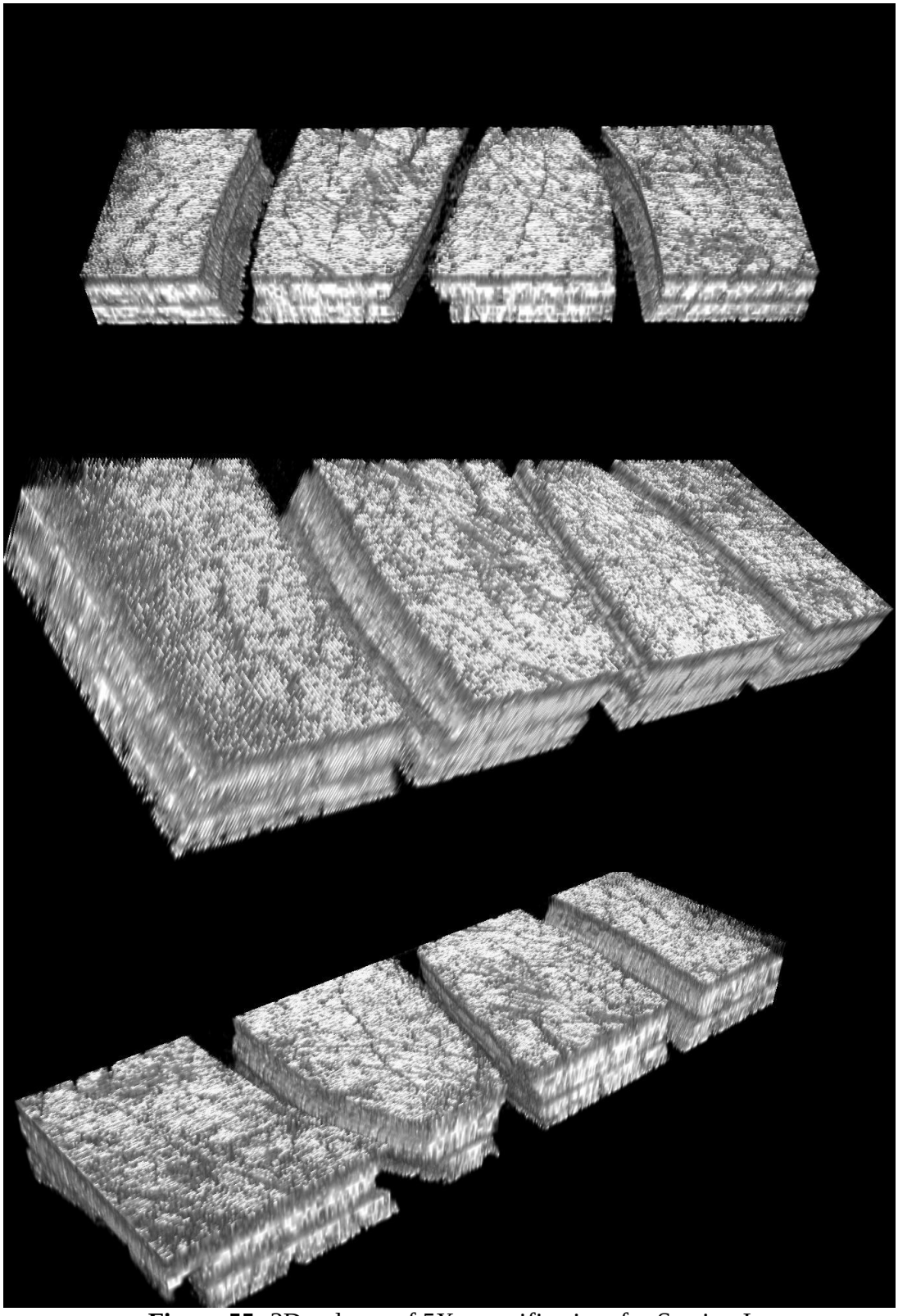

Figure 55: 3D volume of 5X magnification for Section I